9-29-2023

Forest Fire Effects on Snow Storage and Melt Across Scales of Forest Recovery in the Western Oregon Cascades

Megan Nicole Guinn
Portland State University

Forest Fire Effects on Snow Storage and Melt Across Scales of Forest Recovery in the Western Oregon Cascades

by

Megan Nicole Guinn

A thesis submitted in partial fulfillment of the
requirements for the degree of

Master of Science
in
Environmental Science and Management

Thesis Committee:
Kelly E. Gleason, Chair
Yangdong Pan
Max Nielsen-Pincus

Portland State University
2023

Abstract

Snow is the largest component of water storage in the western United States, it serves as a key moisture source for forested ecosystems and is fundamentally linked to streamflow and nutrient cycling. Snow is vulnerable to climatic warming, and a key consequence of declining mountain snowpack is the escalation in wildfire frequency, extent, intensity, and duration across the seasonal snow zone. Fire modifies the spatial extent of snow in watersheds, reducing snow water storage and timing of melt across burned forests. Forested mountain ecosystems and water supplies are facing shifts in their structure, function, and succession. Previous research has focused on short-term forest fire effects on snow hydrology. However, no previous study has empirically investigated the recovery of forest fire effects on snow-storage and melt over decades following fire. With the intensity and frequency of forest fires increasing and snowpack declining in the western United States, a common question is how to reduce forest fire risk while increasing watersheds efficiency at generating water supplies? Here we present a potential answer to such a question, where snowpack observations taken from the western Oregon Cascades illustrate that over decades following fire, snow in burned forests store more snow volume and delay melt timing for similar to an open area. We evaluate the long-term recovery of forest fire effects on snow accumulation and melt. We combined in-situ point based measurements, continuous time-lapse photography within three burned forests, and a remote sensing and multivariate analysis of basin scale forest fire effects on snow cover in the western Oregon Cascades. We found that forest fires increase snow accumulation and eventually delay snowmelt around 10 days later 10 years following fire compared to immediately following fire Decades following forest fire, burned forests may retain more snow longer in spring

and result in long term benefits for water resources. Allowing forest fire to burn in snow dominated headwaters may increase snow storage for water resources management.

Acknowledgements

I would like to thank numerous individuals and institutions that have supported and contributed to this body of work. I have benefited tremendously from your generosity, ideas, and support. First and foremost, to my advisor Dr. Kelly Gleason for taking a chance on me and accepting me into her lab during a very challenging time, a decision which changed the trajectory of my life. She provided me inspiration through her grit, intelligence, and creativity in the field of snow hydrology. I am grateful for her mentorship and for being an example of what it is to be an influential woman in a challenging scientific world.

Thank you to my thesis committee Dr. Yangdong Pan and Dr. Max Neilsen Pinus for the support in data and statistical analysis and serving as graduate school representatives. I am very appreciative for their willingness to provide beneficial knowledge and feedback. Thank you also to the unyielding support of the ESM faculty and my peers at Portland State University. I am also grateful for the financial support for all of these research efforts that was provided by the National Science Foundation Rapid Award # 2102762, NASA award #80NSSC19K0002, and the US Army Corps of Engineers Award # W912HZ2220004. Their generosity provided support for my graduate school attendance and for field and travel support for the countless days of fieldwork, necessary for conducting this research and collecting these data.

I personally benefited from the conversations, friendships, and collaborations with my lab mates within the Snow Hydrology Lab. A major contributor is Anton Surunis, who was always available as support to my work. Through Anton's incredible programming skills, he produced PoleR which was an essential piece of programming for this research effort. His kindness and willingness to help was a true support and I could not have made it through without him. Max Gersh provided field and moral support and paved the way for the rest of us. Nani Ciafone helped with fieldwork, keeping my head on straight and talking through tough problems in science and life. Sage Ebel for the inspiration for what is possible in fieldwork and adventure and Monica

Zapata Villegas for showing up with kindness and providing motivation near the end. I would also like to thank the forecasters at the Chugach Avalanche Center and the Flathead Avalanche Center, Wendy Wagner, Andrew Schauer, John Sykes, and Blase Reardon. Thank you for your mentorship, friendship, and the nerdy conversations on the skin track. It has truly been an honor to learn about snow through your unique perspectives.

Finally, I would like to thank both of my parents for being by my side through this process and for showing me the reward of a strong work ethic and pushing me to pursue my dreams, no matter how big they may seem. Thanks to my Mom, Cheryl Guinn for her lessons in kindness, creativity, and the bravery to look for answers in unconventional ways. Thank you to my Dad, David L. Guinn for pushing me to seek knowledge, the truth, and setting my mind straight during challenging times. They both have provided me with a life from which I could pursue my dreams and passions and there is perhaps no greater gift. And finally, to my partner Ben Grodner for exposing me to the light I couldn't see in myself. For being kind, fair, and an invaluable scientific, adventure, and life partner. You are my rock and I am forever grateful for your limitless patience, support, and love through what was the most trying experience of my life.

Table of Contents

LIST OF TABLES

LIST OF FIGURES

LIST OF ACRONYMS

General Terms
LAI = Leaf area index
LAP = Light absorbing particles
BC = Black Carbon
JD –=Julian Date
NRCS = National Resources Conservation Service
USGS = United State Geological Survey

Remote Sensing Products
MTBS = Monitoring Trends in Burn Severity
fSCA = Fractional Snow cover area
dNBR = Differenced Normalized Burn Ratio
NLCD = National Land Cover Database
NED = National Elevation Dataset

Snow processes
PSD = Peak snow date
SDD = Snow disappearance date
PSWED = Peak SWE date
SMR = Snow melt rate
LSA = Landscape Snow Albedo
SSA = Surface Snow Albedo
SWE = Snow water equivalent
CC = Cold Content

Burn Severity Classifications
MOD = Moderate Severity Burned Forest
FOR = Forested Unburned
OPN = Open Meadow
HGH = High Severity Burned Forest

In-situ Forest Fire sites
LH = Lionshead Burn Complex
BB = B and B Burn Complex
SL = Shadow Lake Fire

Statistical references
ANOVA = Analysis of the Variance
SD = Standard Deviation
PCA = Principal Component Analysis

1.0 INTRODUCTION

1.1 Why is snow important?

Water resource availability has long been a topic of concern throughout the American West, where snow sustains nearly 70% of yearly water usage (Barnett 2005; Li 2017). This is the equivalent of 150 cubic kilometers of water and is the approximate storage capacity of all man-made reservoirs in the Western United States combined (Mote 2018). In 2022, such reservoirs experienced their lowest water levels since their inception (Aaro and Becki 2021; Carlowicz 2022; Bureau of Reclamation 2022). Lake Mead, a crucial resource supplying water and electric power to roughly 40 million Americans, only reached 27% of its capacity (Aaro and Becki 2021; Carlowicz 2022; Bureau of Reclamation 2022). At this critical juncture, 10 Western State Governors declared official water shortages and appealed for federal drought disaster aid (Bureau of Reclamation 2022). Strain on finite but critical water resources has the potential for detrimental impacts on society, the environment, and the economy (Adam 2009).

Winter snow retention is critical for water availability in the drier summer months (Bladon 2014). The timing of differential spring snowmelt drives the occurrence of terrestrial drought (Mueller 2005) particularly in snow-melt dominated mountain basins. In these regions, cyclical snow recession shapes abiotic processes, saturates soils, initiates runoff, exports nutrients, and recharges groundwater (Yarnell 2010; Jeong 2012). For forest and stream biota, snow-melt is a reproductive cue and is closely linked with the hydrologic transitions that exert phenologic controls through the growing season (Contosta 2017; Yarnell 2010). Further, human management of water resources require thresholds of water quality, quantity, and timing to be met for drinking water, agriculture, ecosystem

health, flood control, and myriad other uses. Shifts to the timing of this key hydrologic source may result in dramatic alterations to snow-driven biotic and abiotic systems (Mastrotheodoros 2020).

Snow cover has a large influence on the global energy balance (Henderson 2018; Intergovernmental Panel on Climate Change 2007). Amid widespread early snow loss, the overall surface of the earth darkens, amplifying changes to climate (Marks and Dozier 1992). The subsequent decrease of global albedo instigates a positive feedback loop expected to augment global warming (Cess 991; Marks and Dozier 1992). Concurrently, disturbance such as forest fire, pollution and dust on snow events decrease snow albedo (De Noblet-Ducoudré 2019). After environmental disturbance, the snowpack absorbs more energy accelerating it's rate of warming and melt (Gleason 2013; Wiscombe and Warren 1980; Marks and Dozier 1992). Ultimately, snow decline will exacerbate the climate conditions that cause it (Thackeray and Fletcher 2016).

1.2 Snow is Vulnerable – Climate Change Melting Snow and Increasing Fires

Patterns in snow melt and accumulation throughout the seasonal snow zone are altered by climate warming, causing inconsistency to snowmelt pulses (Musselman 2021; Luce 2014; Yan 2021). As the climate warms, the largest hydrologic fluctuations are in snow-dominated basins of mid to upper latitudes (Barnett 2005). Early melt and declining snow water equivalent are especially apparent in low elevation maritime regions (Mote 2005, 2018; Dyer and Mote 2006; Kapnick and Hall 2012; Lundquist and Cayan 2007) with prominent and consistent declines in April 1st snow water equivalent (SWE) and shifts in precipitation patterns and snow cover (Mote 2018). The ripe Maritime snowpack of the Pacific Northwest has a high internal energy state requiring lower inputs to reach

isothermal temperatures required for melt (DeWalle and Rango 2008). Climate warming readily drives large-scale shifts from snow to rain across the region (Klos 2014; Harpold 2017). Such critical thermal sensitivities disrupted snowmelt timing and response causing flooding, erosion, and even reservior overfill through abnormal melt patterns and pulses (Lyon 2008; Stewart 2004). Larger pulses of precipitation caused by rain on snow provoke higher frequency of flooding and drought (Mote 2018; Us Epa 2016). Water supplied from snow melt varies from year to year and climate warming adds uncertainty in water resources management decisions reliant on snow melt (Stillinger 2021). Inconsistencies in winter melt trends give a false sense of security to water reservoir forecasters who open spillways without fully understanding what is left upstream (Stillinger 2021).

Snow is the largest component of water storage in Oregon and is vulnerable to climatic alterations (Mote 2005). Early melt and declining snow water equivalent are especially apparent in low elevation maritime regions (Mote 2005; Mote 2018; Dyer and Mote 2006; Kapnick and Hall 2012; Lundquist and Cayan 2007) with prominent and consistent declines in April 1st snowpack (Mote 2018; Harley 2020; Us Epa 2016; Barnett 2005) and shifts in precipitation patterns and snow cover (Mote 2018). Maritime snowpack's have a high internal energy state requiring lower inputs to reach isothermal temperatures required for melt (DeWalle and Rango 2008). Therefore, it is easy for climate warming to drive large-scale shifts from snow to rain across the region (Klos 2014; Harpold 2017). Such critical thermal sensitivities disrupted snowmelt timing and response causing flooding, erosion, and even reservior overfill through abnormal melt patterns and pulses (Lyon et al. 2008; Stewart, Cayan, and Dettinger 2004). Simultaneously, in light of regional projected climate warming as well as aggressive fire suppression techniques from the past

century (Gilliam 2016), maritime temperate forests have experienced expanding fire area into once moisture-rich forested watersheds (Trouet 2006; Westerling 2006; Littell 2016; Abatzoglou and Kolden 2013; Cansler and McKenzie 2014; Dennison 2014; Stavros 2014; Westerling 2016; Kitzberger 2017). Decreased fuel moisture and increased duration of arid weather create large quantities of dry fuels where wildfires are more likely to ignite (Littell 2016). With increased fire deficit, exacerbated by climate change, regional risk for high-intensity forest fires has increased (Ager 2019; Hessburg 2016; Kolden 2019; Littell 2016).

Forested watersheds are notably dynamic but increasingly unpredictable with wildfire alteration. Wildfires modify vegetation distribution and structure, which transforms the snowpack energy balance (Vilà-Vilardell 2023). The intractable consequence of wildfire is a spatially heterogeneous landscape at many scales, from small changes in canopy gaps to an entire burn complex. As spatial scale increases, ability to identify the effects of heterogeneous burn severity on snowpack patterns diminishes (Varhola 2010). Previous research has focused on snowpack storage and duration differences between open areas and forested areas in the Pacific Northwest (Dickerson-Lange and Gersonde 2017; Lundquist and Dickerson-Lange 2013; Gleason 2017; Rutter 2009; Storck 2002), as well as the radiative, broad scale, and immediate impacts of forest fire effects on snow hydrology (Gleason 2013; Gleason 2019; Smoot and Gleason 2020; Gleason and Nolin 2016). However, the long-term effect that forest fire has on snow hydrology is not well understood and represents a critical hydrological knowledge gap. No previous study has empirically investigated snow hydrology over varying scales as a function of post-fire recovery. Given the strong effects of fire on the spatial and temporal

arrangement of forest cover and subsequent snow cover, there is a need to understand forest fire-snow interactions during diverse phases of recovery.

This thesis aims to disentangle the long-term influence of forest fire on various spatially variable scales of snow hydrology. I aim to contribute a new paradigm in natural resource and water management for watershed-scale retention tools that not only combat water resource strains, but also work in parallel with strategic prescribed fire management tactics and intentional ignitions management. The proposed idea supplies solutions and quick adaptations as climate warming becomes reality and the western United States enters the third major drought of this century (State of California, 2022).

2.0 BACKGROUND

2.1 Scientific Concepts

2.1.1 Forest Snow Interactions and Management

Measuring and managing water is a piller of human civilization and western US alpine forests benefit from hydrologic management. The first human settlments were intentially placed due to their proximity to springs and rivers (Kenyon 1956). Though a compounding issue is the decline of fresh water in the western US due to a significant decrease in snowpack in alpine systems, disrupting the systems we have built around and come acustom to (Mote 2018, 2005). It is not enough to understand how much water we have, but the mechanisms that drive its distribution through natural and built systems . Novel approaches to imporving water retention in forests through the lenses of both hydrology and ecoloy allows for a more complete understanding of hydrologic functions at catchments scales (Cooper 2018; Huang 2016). There is a need for management that provides a holistic approach to preserving natural resources paramount for Earth's system equilibrium (De Freitas 2022).

Two main approaches have been used: reducing courses of climate disruption and preventing further agrevation (Jennings 2011) by seeking adaptive strategies to reduce vulnerability and increase resiliance to extreame events (Wheeler and Von Braun 2013). Adaptive stratagies focus on the reduction of vulnerabilities and increasing resliance in response to them (Barnett and Adger 2007). Many interesting natural methodolgoies have been proposed to increase water yields within watersheds, by focusing conservation efforts on areas of basins that have greater importance for water recharege, implementing less extreame land use changes and avoiding drastic conversions of native forest areas. One interesting tool proposed through a number of independent and peer reviewed studies

suggests the potenital of Siviculture as a tool in water management (Kittredge 1953; Golding and Swanson 1978; Varhola 2010). Findings proposed in Lundquist 2013, found that lowering forest density in regions with warm winters enhanced snow retention(Lundquist and Dickerson-Lange 2013). Additionally, studies have found that through the removal of vegetaion through either clear cutting or forest fires cause reductions to transpiration and increases in runoff (Bales 2011; Boisramé 2017; Ebel 2012; McLaughlin 2013; Rowse and Center 1998; Schnorbus and Alila 2004; Lang 2017). This has led many to hypothesize that if we apply methods used to reduce forest fire risk there may be both a reduction in catastrophic forest fires but also an increase in snow storage and water yield (Bales 2011; Saksa 2017). Forest clearning through perscribed burn, has been proposed though the relationship is not finite and it is still known that in the short term forest fires do the opposite and put pressures on water resources. Thus a more in-depth analysis in needed to understand the longterm influence fire has on snow hydrology.

2.1.2 Forest Fires Further Alter the Spatial Variability of Snow

Fire modifies the spatial extent of snow in watersheds creating alterations in snow cover across primal zones. Snow serves as the key moisture force for forested ecosystems were forest health is fundamentally linked to snow accumulation, ablation, and streamflow timing (Harpold and Molotch 2015; Barnhart 2016; Bales 2011, Hopmans, and O'Geen 2011; Huntington and Niswonger 2012; Stewart 2009). A key consequence of declining mountain snowpack is the escalation in wildfire frequency, extent, intensity, and duration across the seasonal snow zone (Westerling 2016). Following fire, a 40% augmentation of black carbon and burned woody debris accumulate on the snowpack surface, darkening the snowpack lowering its albedo and modify the surface energy balance (Gleason 2013;

Harpold 2014; Burles and Boon 2011; Winkler 2011). Energy absorbed by the altered snowpack drives a 200% increase in net shortwave radiation (Gleason 2019; Gleason 2013). As a highly reflective substance, snow is sensitive to concentrated impurities, leading to considerable intensification of radiative effects and ultimately faster snowmelt by even minimal depositions (Marks and Dozier 1992; Flanner 2009; Painter, Bryant, and Skiles 2012). The buildup of LAPs alter runoff patterns (Flanner 2009; Wiscombe and Warren 1980; Painter 2007) with clear and immediate shifts to snow retention properties; snow disappearance date increases, snow melt rates spike, and there is an overall loss of snow water storage (Smoot and Gleason 2020). Such influences are dependent on canopy burn severity, vegetation type, region, decreases to post-fire forest structure, and charred forest shedding further altering the snowpack mass and energy balance (Gleason 2013; Gleason 2019).

2.1.3 One to Ten Years Following Fire: Immediate Recovery

A 300% decrease in canopy density and 500% decrease in stem density increases direct solar light transmission to the snowpack surface (Gleason 2019). Reduced longwave radiation emissions from the once healthy forest canopy (Figure 1) and decreased levels of canopy interception by 40% (Roth and Nolin 2017; Storck 2002). During the accumulation period, burned and unburned forests show little change in surface snow albedo, however, during the ablation period LAPs produced by fire, decreased snow albedo by 60% and enhanced the snowpack's radiative exposure (Gleason 2013). Shortwave albedo is directly related to the snowpack energy balance (Dozier 2009; Skiles 2012). Since snow is highly reflective in the visible wavelengths (400-700nm) small changes to surface albedo can have large impacts on net shortwave radiation and accelerate the timing of snowmelt (Dozier

2009; Gleason and Nolin 2016; Painter 2007; Warren and Wiscombe 1980). New light absorbing particles intensify radiative forcing on the snow surface by up to 60% in high severity burnt forests (Gleason 2013). These alterations increase net snowpack shortwave radiation by 200% (Gleason 2013) and subsequently raise snow melt rates by 57%, thus decreasing snow disappearance date by 4-23 days (Burles and Boon 2011; Gleason 2013; Uecker 2020; Winkler 2011).

2.1.4 Five to Ten Years Following Fire: Intermediate Recovery

Decreased snow albedo has been observed for up to 10 years following fire (Burles and Boon 2011; Gleason 2013; Uecker 2020; Williams 2022; Smoot and Gleason 2020). For the years following forest fire, burned woody debris (BWD) including charcoal, and partially charred needles, cones and bark are shed from standing burned trees onto the snowpack (Gleason 2013). Landscape scale snow albedo derived from MODIS (500m resolution) in burned forests continues to brighten through the decade following fire (Gersh, 2022). Gleason 2019 shows that then the impact fire has on snow disappearance date begins to decline 8 years following fire. When this was characterized it was found that composition, magnitude, and duration of LAPs in snow samples collected in early spring began to decline following a fire. This decline was seen starting 4 years following fire increasing broadband snow albedo at the same time and decreasing the radiative forcing to the snowpack (Gleason 2019). Impacts on snow disappearance date begin to decline around 8-10 years post-fire aligning with declines in concentrations of LAPs (Gleason 2019).

2.1.5 Ten to Twenty Years Following Fire: Advanced Recovery

Radiative forcing increases up to 15 years following fire and declines from 32 and 101 Wm^{-2} one-year post fire, to 23 and 44 Wm^{-2} 15 years post fire (Gleason 2019). Declines

in black carbon and organic debris concentrations measured in burned forests 15 years after fire were similar to remote pre-industrial background levels (Gleason 2019). Gersh 2022 found that 10 years following a fire, post-fire LSA in burned forests may be more similar to that of open meadows outside the burn perimeter than to the antecedent pre-fire LSA values (Gersh 2022). If there are background concentrations of LAP on the snow surface, over decades following fire, snow surface will have a higher albedo and there will be a profound decrease on the net snowpack shortwave radiation compared to immediately following fire radiation levels (Gleason 2013; Gleason 2019; López-Moreno 2020; Gleason and Nolin 2016). Antecedent pre-fire conditions do not return in these severely burned forested zones, rather, 10 years following fire, an altered state of forest and subsequent landscape snow albedo (LSA) emerge (Gersh 2022). Balances originally offset by reductions in net longwave radiation emissions from canopy persist (Burles and Boon 2011) and benefits to snow accumulation and retention are seen through lower sublimation and canopy interception (Lundquist and Dickerson-Lange 2013; Jost 2007; Roth and Nolin 2017). It is critical that we understand the spatially variable impacts that forest fires have on snow-water storage and its resulting availability.

2.1.6 Why is the Spatial Variability of Snow Important?

For decades, snowpack has been observed and predictions have been made to forecast summer streamflow and help farmers, reservoir operators, and civilizations plan for their water usage (Anghileri 2016). However, snow falls over spatially heterogeneous landscapes at various scales in space and time, making water availability challenging to predict. Snow accumulation and melt are complex processes governed by a variety of variables. Topography controls snow accumulation and melt through slope, aspect, and

exposure of the snowpack surface. Meteorological accumulation and ablation are impacted by precipitation, wind speed, temperature, and humidity (Saydi and Ding 2020). Localized wind tubulance and variable solar radiation are the main causes of lateral spatial variability (Sturm 1995). Orographic effects such as elevation and northness contribute to solid phase precipitation of snow fall over mountain ranges (Houze 2012; Mott 2014) where snow depth and snow water equivalent increase with elevation (Zheng 2019). Snow depth and volume are affected by localized topographic and vegetative effects (López-Moreno 2017; Marks 1998; Van Heeswijk 1996), which drive snow depth, volume, and timing (Marks 1998). Overall, seasonal snow cover is spatially variable due to various external and internal processes interacting with ground cover and terrain (Schweizer 2008).

Spring snowpack measurments are the foundation for water avaiblibilty forcasting (Zheng 2019), requiring accurate predictions of both precipitaion and snowpack water storage at various scales (Hopkinson 2001). Snow can be measured at different scales in space and time, from the bonds between snow crystals, to slopes, mountain ranges, and climate regions (Schweizer 2008). This hierarchy requires varying horizontal grids for measurments, dependent on the question of concern (Clark 2011). A longstanding challenge for snow hydrologists is quantifying the spatial distribution of snow over complex terrain and forested mountain areas (Golding and Swanson 1986; Winstral and Marks 2014).

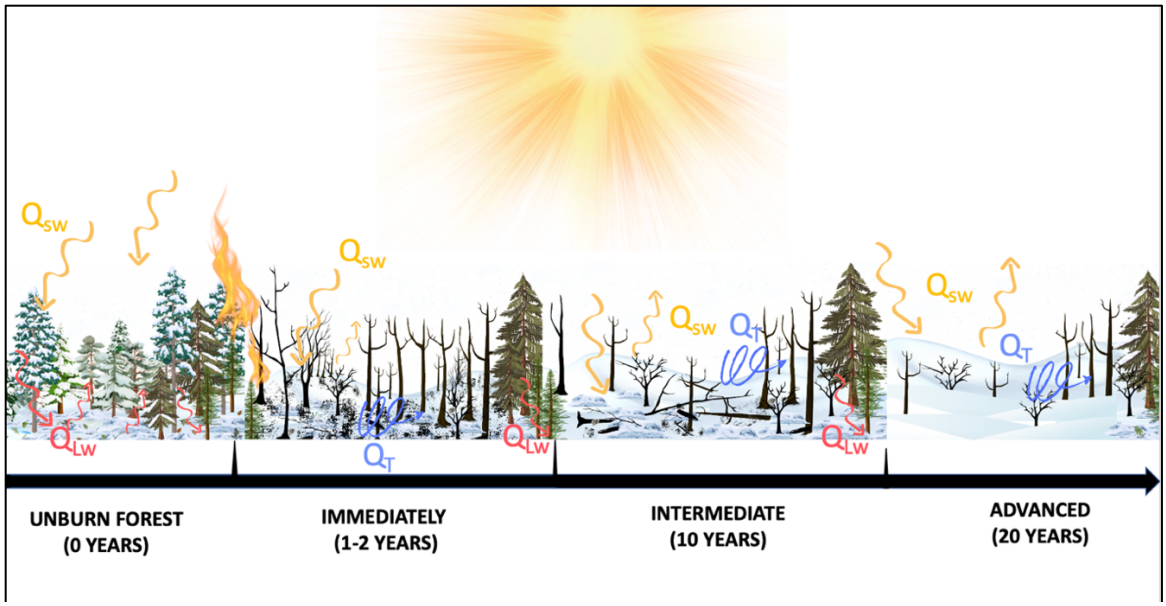

Figure 1: *Conceptual model of Radiative and Turbulent energy exchange within an unburned forest a forest immediately following burn, a forest with intermediate recover and a forest in advanced recovery. Qsw distinguishes shortwave influences on the snowpack energy balance, Q_{lw} represents the influence of Longwave Radiation on the snowpack and Q_T is turbulent flux over the snowpack surface including sensible and latent energy exchange.*

2.2 Hypotheses and Objectives and Method Background

To evaluate the overarching research question, I used multiple methods including field-based monitoring, time-lapse photography (Snowtography), multivariate statistical analysis and remote sensing focused on three primary objectives to answer the following research question:

RESEARCH QUESTION: WHAT IS THE TEMPORAL AND SPATIAL IMPACT OF POST FOREST FIRE RECOVERY ON SNOW HYDROLOGY IN THE WESTERN OREGON CASCADES?

Objective 1: Quantify Immediate Post Forest Fire Effects on Snow Storage Potential and Snowmelt Using Snow Surveys in The Western Oregon Cascades.

The objective of the research performed for the first hypothesis was to evaluate the influence of forest fire effects on snow hydrology, the year immediately following fire utilizing empirically derived snow and depth measurements via snow surveys. The snow survey is a technique that has been used by the USDA since 1984 and is one of the most accurate point-based measurements of snow available today (Pickett 1995). The snow

survey developed by Dr. James Church is a valuable tool used by water resource forecasters to monitor water supply for the coming year (Pickett 1995). Common protocol developed by the NRCS snow survey was utilized to collect snow water equivalent and snow depth. These measurements where used to capture accurate point based immediate post fire accumulation and ablation patterns and addressed the following hypothesis:

> ***Hypothesis 1***: During accumulation snow storage (snow depth, snow water equivalent, snow cover) in burned forests are more like open meadows immediately following fire but melt off earlier.

However, snow surveys have low temporal resolution due to time consuming and exhaustive data procurement were a potential loss of crucial snowpack details are not revealed. This limitation leads to the methodologies utilized in Objective 2.

Objective 2: Characterize Recovery Over Time of Post Forest Fire Effects on Snow Storage and Snowmelt Using Continuous In-Situ Snow Time-Lapse Photography and Peak SWE Surveys in A 2-Year Old, 10-Year Old, and 20-Year Old Burned Forest Relative to High Severity, Moderate Severity, Unburned and Open Areas Using Time-Lapse Photography And Snow Stakes In Western Oregon Cascades.

The objectives performed to answer hypothesis 3 considered that the variability of snow accumulation and duration within forested watersheds is difficult to accurately estimate from sparse point-based observations alone (Meromy 2013). Snow survey measurements are highly accurate so peak SWE surveys were conducted in all 3 burn regions, but only once for April 1st SWE, however they lack temporal resolution. Observing a complete snow depth time series of seasonal snow accumulation and ablation can provide increased precision of estimates for date of peak SWE (PWED), ablation and accumulation rates, snow disappearance date (SDD), and peak snow depth (PSD), providing elevated comprehension of snowpack seasonality between diverse burn areas. Dispersed and highly regular snowpack measurements are critical for building process-based representations of

snow distribution within forested watersheds impacted by forest fire. By utilizing time-lapse photography, it was possible to use semi-automated instrumentation to aide in snow depth retrieval. These stations have a high temporal resolution with conservative installation times and low cost so stations could be widely dispersed. a deeper insight into the response of snow ablation and accumulation following forest fire while allowing ample spatial distribution through recovering burns and answer Hypothesis 2:

> ***Hypothesis 2*** As a forest recovers from fire, snow within the burned region at peak SWE, ablation, and snow disappearance date begins to resemble similar characteristics of an open meadow.

Spares point-based measurements alone limit the applicability of results and fails to acknowledge the influence of variables that change throughout a watershed. This limitation leads to Objective 3.

Objective 3: Evaluate the Spatial Variability of the Recovery of Forest Fire Effects on Snow Covered Area Using Remote Sensing Derived Snow Extent and Multivariate Analysis in The Western Oregon Cascades.

The objectives performed to answer Hypothesis 3 used remote sensing, which is a suitable technique for measuring snow pack extent at the catchment scale. Satellite snow cover observations have been used for many decades and there are numerous satellite derived products that exist at the global scale (Frei 2012). Remote sensing can offer regional observations of seasonal snow and snowpack processes (Nolin 2010) due to the nature of the interactions between snow cover and electromagnetic radiation (Nolin 2010; Dozier 1989). Using remotely sensed data in conjunction with multivariate analysis will help to parse out noise in complex environmental data to answer Hypothesis 3:

> ***Hypothesis 3*** The spatial variability of snow cover in burned forests over time is decided primarily by forest fire recovery, where intermediate and advanced

recovered burns represent snow extent of an open meadow where snow extent and snow disappearance date increase with phase of recovery.

The evaluation of the differing spatial scales aided in drawing conclusion throughout this study. The strengths of each data methodology helped answer each hypothesis and derive an overall answer to our research question. Utilizing different scales and methods helped increase confidence in our results that could otherwise be confounded due to error associated with each method. Many studies constrained to one domain limit their scalability and representativeness for more variable vegetation and topographic conditions (Goodell 1952).

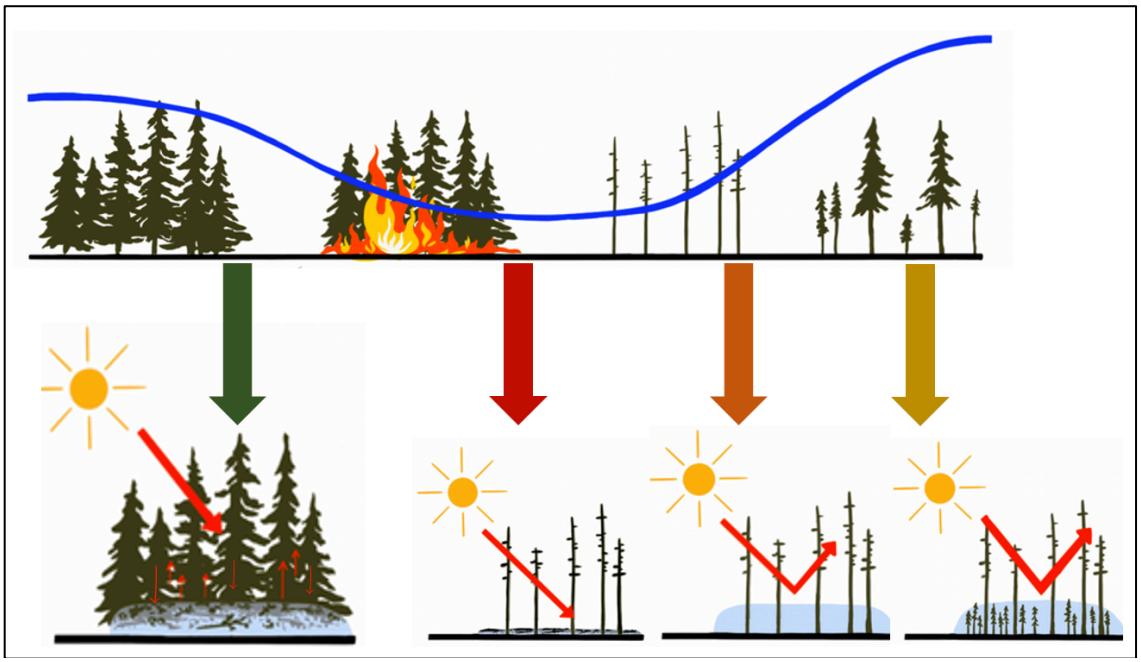

Figure 2: *Synthesis of snowpack quantity over time within a high severity burn forest over time. Far left is unburned progressing through advanced forest recovery. Arrows show net radiation at the snowpack surface over time and recovery.*

3.0 METHODS

3.1 Study Regions

3.1.1 The Willamette Watershed

The heart of the western Oregon Cascades is the historic lands of the Kalapuya, Chinook, and Clackamas and is otherwise known as the Willamette Watershed, which bounds our study region (Figure 3a, 45˚ 20' 39" N and 122˚ 39' 14"). Notably, this watershed has had an increasing proportion of burned forest, with fires ranging in age and extent (Walsh 2008). The Willamette watershed at 30,000 km^2 is the largest watershed in the State of Oregon, contributing to major municipal water resources in Eugene, Corvallis, Salem, and Portland (Portland Environmental Services 2017). Seventy percent of Oregon's population lives in the Willamette Valley where the North and South Santiam river converge and flow into the Willamette (Lane 1969). The Watershed is made up of a significant portion of volcanic and mountainous National Forest, specifically the Willamette, Mt. Hood, and Deschutes National Forests. It is delineated by the Coastal Mountain Range to the west and the Cascade Mountain Range to the east. Elevations range from 3,200 meters at Mount Jefferson to 3 meters at the mouth of the Columbia River (Portland Environmental Services 2017). Our study area receives between 165-330 cm of annual precipitation, falling as snow and rain depending on topography (Prism Climate Group 2022).

Vegetation varies from high mountain subalpine of Montane Conifer Forest and Lodgepole Pine to closed conifer and Red Fir (Atzet and McCrimmon 1990). The spatial complexity of the forest types and connected fire regimes contribute to variable snow conditions (Atzet and McCrimmon 1990). Snow storage in the headwaters of the Willamette subregion in Western Oregon, directly contributes to the stream habitat of sensitive species, hydropower generation, and municipal water supply (Portland Environmental Services

2017). Defined as a Maritime climate, the western side of the north-south trending Cascade Range typically sees a large amount of winter precipitation and temperatures that fluctuate around freezing (Sturm 1995). The western Oregon Cascades depends on sufficient snow storage to augment the summer dry seasons for water resources and fire suppression (Hamlet and Lettenmaier 1999; Nolin and Daly 2006; Adam 2009).

Management within the Willamette watershed is complex as the fertile agriculture drives water resources necessity (Portland Environmental Services 2017), in addition to the water resources need of the extensive urban and suburban development and interface (Lane 1996) . The forest and valley floor has been shaped by numerous forces that exult environmental upheaval, including the influence of forest clearance and naturally and human ignited fires (Walsh 2008).

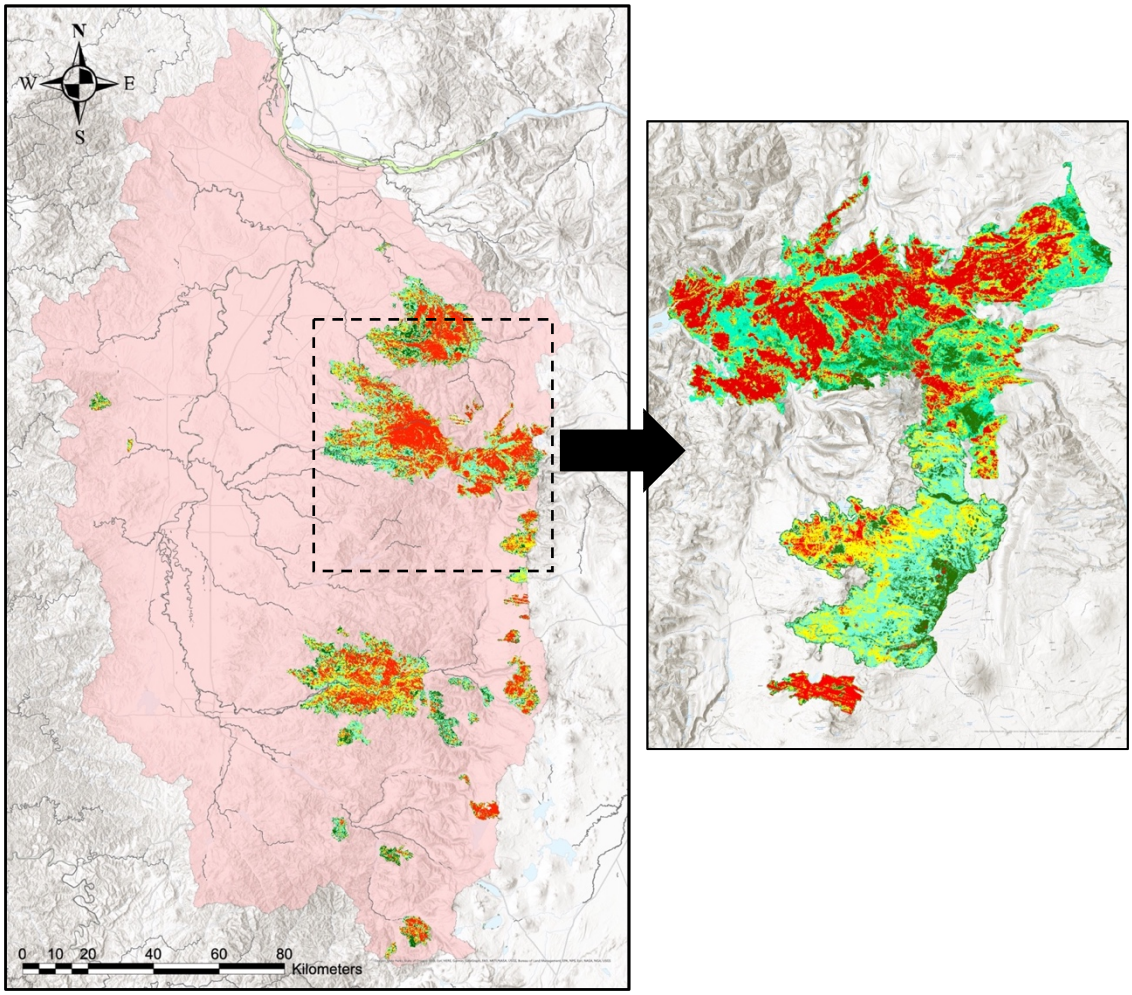

Figure 3: *Overview of the Willamette Watershed and all fires studied during the remote sensing phase of study. B: Locations of the Lionshead (Top) B and B (Middle) and Shadow Lake (Bottom), in relation to other burn areas of concern are the field based study areas.*

3.1.2 The 2020 Lionshead Burn Area (2-year-old fire)

During the late summer of 2020, record-setting wildfires swept through the western United States. In that year alone 250 wildfires burned 41.500 km^2 – the most acreage impacted by wildfires in any year on record (Hoover, Hanson, and the Congressional Research Service 2021). The fires that moved through the temperate forests of the Oregon Cascades were ignited by lightning on August 16th, 2020. Three weeks following the outbreak, a historic wind storm ("Incident Information System" 2021) caused the fires to expand to over 530 km^2 in one night, about 70% of the final burned acreage. By the time

the fires were considered contained on October 1st, 10 weeks after the burn had initially begun, ("Incident Information System" 2021) the Beachie Creek - Lionshead Burn Complex covered nearly 830 km^2 of municipal, public, and private forested land (Figure 4a).

Our major *in-situ* study was conducted within the Lionshead Burn Area on the west side of the Cascade Crest at about 1350m (Lat: 44:724, Long: -121.967) dominated primarily by conifer closed canopy stands where moisture levels are that of a rainforest. A significant portion of this region is National Forest, specifically Willamette, Mt. Hood, and Deschutes National Forests. The Beachie Creek-Lionshead burn complex destroyed several communities in the Santiam River and Breitenbush River watersheds, including the loss of 264 residences in Detroit, OR ("Incident Information System" 2021). These fires also threatened highly valued natural and cultural resources: water supply, timber supply, and public lands (Portland Environmental Services 2017). Watersheds affected by the Beachie Creek-Lionshead fire feed into the Detroit reservoir, which has a capacity of slightly more than half a cubic kilometer and is the main drinking water source for the city of Salem and other nearby communities (Portland Environmental Services 2017).

3.1.3 The 2011 Shadow Lake Burn Area (15-year-old fire)

The Shadow Lake fire was started by lightning and burned 42 km^2 of the high Oregon Cascades (Figure 4b). The fire started on August 28th, 2011, in the Mt. Washington Wilderness and devastated the headwaters of the McKenzie River Basin, a major tributary to the Willamette Watershed and a large contributor to groundwater recharge. A majority of the burn occurred between the elevations of 1500m – 2000m, at the high end of the seasonal snow zone (Gleason 2017; Taylor and Hannan 1999). Most of the 3000mm of precipitation that this region receives falls as snow from November to April (Taylor and

Hannan 1999). The McKenzie River Basin has a low to mid elevation snowpack making it vulnerable to small changes in air temperatures. Snow in this mid-elevation snowpack contributes over 90% of flow in the McKenzie River (Tague and Grant 2004, 2009), and 25% of low flow during the later dry summer months (Jefferson 2008). On September 3rd, dry and hot conditions were such that the fire grew to over 40 km^2 and resulted in the evacuation of the Big Lake Recreation area (St Denis 2012). The primary flora burned were beetle kill snags and a variety of pine, as well as dense fir and hemlock forests. About 50% of the area burned at moderate-to-high burn severity, with near total loss of forest canopy (Gleason 2015).

3.1.4 The 2003 B&B Burn Complex (20-year-old fire)

The B&B complex is the result of a pair of fires ignited by lightning during the summer of 2003 that burned 367.3 km^2. The B&B fires were ignited by lightning following high local temperatures and dry conditions. The fires started as the Booth fire and the Bear Butte fire, which combined to become the mega-fire known today as the B&B fire Complex (Zybach 2011). The storms that started the fires also brought high winds that peaked on August 19th at 19 mph. Starting on the North end of the Mount Jefferson Wilderness, the fire complex burned through the Cascade range for over a month, eventually reaching Mount Washington (Figure 4c, Zybach 2011). The burn sprawled on both sides of Highway 20 through the central Cascades and took down a variety of forest types, from Douglas-fir and western hemlock on the western side of the western cascades to yellow pine and jack pine forests on the eastern side of the crest (Zybach 2011). The B&B Complex burned mostly on federal forest service lands: 93.55 km^2 in the Deschutes national forestland and 11.08 km^2 of Willamette National Forest, as well as 70 km^2 of Mt. Jefferson Wilderness.

There were also 0.33 km^2 Oregon State lands and 15.4 km^2 of Confederated Tribes of Warm Springs lands, and 4.4 km^2 of various private land owners burned within the boundaries of the B&B fire. Thirteen structures were destroyed, and 8 firefighters were injured. The total cost in suppression efforts was over 38.7 million dollars (Deschutes and Ochoco National Forests 2005).

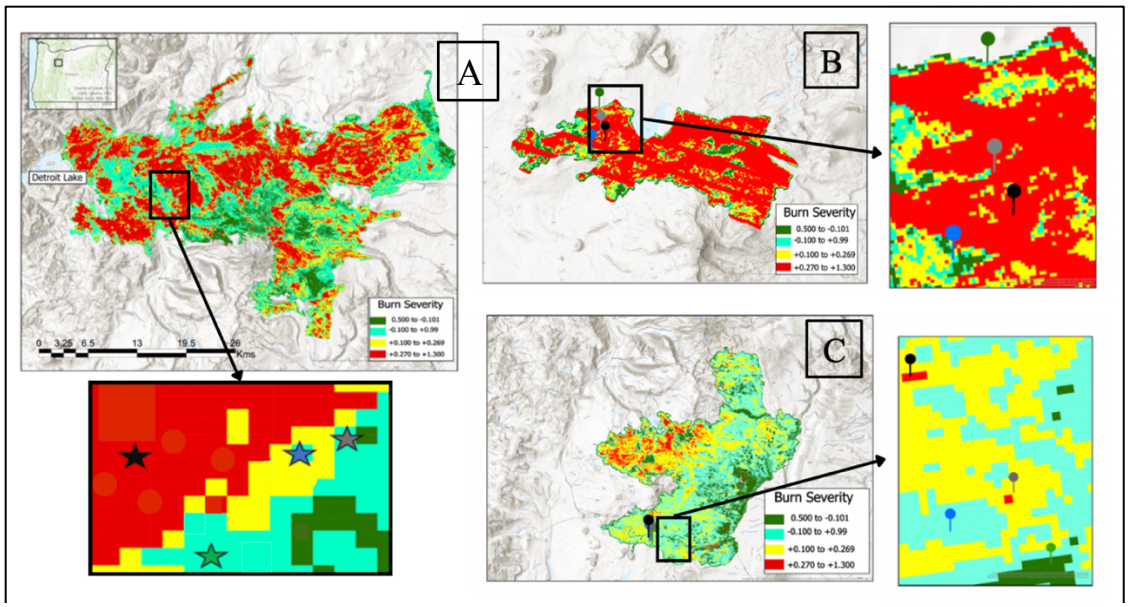

Figure 4: *Distribution of timelapse cameras across all three burn areas, where A is the Lionshead burn area, B is the shadow lake burn area, and C is the B and B burn area. D illustrates a plan view timelapse site setup where three cameras surround the depth staff. Each SWE measurement is taken near the black dot for each snow survey date. E is the profile view of one camera at a site, showing how the timelapse camera captures the entire extent of the pole.*

3.2 Study Design

Study sites were located on the western side of the Central Oregon Cascade Mountain range and selected from three burn areas within the Willamette Watershed. We selected the Lionshead Burn Complex, the Shadow Lake burn area, and the B&B burn complex, since all had burned a portion of the Western Oregon Cascades within the last 20 years.

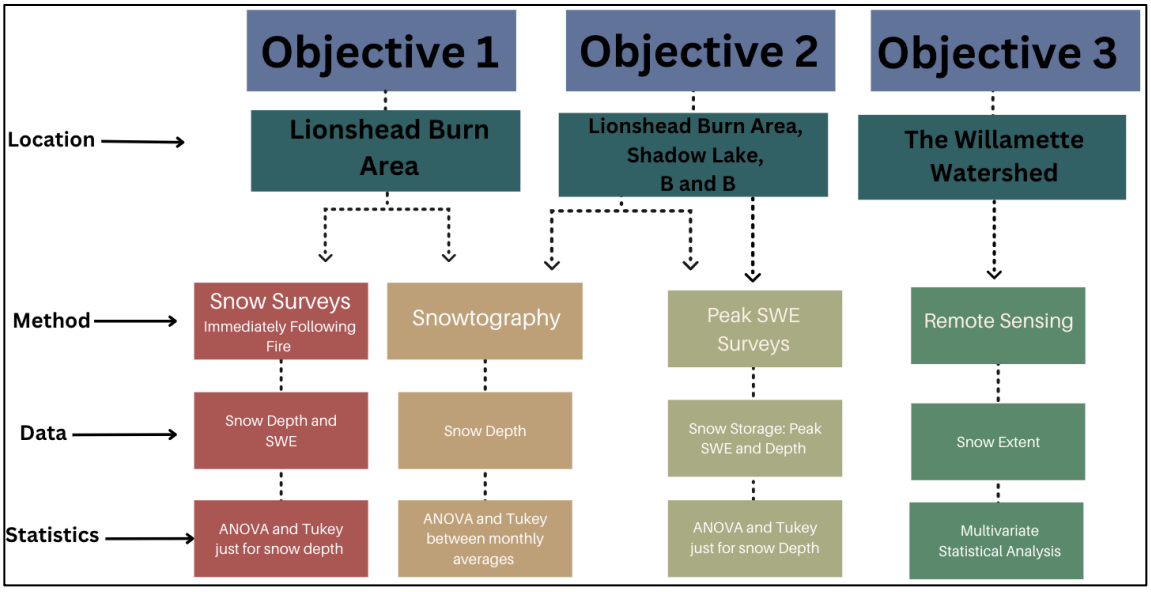

Figure 5: *Flowchart of methodologies and regions utilized throughout the length of study. The Lionshead burn area was used to study fire effects immediately following burn year 1 and year 2 for objective 1. The Shadow Lake and B and B were used to answer objective 2, The Willamette watershed was used to answer objective 3.*

3.2.1 Lionshead: McCoy Site Selection Winter 2021

To quantify immediate post forest fire effects on snowmelt in the western Oregon Cascades we chose site locations within the Lionshead burn area in proximity to the McCoy snow shelter at an elevation of 1350 m (Figure 5). This location served as an ideal field laboratory due to varying burn severities within a localized 1 km zone. Topographic variables (slope and aspect) were kept constant to limit data variability. The moderate topographic complexity near the McCoy site provided choice survey locations with

consistent aspect (SSE) and low slope angles (<20˚). Close proximity along Forest Service road 2233 created accessibility for summer and winter field visits.

Table 1: *Burn severity levels calculated based on the formula for dNBR. A higher value of dNBR indicates more severe damage while areas with negative dNBR may indicates regrowth following fire* (Eidenshink et al. 2007)*, enhanced regrowth was not utilized for this study.*

Severity Level	dNBR Range (Scaled)	Associated Color
Enhanced Regrowth	< -0.100	
Unburned	-0.100 to 0.990	
Low Severity	0.100 to 0.269	
Moderate Severity	0.270 to 0.659	
High Severity	0.660 0.130	

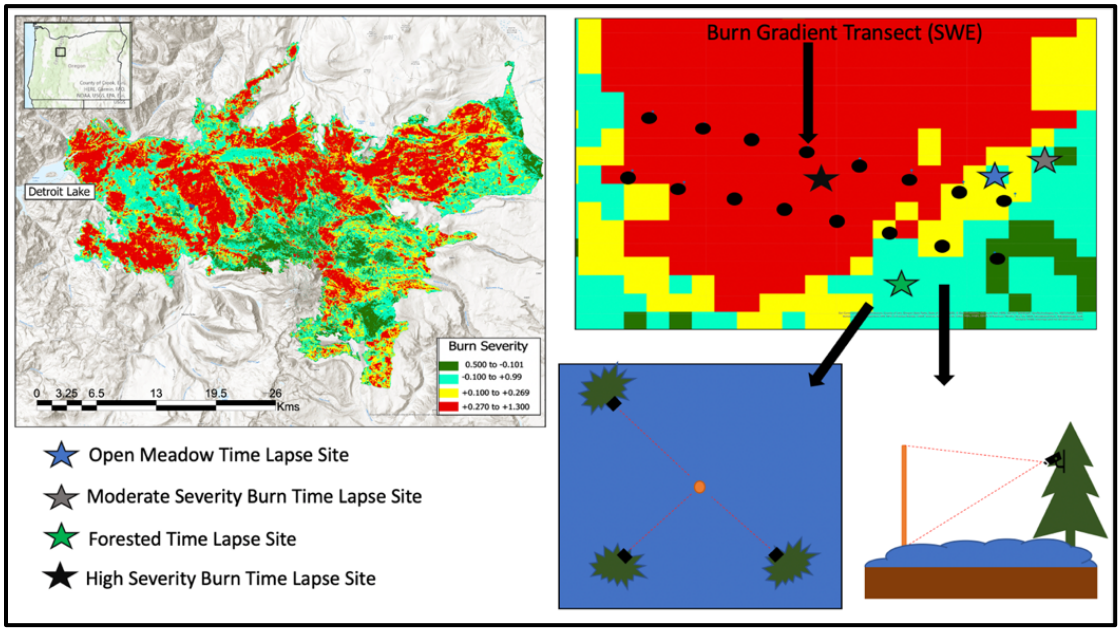

Figure 6: *The 2020 -Lionshead Fire complex perimeter, burn severity scale from -2 to 2, and site, Field set up during the first year of data collection along 2 x 100 m transect along a gradient of burn severities. Pixels are 30x30 meters where aspect was held relatively constant as well as aspect and elevation. B illustrates the field set up for the winter 2021 collection season. Black dots represent SWE measurment locations where snow depth occurred 10 times between each sites. Stars reprsent the location of timelapse imagergery and C and D display the plan and profile view of the cameras sites set up, respectively.*

Site locations with varying burn severity were selected in ArcPro 2.8. The Monitoring Trends in Burn Severity (MTBS) dataset from 1984 – 2019, (Eidenshink et al. 2007) which calculates burn severity from the Differenced Normalized Burn Ratio, (dNBR) was used to estimate locations based on forest burn severity. In the field forest

stands with trees that had been completely burned to their tips and lacked pine needles where characterized as high severity (Figure 7). Moderate severity generally created the border between high severity and unburned forest sites and had primarily burned pine needles lower on the trunk with some green up higher. A mix of completely charred to partially alive trees would be mixed in (Figure 6). Nearby meadows and openings in trees defined our open forest plot and high-density pine trees to define for unburned (Figure 6).

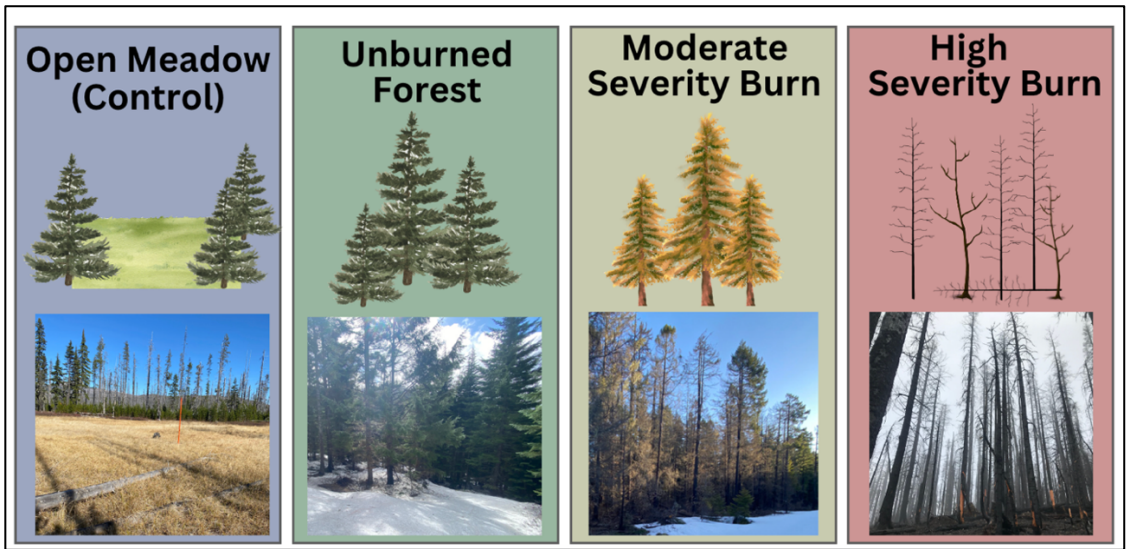

***Figure** 7: Four forest types were evaluated throughout each burn region. High-severity burns remove the forest canopy while in a moderately burned forest remove some canopy, and many trees remain alive. We utilize the open meadow as a control and the unburn forest as a proxy for the pre- fire state.*

3.2.2 Lionshead, Shadow Lake, and B and B Site Selection: Winter 2022

Survey locations differed slightly for the second winter of data collection. The Lionshead sites remained to the west of the McCoy snow shelter at an elevation of 1350m (Figure 7a). To improve site selection from the previous field season, we utilized a variety of open-source spatial datasets (Table 1). A 10m National elevation dataset (NED) was bound within 1300_m and 1500_m so it was restricted to the prime snow zone as defined by Gleason 2017. Site burn severities limited to high or moderate severity utilized the USGS Landsat difference Normalized Burn Ratio (dNBR) product sourced through Monitoring

Trends in Burn Severity (MTBS). The remote sensing product, dNBR, uses land surface reflectance to identify burn areas and quantify burn severity. It indexes canopy reflectance on a scale of -0.5 to 1.3 were healthy vegetation is defined within its lower bounds and severely burned vegetation is within its upper bounds (Table 2 Appendix B, Eidenshink et al. 2007). Aspect and slope angle rasters were created using the associated geoprocessing tools where sites were limited to slope angles less than 20 degrees with constraints set for aspects at south to east orientations.

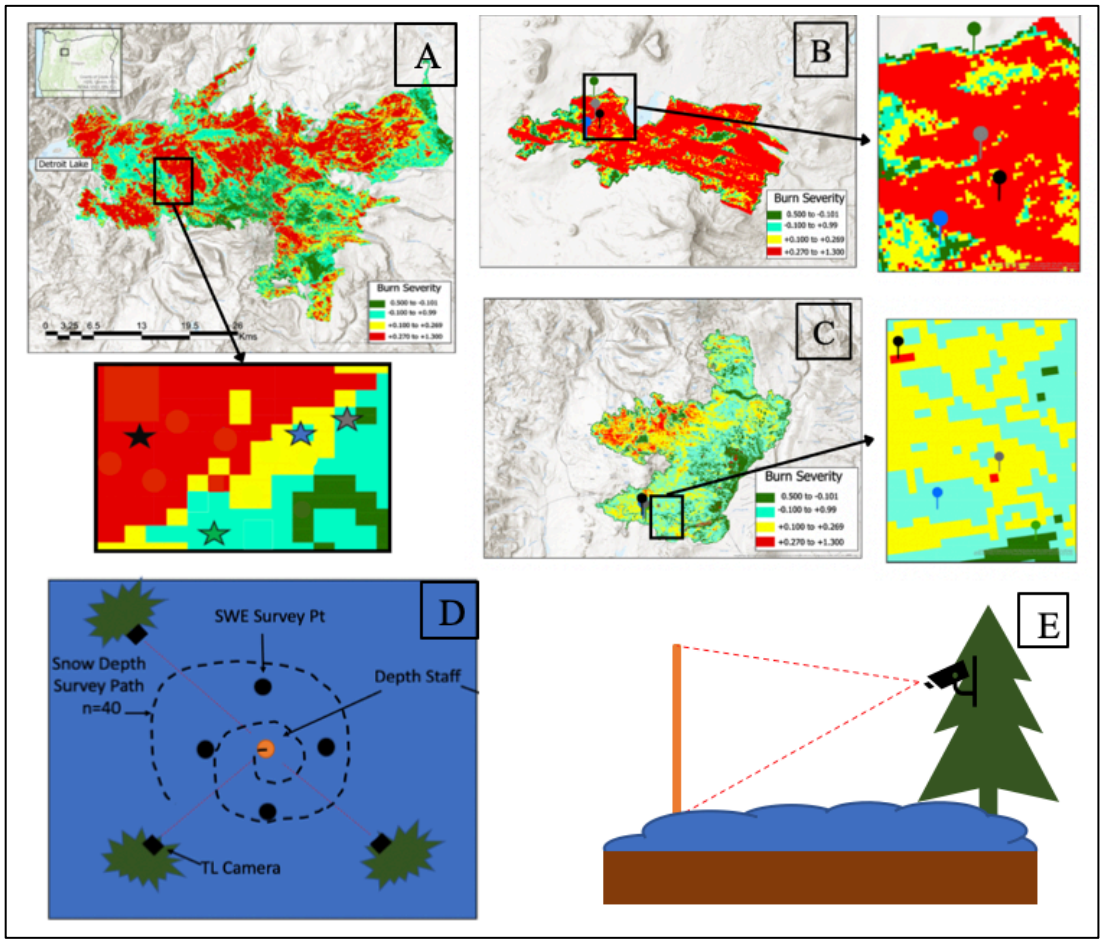

Figure 8: *Distribution of timelapse cameras across all three burn areas, where A is the Lionshead burn area, B is the shadow lake burn area, and C is the B and B burn area. D illustrates a plan view timelapse site setup where three cameras surround the depth staff. Each SWE measurement is taken near the black dot for each snow survey date. E is the profile view of one camera at a site, showing how the timelapse camera captures the entire extent of the pole.*

3.3 Snow Surveys

Objective 1: *Quantify immediate post forest fire effects on snow storage potential and snowmelt using snow course transects in the western Oregon Cascades.*

Snowfall is temporally heterogeneous, empirically derived snow depth and SWE measurements via snow surveys provide reliable information for drawing conclusions concerning snow water content and its potential variability (Lundberg, Granlund, and Gustafsson 2010). Snow water equivalent (SWE) is the most informative variable when measuring snowpack water content (Avanzi et al. 2014; De Michele et al. 2013).

3.3.1 Lionshead Snow Survey Field Methodology Winter 2021 and 2022

We conduct snow surveys the two years following the Lionshead burn to quantify SWE and snow depth accumulation and ablation dynamics relative to forest burn severity and structure (Fig. 6 and 8a). In 2021 we measured SWE along two 800m parallel transects located to the west of the McCoy snow shelter (Fig.5). SWE was measured 16 times per field day spread out every 100 meters along the transects and snow depth measurements were taken every 10 meters along each transect (between SWE measurement sites). Snow course surveys were conducted using a Federal Sampler, a tool used widely by the NRCS snow survey and water supply forecasting system. An Avalanche Probe in centimeters was used to collect snow depth. Snow Surveys were performed once monthly during the accumulation period (January 1st, February 1st, and March 1st) and following the start of ablation (April 1st) we performed bi-weekly surveys within 4-5 days of April 1st and 15th and May 1st and 15th, exact dates of field visits were dependent on timing and weather. These measurements were used to capture point-based accumulation and ablation response of snow immediately post-fire and relate canopy structure to burn severity and thus SWE and snow depth.

SWE surveys the winter of 2022 continued to be located to the west of the McCoy snow shelter (Figure 8a) but the transect method was retired and instead SWE was taken 4 times at each time-lapse camera location. It was advantageous to plot in-situ SWE and snow depth at these locations as coincident time series snow depth retrieved from the time-lapse photography could be validated. Four SWE measurements were taken at each site two meters away from the snow stake at its cardinal directions (N, E, S, and W, Figure 8d). In-situ snow depth was measured 40 times with an avalanche probe spiraling away from the snow stake (Figure 8d). Measurements would start approximately one meter from the staff moving slightly outward with every new measurement. The 2022 field season's measurements started within the first week of February and were taken every two weeks after the start of ablation (April 1st), with a focus on ablation characteristics such as snow storage potential (peak SWE), snow melt rate, and snow disappearance date.

3.3.2 Snow Survey Statistics

With varying burn severities, the magnitude of snow depth designated by burn class was tested immediately following fire. To test the significance of hypothesis 1 and 2 we used snow depth as it provided a large enough sample size for useful snow survey measurements ($n = 40$). Additionally, the mean and standard deviation of each burn severity type for each collection date was calculated. Most relationships in the dataset achieved normality in January, February, March, and April. Though a smaller sample size and the decline of snow depth created skew in the data for the month of May. To evaluate the results of the ANOVA test, we used the post-hoc Tukey's Honestly Significant Difference (HSD) to analyze each comparison separately.

3.4 Snowtography

Objective 2: *Characterize recovery over time of post forest fire effects on snow storage and snowmelt using continuous in-situ snow time-lapse photography and peak SWE surveys in a 2-year old, 10-year old, and 20-year old burned forest relative to high severity, moderate severity, unburned and open areas using time-lapse photography and snow stakes in western Oregon cascades.*

3.4.1 Study Design and Site Installation

We used time-lapse photography to characterize continuous in-situ snow depth during a winter season as a function of forest recovery (Figure 8). We measured snowpack in zones immediately following fire (winter 2021) and in 2-year old, 10-year old, and 20-year old burned forests (winter 2022). At each burn area we established 4 sites consisting of one snow stake and three cameras within high and moderate severity groves in addition to unburned forest and open meadow. In December of 2020 we deployed 12 cameras through the 4 different forest and burn classes within the Lionshead burn area. The following year, we installed a similar set of cameras in the Shadow Lake Fire and the B&B burn area in addition to the Lionshead burn area in October of 2022.

We used Wingscape's Moultrie Time-lapse Cam Pro, a consumer-grade weather-proof outdoor time-lapse camera equipped with a 20-megapixel 2-in TFT. The cameras were tightly harnessed to surrounding trees and programmed to capture an image every 2-hours starting at 8:00 am and ending at 4:00 pm from October to June. Each site had three cameras to ensure data preservation during harsh winter conditions. Hourly images were stored on internal 96 MB SD cards. When placing cameras, we considered and limited surrounding canopy that could cause photo interference, considering branch movement with a snow load mid-winter so that line of site was not obscured. The time-lapse cameras were set up with direct line of site to 10-foot PVC pipes as snow stakes. To provide maximum contrast with the surrounding environment the PVC was wrapped in neon orange

tape and gradually at one-meter intervals for depth validation place holders. The PVC pipes were set through t-posts a-foot into the ground to ensure limited movement through harsh winter conditions (Figure 9).

Figure 9: *View of each snow depth staff taken from time-lapse camera near peak snow depth. Far left is snow immediately following the burn within the Lionshead burn region, center are the sites 15 years following burn, far right are the sites of the 20 year post burn B and B fire. A or the top photos are forested regions, B are open regions, C are high severity burn regions and, D are Moderately burned.*

3.4.2 Semi-Automated Retrieval of Snow Depth

Camera images where analyzed to derive snow depth. To achieve this, we refined remote sensing methodologies to develop an R-based tool that extracts snow depth from time-lapse imagery. The retrieval procedure of snow depth is articulated in the following steps:

1) Subset photos based on time step: the time of day from which the photo is retrieved is reduced to one per day for the best balance of low processing time and high temporal resolution. We selected the photos taken at 14:00 as they had the best light contrast between the snow stake, the snow, and the background terrain (Figure10a).

2) ROI Identification: starting from an image without snow cover, we selected a region of interest by drawing a polygon, which defined a quadrilateral around the snow stake. This allowed the pixel clipping algorithm to consider only pixels inside of clip, helping to cut out background noise and further limit processing time. A new ROI was defined every 10 days to keep up with variations in fine snow deposition and melt events. Re-defining the ROI provided a suitable interval to keep processing time tractable and contour accuracy high (Figure10a).

3) Run as a batch analysis through image processing algorithm a routine used to load and analyze each set of camera images through the image processing algorithm helped to cluster pole pixels away from other pixels. The process defined in figure 10b shows the applications of an orange filter to the base image to brighten the orange pixels. The image is then inverted which makes the bright orange images dark. A grey scale then separates black pixels from the colored and a transformation is applied to the separated pixels diverging all other pixel properties to a value of 0 or 1. Finally, k-means clustering groups pixels with similar means together. Images taken in fog, intense snowfall, and at night caused errors and were discarded. Polar was run three times for every camera to fill in gaps and increase the robustness of snow depth derivations.

4) Algorithm Edge Detection To define the height of the visible pole the cropped image based on the pre-defined ROI has a contour applied to like pixels. The contour edges select

the top x contours where x varies with the height of ROI. The contours are then applied to the original base image where by the y-max and y-min can be defined (Figure 10c).

5) Retrieving Pixel Height to Convert to Snow Depth The depth of the snow stakes as pixel depth was derived from the ROI contour of the pole. To extract the number of pixels of the depth staff covered by snow, the number of pixels of the entire stake were read from the image and verified (Hs). The height of pixels of the pole with snow on (Hn) was subtracted from the height of the pixels with snow off:

$$Hs - Hn = Hp\ [no.of\ pixels]. \qquad \text{(Equation 1)}$$

Where Hp is snow depth derived from the number of pixels within the snow depth. The number of pixels is converted into a snow depth in meters, multiplying by the ratio between the real snow stake length (Ls) in meters and the number of pixels of the whole stake (Hp):

$$SD = \left(\frac{Ls}{Hp}\right)(m) \qquad \text{(Equation 2)}$$

m is the height of the snow pole in meters. We used a conversion factor for the accumulation period and peak SWE period (Fig.6c). This experiment produced a snow disappearance date (SDD) and peak snow depth (PSD) for each forest type. Snow ablation rates were calculated taking the maximum snow depth and dividing it by the number of pixels identified for the entire pole. Snow disappearance was recorded beneath the snow stakes.

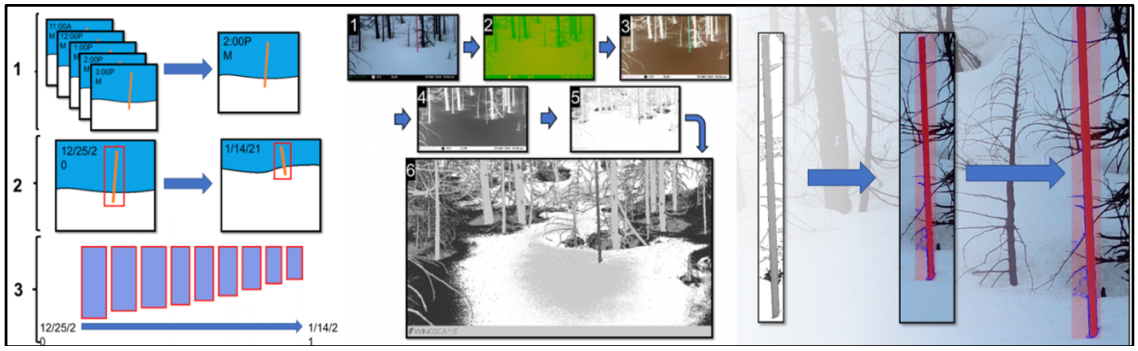

Figure 10 *PoleR workflow snow depth retrieval procedure from time-lapse imagery. Adapted by Anton Surunis. Starting from the left the program subsets photos based on time step 2) it asks for a defined region of interest 3) a new region of interest is defined every 10 steps or to whatever the user believe is best. In the middle the program runs the selected image ROIs as a batch analysis through the image processing algorithm. On the program runs through an edge detection and 6) finally the pixel height is received and can then be converted to a snow depth.*

3.4.3 Snowtography Statistics

The mean and standard deviation of all snow depths were calculated for each month and split between severity treatments to evaluate mean snow depth per treatment per month during the ablation period. The overall treatment effect was tested using a one-way analysis of the variance (ANOVA). Having received significant results via the ANOVA test ($p<0.05$), a Tukey's Honestly Significant Difference (HSD) test was used to simultaneously compare all pairwise treatment relationships and identify relationship with significance. With varying burn regions, our second year we tested the magnitude of the treatment effect for differences in snow depth within each burn region using the interactions between the four varying forest blocks at one time period. Prior to testing the sample-level data we accounted for spatial autocorrelation by randomly subsampling snow depth and its associated data from each month and treatment block. The data was partitioned to be randomly sampled and statistically evaluated. We calculated the mean and standard deviation for the entire winter within each burn area and then the mean and standard deviation of each burn severity type. Additionally, further summary statistics are provided to fully interpret the skew of the dataset. Homogeneity was assessed by looking

at the distribution of the dataset displayed on a histogram plot and looking for the bell-shaped curve, as well as the Shapiro Wilks normality test where a value greater than 0.05 indicated a normal distribution (Tables 3 Appendix C). To avoid pseudo-replication, we averaged all measurements within a treatment month. Differences in snow-depth for each forest burn severity class were analyzed using a one-way analysis of the variance (ANOVA), followed by Tukey's Honestly Significant Difference (HSD) for the test in which the true variance in the data could be explored.

3.5 Remote Sensing Analysis

Objective 3: *Evaluate the Spatial Variability of Snow Cover Area Relative to Recovery of Forest Fire Effects on Snow Covered Area*

3.5.1 Experimental Design

Expanding the spatial extent of our study area allowed us to study the spatial variability in snow cover area relative to the recovery of forest post wildfire. Our approach utilized a variety of satellite derived remote sensing products and spatial analysis. We developed a masked combination of Landsat08 datasets at a 30 m spatial resolution. We compared snow cover area in high severity burn forests and open areas as a control to evaluate these effects. The temporal discrepancies through a chronosequence of 23 burns and adjacent open areas were used to determine snow extent characteristics in the burn areas representative of open areas as fire rehabilitation occurs. Two snow cover area masks were developed: the first mask solely reflected snow cover which overlapped dNBR high severity burn designations and the second isolated snow cover of Oregon Statewide Habitat Maps, derived via open vegetation regimes.

Table 2 *Relevant remote sensing products and course information used throughout the study.*

Data Type	*Data Source*	*Resolution*	*Features*
Burn Perimeter and Severity	Relative Normalized difference burn ratio (RnDBR) and burn perimeters from MTBS (Eidenshink et al. 2007)	30 m	MTBS forest fires burn perimeters and burn severity scaling post -fire change to forest landscape (1984 – 2020)
Landcover Class	National Land Cover Data Set (NLCD) (Collin Homer, Joyce A. Fry, and Christopher A. Barnes 2012)	30 m	NLCD 2022 used to classify landcover
Hydrologic Unit Boundaries	Oregon Watershed Boundary Dataset -Hydrologic Unit Boundaries (Niknami 2012)	Polygon	Comprehensive base-line drainage data that delineates the extent of surface water drainage
Prism 30 Year Normal Precipitation and Temperature	PRISM Climate Group – Northwest Alliance for Computational Science and Engineering (Oregon State University data created 4 Feb 2014, accessed 16 Dec 2020. 2014)	800 m	Average monthly and annual precipitation and temperature conditions over the most recent three full decades
Fractional Snow Cover Area	UGSG Landsat Fractional Snow Cover Area Science Products (Selkowitz, Painter, and Rittger 2017)	30 m	Landsat 8 fSCA used to detect snow cover duration and persistence variations
Oregon Statewide Habitat Map	Oregon Biodiversity Information Center and Oregon Department of Fish and Wildlife (Jimmy Kagan, Kyla Zaret, Joe Bernert and Emilie Henderson 2018)	30 m	Spatial origin of 77 habitat types 2018
Vegetation Height	Existing Vegetation Height LANDFIRE (“Existing Vegetation Height” 2022)	30 m	Existing Vegetation Height (EVH) representing the average height of the dominant vegetation
Canopy Bulk Density	LANDFIRE’s (LF) Forest Canopy Bulk Density (“Existing Vegetation Height” 2022)	30 m	Describes the density of available canopy fuel in a stand defined by the mass of available canopy

3.5.2 Bounding the Study Area

Of the 23 wildfire boundaries and 6 snow cover area maps few would extend beyond our region of interest, therefore the Willamette watershed boundary perimeter placed over the burn mosaic raster dataset would constrain all study areas to the west side of the Cascade

Range (Figure 3a). To bound input raster datasets we utilized the Oregon Watershed Boundary Dataset Hydrologic Unit Boundaries HUC 4 watershed perimeter map within the Oregon Spatial Data Library (Niknami 2012). By constraining all studies to this region, we assumed that all weather, temperature, and ecological regimes within each fire boundary were comparable. Spatial datasets were re-projected to a UTM Zone 10 N based coordinate system.

3.5.3 Development of Snow Cover Area Masks

We examined fractional snow cover area (FSCA) extent through the winter of 2021 within a week of our field reported snow survey dates (Figure 10). Imagery downloaded through the USGS Earth Explorer on March 1st, 13th, and 28th, April 15th, May 1st and 18th, as well as June 1st were selected based on cloud cover being less than 10%. Fractional snow cover area, a USGS algorithm developed to classify factional snow cover of a 30 m^2 cell as a percentage (Selkowitz 2017), designated pixels with 50% snow cover area and greater. The resulting snow cover was restricted to the bulk snow zone, defined between 1300 to 1500m in elevation (Gleason 2017) utilizing the ArcPro 2.8 Live Atlas 30m DEM (ESRI 2022).

3.5.4 Development of High Severity Burn Masks

Burn severity datasets secured through MTBS from burn years between 2020 and 1988, the same data set used to determine site locations in the above methodology, were mosaiced. The fires ranged in size, age, and burn severity extent; however, we limited our evaluation of burn areas to high severity burned forests under the assumption that lower severity burn areas would produce errors due to canopy interference. High severity burned regions were defined as being an dNBR index reading of 0.66 and higher (Table 1) were isolated through reclassification. The fires ranged in size, age, and burn severity extent.

3.5.5 Development of Snow Cover Area Within High Severity Burn Regions and Open Meadows Within 5 km Buffer

FSCA were mosaiced and reclassified, transforming the continuous measure of snow cover into a binary snow on/snow off raster. This half snow-on classification was used to build both the open meadow snow cover area within the buffer as well as snow extent masks in high severity zones (Figure 11a). Following, was the intersection of a snow extent raster by the high severity burn raster confined to snow extent to corresponding burn regions (Figure11b). Five more iterations were run for every snow cover area date collected. The output would result in a pixel count of snow cover area for each burn area and for each collection date.

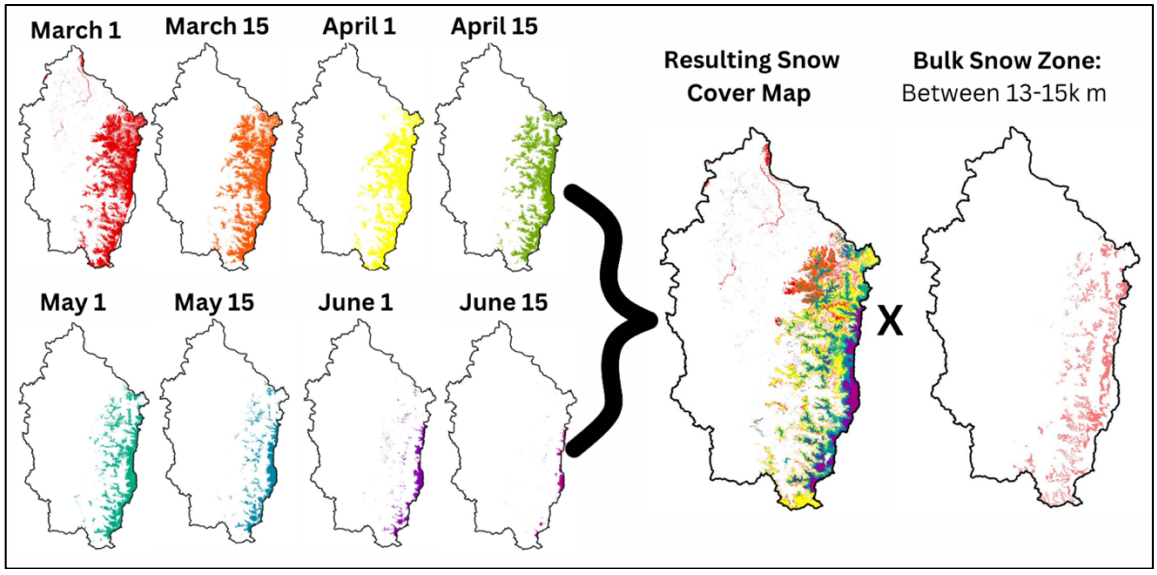

Figure 11 *Snow cover area work flow derived via the landSAT fractional snow cover area product. Each image was selected through the winter of 202, within a week of snow survey dates. Imagery downloaded through the USGS Earth Explorer were selected based on less than 10% cloud cover. FSCA were mosaiced and reclassified, transforming the continuous measure of snow cover into a binary snow on/snow off raster. Where values with greater than 50% snow cover were considered snow on and otherwise were considered snow off. The resulting snow cover was restricted to the bulk snow zone, defined between 1300 to 1500m in elevation (left).*

A 5 km buffer was drawn outside the burn perimeter to evaluate open areas as controls and account for interannual variability of snow cover relative to forest fire recovery (Figure 11a). Oregon Statewide Habitat area and landcover data was used to

categorize each land cover type as either “No Data” or open meadow. Land cover area classified as sagebrush, shrubland, barren, herbaceous, planted/ cultivated, and grasslands where all considered open. While “No Data” were defined as deciduous, mixed, or coniferous, essentially forested areas with the potential of canopy obstructing the fSCA view. The new land surface mask would intersect one of the 6 independent snow cover area masks producing a map of snow extent within the open areas for that time step (Figure 11a). This would be repeated 5 more times to get a capture of snow cover area for each date of fSCA data collection.

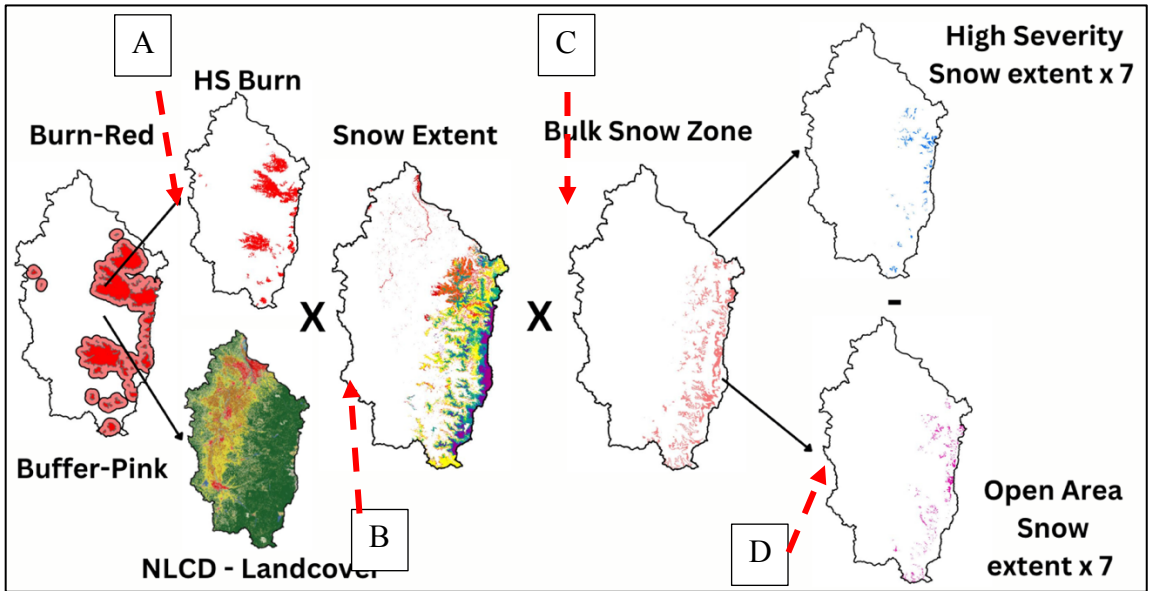

Figure 12 *To evaluate snow extent differences between HS burn areas and open a 5 km buffer was drawn outside the burn perimeter shape fire to evaluate open areas which were defined using the NLCD land cover (A). MTBS's high severity burn area maps were used to define burn areas within our regions of interest (B). The new land surface mask would intersect one of the 6 independent snow cover area masks producing 7 maps of snow extent within the open areas(C) and high severity regions for that each time step (C). The data was constrained to the bulk snow zone where the area of the HS region was subtracted by the open (D). The data was then normalized by the maximum snow extent and then by forest fire area.*

3.5.6 Data Analysis and Normalization

A bi-weekly pixel count of snow cover during the 2021 ablation period resulted in 12 datasets that satisfied all above criteria for each time step. “Snow on” pixel counts within high severity burn areas were compared against the “snow on” within the defined open

meadows of the buffer region (Figure 12). Specific to date of collection, fire pixels were divided by their highest potential snow extent, defined as the maximum number of "snow on" pixels that could be collected within an independent burn region. Under the assumption that "highest potential snow extent" is the maximum amount of snow cover that could be experienced in this burn zone throughout the winter season. We can assign a quantity to the maximum amount of snow cover pixels that can be derived within that burn. Additionally, the proportion of a given snow cover pixel count for a timestep to the maximum snow cover pixel count needed to be considered as each of these proportions was distinct to that particular fire area. Differing high severity burn proportions had to be considered in order to normalize for differing open to burn proportions.

The same process was repeated with snow extent in the buffered regions. Snow extent normalized by total possible snow within the burn region was subtracted by the same ratio in the open meadows for the corresponding fire and time. The ratio of the total burn to total area of the buffer was multiplied by differenced snow extent to normalize snow cover by burned area included in the analysis. In depth steps explained below.

1) Find Highest Potential Snow Extent Pixel Count for each burn area **(PSnb and PSno)** and corresponding open area in buffer: **PS_{bmax} & PS_{omax}**
2) Divide specific date pixel count by the maximum potential snow extent for all open and burn pixel counts to get: ratio of pixel date/ratio pixel total potential **(PS_{nb}/ PS_{bmax})=S_{nb} and (PS_{nb}/ PS_{omax})= S_{no}** – where n is the time-step to each ratio
3) Subtract **S_{nb} - S_{no} = S_n -- Difference of snow extent in burn to snow extent in open**
4) Divide the total count of all snow covered burn pixels for each fire by the corresponding snow-covered open pixels **(PC_b/PC_o)**

a. Gives the ratio of total burn pixels to ratio of open pixels **Pt**

5) Multiply $\mathbf{S_n}$ x **Pt** to normalize the area of snow extent by the ratio of burn pixels to open pixels
6) Average each fire for each year

3.5.7 Multivariate Statistical Analysis

To synthesize the broad scale spatial ablation for the Willamette watershed, we begin by explaining the data preparation methodology to distill the collection of biweekly images within the season of 2021 into the essential information, then develop the PCA model, explain how to apply the model to an image and, finally describe how to assess the spatial accuracy of the model (Figure 13).

In order to identify the factors or sources which were responsible for snow disappearance date relative to forest fire recovery variations in our remote sensing data, PCA was applied (R Core Team 2023). PCA is a data reduction method commonly used in remote sensing that linearly rotates and scales a data matrix. The *D* vectors which comprise the *D* matrix each contain a large amount of redundant or correlated information with respect to the other *D* vectors, as well as information which only appears in a few of the vectors and some information unique to individual vectors. PCA reorganizes this information into a collection of new vectors each of which is orthogonal to or uncorrelated with the others.

To assess different environmental drivers of snow disappearance with regard to forest fire recovery, we compared all variables using principal component analysis (PCA) to reduce dimensionality of highly correlated explanatory variables. First, all variables were scaled before conducting PCA and all NA values omitted and centered around the mean. The number of principal components with eigenvalues greater than one explained

little less than 80 percent of the total variance (Kanyongo 2005). We then used the broken stick model for retaining principal components (Jackson 1993). The model retains components that explain more variance than randomness. The goal being to capture as much variance in the data with as few dimensions as possible. After performing PCA we picked the top number of features that contain the most variance, which reduces dimensionality and keeps the highest amount of information.

To further parse out noise or identify key relationships that might develop with a large, wide reaching spatial dataset, we used a decision tree-based framework since the dataset is too complex for linear regression alone. PCA is applied before a Decision tree, as it explicitly transforms the dataset to highlight the directions that have the highest variance, which often have the highest amount of information. Decision tree analysis uses a machine learning algorithm to build a tree-like classification structure and regression model to identify a set of characteristics that can best differentiate between individual classes base on a categorical feature variable. It has proven to be a very useful and efficient technique to process remote sensing data (Yang 2017). Fitting a decision tree will highlight major variables contributing to snow disappearance in burn forests including both continuous and discrete measurements. An R based package "rpart" or recursive partition and regression trees was used to develop the decision tree (Archer 2010). Making the decision tree achiever high accuracy within the least number of decisions layers, we discarded 3 variables (aspect, slope angle, and canopy bulk density) as they had little to no influence on the variance of PC1 (Appendix B). PC1 was the only PC kept, because only the first observed proportion of variance was higher than the corresponding broken-stick proportion (Appendix B - Figure 24). This tree explains the variations of the single

response variable snow disappearance date (SDD) by repeatedly splitting the data into more homogeneous groups.

A simple rule, in our case an ANOVA, is responsible for repeatedly splitting on a single explanatory variable. At each split, the data is partitioned into two mutually exclusive groups. The categorical variables all have greater than 2 levels, so any combination of levels can be used to form a split. For the numeric explanatory variables, the split is defined by values less than, and greater than some chosen value. Thus, only the rank order of numeric variables determines the split, and for "u" unique values, "u"-1 possible splits. From all the possible splits, the one that maximizes the homogeneity of the two resulting groups will be selected.

Following the production of the model, the tree was represented graphically (Appendix B). The root nodes represent the original data at the top, the branches split the groups and the leaves represent one of the final groups. At the bottom most leaves, the samples size and snow disappearance date described by Julian days are displayed. The number of splits will increase until they reach a plateau indicating that further splits will not improve the model's predictive power.

To prune the decision tree cross validation was utilized to help select the proper tree size and obtain honest estimates of true (prediction) error for the trees (Gordon 1984). A separate methodology was utilized to prune the decision tree where the final model was generated using the lowest cross-validation predictive error instead of an ANOVA (Cp, Appendix B). Cp values are plotted against a random subset of half of dataset used to calculate geometric mean to depict the deviation (Appendix B). The final pruned decision tree was generated.

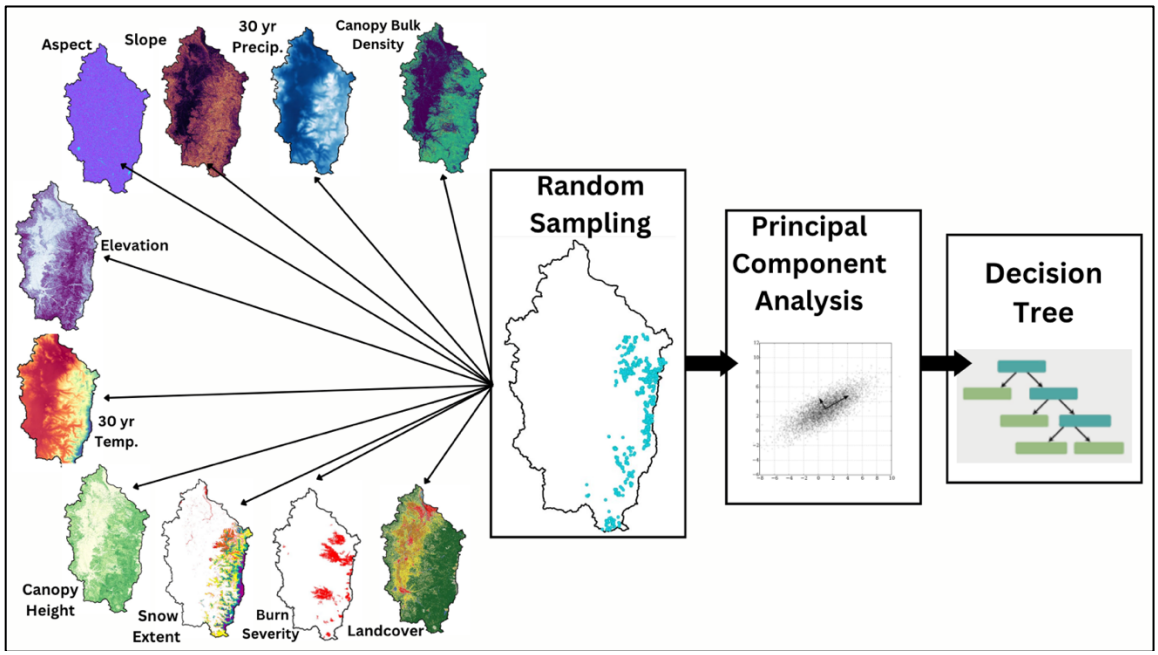

Figure 13 *To identify the factors responsible for snow disappearance relative to forest fire recovery all environmental spatial datasets where overlaid and 500 random points where chosen over the defined high severity burn are within the bulk snow zone. All information for environmental variables were derived with these points. A Principal Component Analysis (PCA) was applied, the multivariate statistical data reduction method, linearly rotates and scales a data matrix and reduces noise in a dataset. The PCA was applied before a Decision Tree, to parse out variables with little influence to the variance of the data. The remaining variables were applied to the analysis of the decision tree.*

4.0 RESULTS

4.1 Immediate post forest fire effects on snow storage and snowmelt (1 year following fire 2021)

Objective 1: *Quantify immediate post forest fire effects on snow storage potential and snowmelt using snow course transects in the western Oregon Cascades.*

4.1.1 Snow Accumulation

The first year following fire, more snow accumulated in the burned forest and open areas, than in the unburned forest mid-winter. Snow depth within the high and moderate severity burned areas (mean= 130.62cm, SD =25.87cm, Figure 14b) was like the nearby open meadows, (mean = 127.70cm, SD = 24.10cm) and was greater than snow depth in unburned areas (mean = 72.00cm, SD = 22.53cm, $p<0.05$). Less SWE accumulated in the high and moderate severity burned area (mean = 32.00cm, SD =12.50cm) than in the open areas (SWE = 41.00cm, SD = 4.94cm) through the month of January (Figure 14a). Average snow depth (snow depth = 149.00cm, SD = 12.03cm) and SWE (SWE = 27.50cm, SD = 1.76cm) in the open areas exceeded those of the burned forest (snow depth = 127.23cm, SD = 37.30cm, SWE = 20.50cm, SD = 7.85cm) for the beginning of February (Figure 14 a&b, $p<0.05$).

4.1.2 Snow Storage

The most snow accumulated in the open areas, but more snow accumulated in the burned forest compared to the unburned forest during peak SWE in March. SWE (Mean = 50.30cm, SD = 7.25cm) and snow depth (Mean=224.96cm, SD =48.96cm) in burned regions were similar to open meadows. On the March 2nd snow survey, (Figure 14a&b) average SWE and snow depth were highest in the open meadow and burn (Depth=252.08cm, SD = 30.94cm; SWE = 50.03cm, SD=7.25cm) and close in the burned areas (Depth = 224.96 cm, SD =48.96cm, SWE=44.50cm, SD= 13.41), where average

SWE and snow depth were 12% and 10% greater, respectively. Mean SWE in the burned area was 15% higher than in the forested areas (SWE = 30.50cm, SD =4.52) and snow depth (Depth =213.77cm, SD =44.55cm) was 5% higher in the burn relative to the forest. Snow remained the highest in open areas through the month of March, only losing 3 cm of SWE by the April 1st SWE survey date (SWE = 48.00cm, SD =10.15cm). At this point SWE was 16% greater in the open than the burned areas, (SWE= 40.03cm, SD =15.32cm) though the difference was not significant. Snow in the forest had the lowest mid-winter snow retention potential, losing 13 cm of SWE during the month of march (SWE = 20.06cm, SD = 20.64cm) and only being 50% of the mean SWE at the burned site ($p<0.05$). Snow melt was faster in the burned areas during the ablation period then during the midwinter melt event.

4.1.3 Snow Ablation

Snow melt was faster in the burn region compared to the open meadow with advanced melt moving toward an earlier snow disappearance date, though these dates were not captured. Snow melt was faster in the burned areas during the ablation period then during the midwinter melt event. The difference in snow depth was not significant between the burned (Depth = 154.34cm, SD=68.46cm) and forested areas (Depth =150.05cm, SD =49.59cm). By April 20th, SWE had declined by almost half in the burn area, (SWE =25.26cm, SD =14.16cm) while the open area only lost 8 cm of SWE, or 16% of its original value (SWE =40.01cm, SD = 5.48cm). Because more snow accumulated in the burned forest but melting earlier in spring, snow depth of both the burned forest and unburned forest was similar at the April 15th survey.

Late spring snowpack persists longer in the open areas the first year following. On May 4th, snow depth was 30% higher in the forest (Depth = 87.94cm, SD=52.18cm) than the burn area, (Depth= 65.34cm, SD =56.53) and snow depth in the burn and open regions were significantly different ($p<0.05$). On the final survey date (May 17th) snow was absent from most burned sites but persisted in the open meadow (Depth =20.91cm, SD =21.73cm) and in some forested areas (Depth = 21.22cm, SD = 33.87cm). SWE was almost 500% greater in the open area than the burned and forested areas on the final collection date, though this might be a product of poor ability to collect SWE in the federal sampler with such low snow volumes.

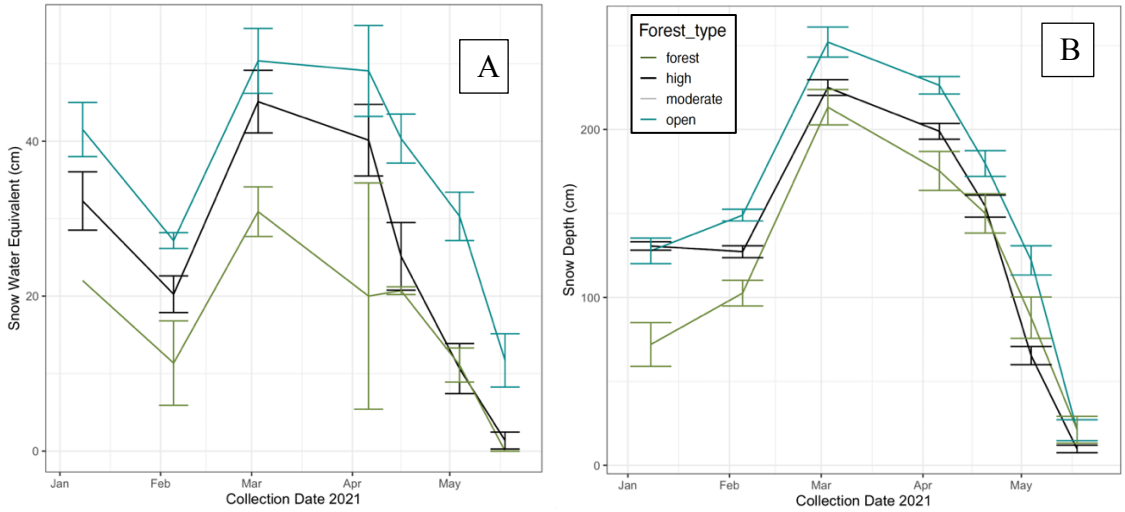

Figure 14: *Snow Survey Results through the 2021 Lionshead survey year. Plot A is average SWE (cm) and plot B is Average snow depth (cm), the error bars represent standard error in the dataset.*

Table 3: *Lionshead Snow Survey 2021 mean and standard deviation of snow depth and SWE by collection date and forest type.*

Date	Severity	Mean Snow Depth (Cm)	Sd Snow Depth (Cm)	MEAN SWE (CM)	SD SWE (CM)	P-ADJ Tukey
JAN-8	burned	130.62	25.87	32.0	12.49	opn-brn p=0.93
	open	127.70	24.08	41.0	4.94	unb-brn p<0.05**
	unburned	72.00	22.53	21.25	-	unb-opn p<0.05**
FEB-8	burned	127.23	37.30	20.50	7385	opn-brn p=0.11
	open	149.00	12.03	27.50	1.76	unb-brn p=0.01
	unburned	102.55	32.43	16.50	7.70	unb-opn p<0.05**
MAR-3	burned	224.96	48.96	44.50	13.41	opn-brn p=0.14
	open	252.08	30.94	50.30	7.25	unb-brn p=0.59
	unburned	213.277	44.55	30.50	4.52	unb-opn p<0.05**
APR-6	burned	198.93	49.26	40.03	15.32	opn-brn p=0.14
	open	226.33	18.46	48.00	10.15	unb-brn p<0.01
	unburned	175.33	49.23	20.06	20.64	unb-opn p<0.05**
APR-20	burned	154.34	68.46	25.26	14.15	opn-brn p=0.39
	open	179.75	26.57	40.01	5.48	unb-brn p<0.96
	unburned	150.05	49.59	21.00	0.71	unb-opn p<0.43
MAY-4	burned	65.34	56.53	12.00	10.70	opn-brn p<0.05**
	open	122.08	30.16	32.01	5.39	unb-brn p=0.23
	unburned	87.94	52.18	13.02	3.11	unb-opn p=0.21
MAY-18	burned	9.75	23.66	2.03	3.6	opn-brn p=0.31
	open	20.91	21.73	14.05	5.9	unb-brn p=0.17
	unburned	21.22	33.87	0.00	0	unb-opn p=0.99

4.2 Immediate Post Forest Fire Effects on Snow Storage and Snowmelt (2 Years Following Fire 2022)

4.2.1 Snow Accumulation

The second year following fire, snow depth was similar in high and moderate severity burned forests and lower than the open areas midwinter, which was significantly higher than the forested region (Figure 15, $p<0.05$). Average SWE in both burn regions (SWE_H = 30.16cm, SD_H = 6.72cm, SWE_M = 29.13cm, SD_M = 6.98cm) was 16% higher than SWE in the open region (SWE = 24.85cm, SD = 19.93cm, Figure 15a). Snow depth in February was lower in both burn areas ($Depth_H$ = 136.10cm, SD = 24.14cm, $Depth_M$= 136.32cm, SD = 27.01cm) than in the open areas (snow depth = 147.13 cm, SD = 21.00cm) and open had 9% greater snow depth than the burn (Figure 15b) though these differences were not significant.

4.2.2 Snow Storage

The second year following fire, 2022, snowpack accumulation was bimodal with peaks after the start of March and the second in mid-April, were peak SWE (early March) was greater in the burned forest and open areas than the unburned forest at both peaks. Accumulated SWE values in the open areas (SWE = 67.33cm, SD =4.16cm) surpassed the burn areas (SWE_H = 54.00cm, SD 5.36cm, SWE_M=) by 25%. Concurrently, snow depth was significantly different between the burn areas ($P<0.05$, snow $depth_H$ = 101.57cm, SD =24.92cm, snow $depth_M$ = 113.61, SD = 20.80cm) and the open sites (snow depth=138.25cm, SD=20.80cm, $p<0.05$). SWE was 43% lower and significantly different ($p<0.05$) in the forest (SWE = 86.96cm, SD = 34.19cm) compared to the average of all other sites (Figure 15a).

4.2.3 Snow Ablation

In the second year following fire, snow melted faster in the burned forest than the open area, while snow disappearance date occurred earliest in the burned and unburned forest but persisted into spring in the open area. Snow depth in the burned areas ($Depth_H$ = 79.21cm, SD = 10.67cm, $Depth_M$ = 82.50cm, SD = 13.89cm) at the start of ablation was approximately 5 times the snow depth of the forested region (Depth = 15.70cm, SD=13.89, $p<0.05$). SWE in the burned forest (SWE_H = 173.78cm, SD = 8.90cm, SWE_M = 162.40cm, SD = 22.45cm) melted on average 1.46 cm/day following peak SWE, melting nearly three times as fast as snow in the open meadow (SWE = 208.25cm, SD = 6.29, $p<0.05$). Snow disappearance occurred sometime between the May 21st and May 30th survey dates in high severity and forested areas. However, snow disappearance occurred sometime between the May 30th and June 15th survey dates for moderate severity and open meadow areas.

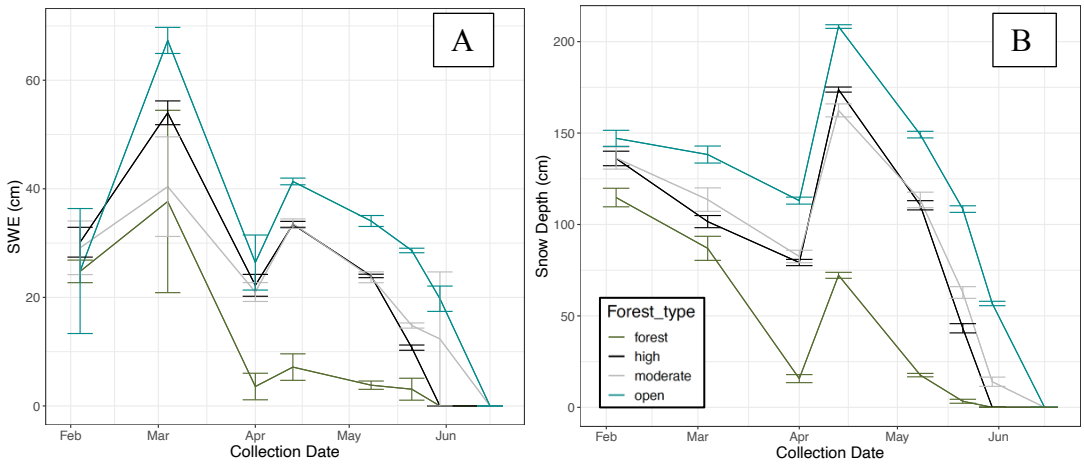

Figure 15: *Snow Course Results for the 2022 survey year. Where A are the results for SWE (n=4) and B are the Snow Depth Results (n=40). Snow depth and SWE reaching zero are not the true dates of them reaching 0 but are readings for the snow survey at that collection date.*

***Table 4**: Lionshead Snow Survey 2022 Average and standard deviation of snow depth and SWE based on collection date and Forest and burn severity type.*

Date	Severity	Mean snow depth (cm)	SD snow depth (cm)	Mean SWE (cm)	SD SWE (cm)	P-Adj Tukey
Feb-4	high	136.10	24.14	30.16	6.72	mod-hgh p = 0.99
	moderate	136.32	27.01	29.13	6.98	opn-hgh p = 0.30
	open	147.13	21.00	24.85	19.93	unb-hgh p = 0.07
	unburned	114.74	26.36	24.78	4.65	opn-mod p = 0.44
						unb-mod p = 0.14
						unb-opn p < 0.05**
Mar-4	high	101.57	24.92	54.00	5.36	mod-hgh p = 0.35
	moderate	113.61	27.18	40.40	20.51	opn-hgh p <0.05**
	open	138.25	20.80	67.33	4.16	unb-hgh p =0.10
	unburned	86.96	34.19	37.66	29.09	opn-mod p <0.05**
						unb-mod p <0.05**
						unb-opn p <0.05**
Apr-1	high	79.21	10.67	22.22	4.03	mod-hgh p = 0.77
	moderate	82.50	21.61	20.98	3.48	opn-hgh p <0.05**
	open	113.05	12.07	26.41	10.13	unb-hgh p <0.05**
	unburned	15.70	13.89	3.50	4.89	opn-mod p <0.05**
						unb-mod p <0.05**
						unb-opn p <0.05**
Apr-13	high	173.78	8.9	33.45	1.09	mod-hgh p <0.05**
	moderate	162.40	22.45	33.57	1.75	opn-hgh p <0.05**
	open	208.25	6.29	41.35	1.23	unb-hgh p <0.05**
	unburned	72.20	10.33	7.160	1.52	opn-mod p <0.05**
						unb-mod p <0.05**
						unb-opn p <0.05**
May-8	high	110.50	15.95	23.94	0.63	mod-hgh p = 0.87
	moderate	113.42	26.88	23.70	2.01	opn-hgh p <0.05**
	open	149.15	11.44	34.07	2.01	unb-hgh p <0.05**
	unburned	17.62	5.94	3.82	1.52	opn-mod p <0.05**
						unb-mod p <0.05**
						unb-opn p <0.05**
May-21	high	43.23	16.35	10.74	1.36	mod-hgh p <0.05**
	moderate	62.80	20.22	14.81	1.16	opn-hgh p <0.05**
	open	108.42	11.36	28.64	1.18	unb-hgh p <0.05**
	unburned	3.32	7.13	3.08	5.71	opn-mod p <0.05**
						unb-mod p <0.05**
						unb-opn p <0.05**
May-30	high	0.00	0.00	0.00	0.00	mod-hgh p <0.05**
	moderate	14.00	16.73	12.34	24.69	opn-hgh p <0.05**
	open	56.79	7.49	19.75	4.04	unb-hgh p =0.91
	forest	0.00	0.00	0.00	0.00	opn-mod p <0.05**
						unb-mod p <0.05**
						unb-opn p <0.05**

4.3 Time-Lapse Photography Derived Daily Snow Depth From Three Burned Forests (1, 2, 10, And 20 Years Following Fire)

Objective 2: *Characterize recovery over time of post forest fire effects on snow storage and snowmelt using continuous in-situ snow time-lapse photography and peak SWE surveys in a 2-year old, 10-year old, and 20-year old burned forest relative to high severity, moderate severity, unburned and open areas using time-lapse photography and snow stakes in western Oregon cascades.*

4.3.1 Time-Lapse Photography Derived Snow Accumulation the First Year Following Fire

Using time lapse photography derived snow depth data. The first year following fire, snow depth and accumulation rates were greatest in the open meadow (Figure 16, Depth= 89cm, SD =10.45cm) and lower in the unburned forest (Depth = 53.00cm, SD = 5.96cm), moderate (Depth = 40.45cm, SD = 9.28cm), and high severity burn forests initially had snow depths more similar to the unburned forest (Depth = 36.11cm, SD = 8.17cm). However, Snow accumulation from February 2nd to March 2nd in the high severity burn region (SAR_H= 5.5 cm/day) was slightly greater than the rates in the open meadow (SAR_O = 5.2 cm/day) allowing burn areas to catch up to the open meadow depths and contain more snow then the unburned and moderate severity areas. Snow accumulation was highest in the open meadow, and the high and moderate severity burns similar to open. Snow accumulation in open and burned areas the following year (2-years-post-fire) differed from the first year of data collection (Figure 19a). Up to peak snow depth, the unburned forested site had notably lower accumulation rates likely due to greater interception from trees (SAR_{for}= 6.6 cm/day) compared to the burned and open sites ($SAR_{H,M,O}$ ~ 10 cm/day, Figure 10a).

In the 10-year-old fire, snow accumulation was the greatest in the burn areas (SMR = 7.5cm/day) and the open meadow had the lowest snow accumulation rate (SMR = 4.1

cm/day, Figure 10b) varying from trends of the Lionshead forests. Open meadow sites had lower accumulation rates were approximately half the accumulation rate of the burn sites in the and is most likely attributed to site selection error (Figure19b). Peak accumulation in the moderate and high severity burn exceeded snow depth in the open and forested areas of the 20-years-old fire. Accumulation rates within high and moderate severity burn areas were the highest at 6.5 cm/day. Interestingly, open and forested sites had similar rates of accumulation around 6.0 cm/day (Figure 19c), though site selection error again needs to be considered for open regions of the 20-year-old fire.

4.3.2 Time-Lapse Photography Derived Snow Storage the First Year Following Fire

The open meadow had the greatest snow depth and high severity had the second greatest snow depth the first year following fire. The open area had the greatest snow depth at 278.65 cm and the high severity burn areas had the second greatest snow depth of 248.74 cm. Snow depth at the moderate severity site (Depth = 200 cm, Figure 16a) was notably lower than the high and open meadow sites. Open meadow and high severity snow depth values began to diverge near April 1st when snow at the high severity sites began to melt at faster rates (4.14cm/day) than open meadow sites (2.23cm/day, Table 5). Open meadow and high severity burn area snow depths decreased by 10% to 40%, respectively during the month of March (Figure16).

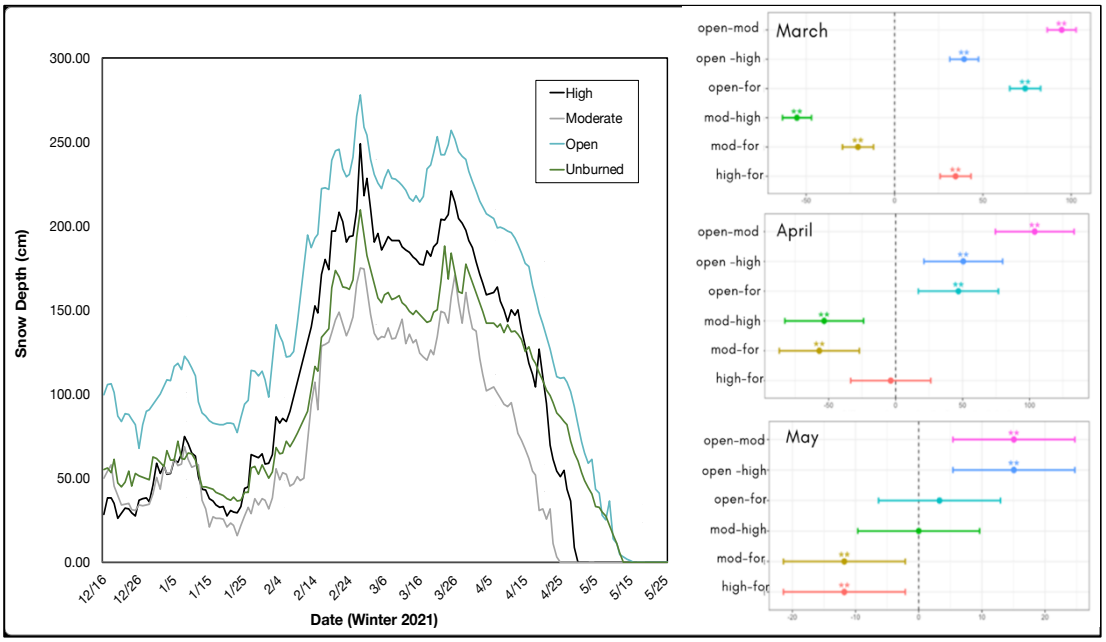

Figure 16: *Cumulative averaged snow depth data between four forest sites consisting of severely burned, moderately burned, forested, and open areas (left). Data reveals accelerated ablation in the high severity and moderately burned forest plots and snow disappearance in the forested and unburned. Additionally, peak snow depths are highest within the open and burned region. Tukey plot and significance values representing significant within the dataset for the LH 20200.*

4.3.3 Snow Accumulation Using Peak SWE Surveys and Time-Lapse Photography Derived Snow Depth Over 2,10, and 20 Years Following Fire

Using April 1st snow course measurements in the Lionshead Fire (2nd year following fire, Figure 17a), we observed peak SWE as18% greater in the open meadow (SWE =26.42cm, SD = 10.13cm, Figure 17a) compared to the burn areas (SWE_H = 22.22 cm, SD = 4.03cm, SWE_M = 20.98 cm, SD = 3.48cm) and was 83% lower in the forest (SWE = 3.58cm, SD = 4.89cm) than in burned areas. Peak snow depth in the two-year-old fire had similar trends, with the highest snow depth occurring in the open meadows (SWE = 113.3cm, SD = 12.13cm) and lowest in the unburned forest (Depth = 15.7cm, SD = 13.89, Figure 17b). High (Depth = 79.67cm, SD = 10.14cm) and moderately burned sites (snow depth = 82.50cm, SD = 21.61 cm) had similar snow depth and on average 80% greater depth than the forested region.

Snow in the high severity burn was the most similar to snow in the open via the time-lapse photography derived snow depth of the Lionshead Fire (2nd year following fire). High severity burned forests (Depth= 225.13cm) and open meadows (Depth = 235.1cm) shared similar peak characteristics and melt rates (SMR_H = 1.83cm/d, SMR_O=1.77cm/d) for the peak snow values. The forested region had 34% less snow (Depth = 153.58 cm) than the high severity region and was significantly different for the month of March ($p<0.05$). In April this relationship persisted ($p<0.05$). At the time of the peak SWE survey, the time-lapse imagery derived similar values of depth as those from in situ surveys. Open areas peak accumulation was the greatest (Depth = 110cm) high severity and moderate severity burned forests snow depth peak accumulation was greater than the unburned forest (Depth = 6.5cm, $p<0.05$), resembling snow accumulation patterns of the open meadow (Figure19a).

4.3.4 Shadow Lake Fire)- 10 years following fire

Peak SWE measurements in the high and moderate severity burn regions of the Shadow Lake Fire (Figure 17b, 10-years following fire) moved closer to the open meadow. Peak SWE differed by only 5% among all burn and forested types within the 10-year-old fire (SWE = 29.13, SD = 5.72cm), SWE was slightly higher in the open meadow (SWE = 32.49cm, SD = 6.42cm) than the moderately burned area (SWE = 29.57cm, SD = 3.08cm, Figure 12b), high severity burn (SWE = 29.99cm, SD = 4.44cm) and forested areas.

Average depth was significantly greater within the open, high, and moderate severity burn areas as compared to the forest ($p<0.05$) according to time-lapse photography derived snow depth. In the Shadow Lake Fire (10 years following fire), the open meadow (Depth = 149.32cm) was 32% lower than snow depth within the high severity burn area

(Depth = 218.62cm, Figure 19b) and 36% lower than snow depth in the moderate severity burn area (Depth = 233.97cm, Figure 13b). Peak snow depth in the high and moderate severity burn was only 5% and 10 % greater than snow depth in the forested plot, respectively (Forest = 207.71 cm). In March, snow depth was significantly different between the open meadow and all other sites ($p<0.05$, Figure 19a). Snow melt rates during the mid-winter melt period were highest in the open region (SMR=1.05cm/d) and lowest in the burned regions (SMR_H= 0.55cm/d, SMR_M = 0.57cm/d) and by the month of April the only sites significantly different where open and moderate sites ($p<0.05$).

4.3.5 B and B Fire -20 years Following Fire

SWE values in the high severity and moderate severity burn areas exceed SWE in the open meadow (Figure 17c). The high severity burn area (SWE = 18.15cm, SD = 0.84cm) and moderate severity burn area (SWE = 19.38cm, SD = 3.10cm) had the highest SWE values. SWE of the moderate severity burn area had the highest retention capabilities while the forested site had the lowest (Figure 17c). Of all study regions, B and B sites had the lowest variation in snow depth between measurements. High severity burned areas had become less variable across classes (Depth = 79.67cm, SD = 10.14cm), more closely resembling open meadow peak snow (Depth = 113.3 cm, SD = 12.13cm) however it was the moderate severity snow depth (Depth = 89.18cm, SD17.00) that was closest to the open meadow (Depth = 94.75cm, SD = 20.99). Mean peak snow depth of open, high, and moderately burned sites all had similar mean snow retention patterns

Average depth was significantly greater within the open, high, and moderate severity burn areas as compared to the forest ($p<0.05$). Time-lapse derived snow depth was greatest in the burned forests compared to the open and unburned forests. Snow depth

peaked in the moderate severity burn region (Depth = 211.95 cm, Figure 19c) and was 5% greater than snow depth in the high severity burn (Depth = 200.96cm). Snow depth in the high severity burn was approximately 14% greater than snow depths in the open area (Depth = 176.73cm, $p<0.05$) and forested region (172.74cm, $p<0.05$) at their peak snow depth on January 5th. Snow melt rates of the high severity (SMR = -1.55cm/d) and moderate severity sites (SMR = -1.60cm/d) were lower than the mid-season melt rates in the forest (SMR = -1.72 cm/d). Snow depth decline considerably in the forested region (snow depth = 117.45cm) was now 20% lower than snow in the high severity burn area (Depth = 149.79cm). Snow depth in the moderate severity (Depth = 144.65) region was now within 1% of the high severity burn. The drastic decline of snow depth within the forested region caused the difference between the forest and all other sites to remain significant ($p<0.05$, Figure 19c).

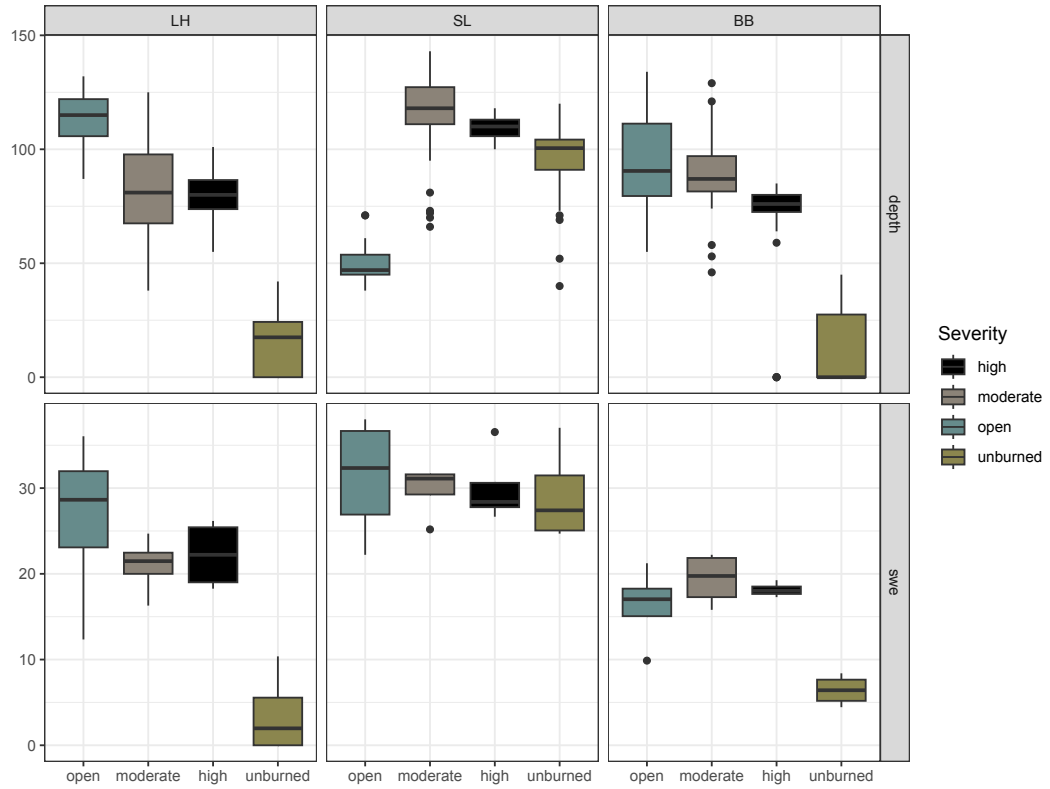

Figure 17: *Lionshead (LH)~Immediately Post Burn (a), peak SWE was highest in open areas and lowest in unburned, depth follows very similar trends as SWE. Moderate and high severity have similar depth to SWE trends, but we see greater variability of snow depth in moderate severity sites than high. Burn areas generally follow immediate post fire trends where moderate and burn sites have accumulated similarly. Shadow Lake (SL)-10 (b) years post burn SWE at moderate and high severity sites followed similar trends to SWE at open and unburned site though, variability of SWE at open sites was more significant. In the shadow lake fire SWE and open are even more similar to high severity. B and B (BB) ~20 years post fire (c) open moderate and high severity all follow similar depth and SWE trends. Depth and SWE at unburned sites was about half the SWE of open, moderate, and high severity. Moderate and High severity SWE had surpassed the open site retention during peak SWE.*

Table 5: *Mean and standard deviation of peak SWE and peak snow depth values across a 2-year-old fire, 10-year-old fire, and 20-year-old fire, following Peak SWE survey during the 2022 winter collection season.*

Mean Peak SWE (cm)	**Lionshead Mean (cm)**	**Lionshead SD (cm)**	**Shadow Lake Mean (cm)**	**Shadow Lake SD (cm)**	**B and B Mean (cm)**	**B and B SD (cm)**
Open	26.42	10.13	31.11	6.42	16.29	4.72
High	22.22	4.03	29.99	4.44	18.15	0.84
Moderate	20.98	3.48	29.75	3.08	19.38	3.10
Forested	3.58	4.89	29.13	5.716	6.42	1.80
Mean Peak Depth (cm)	**Lionshead Mean**	**Lionshead SD**	**Shadow Lake Mean**	**Shadow Lake SD**	**B and B Mean**	**B and B SD**
Open	113.3	12.13	49.83	7.77	94.75	20.99
High	79.67	10.14	109.50	110.0	68.425	23.60
Moderate	82.50	21.61	115.40	19.63	89.18	17.00
Forested	15.7	13.89	95.28	100.5	11.55	16.31

4.3.5 High severity burned forest SWE recovered to resemble that of the open meadow SWE over 20 years following fire

Normalized SWE (relative to open meadow SWE as reference SWE) 2 -year old high severity burned forest and the moderate severity burned forest varied little from each other but considerably from the forested sites (Figure 18) in the 2-year-old fire. Differences between the burns and the open area was 78% greater in the 2-year-old fire than the 20-year-old fire. Normalized measurements in a 10-year-old fire showed that the difference in SWE between the high severity burn area (NSWE = 4.44, SD = 2.49cm) and open region was higher than the 2-year-old burn by 5%, while the difference between SWE in the open and the moderate severity burn was lowered by 43% (NSWE = 3.08, SD= 2.74cm). Normalized peak SWE values for the 20-year-old fire saw high severity SWE (NSWE = -1.85, SD=0.84cm) being the most similar to the open areas but had negative values indicating that high severity had higher peak SWE than the open region. Snow within moderate severity burn areas also surpassed peak SWE retention of open (NSWE=-3.08, SD = 3.11cm).

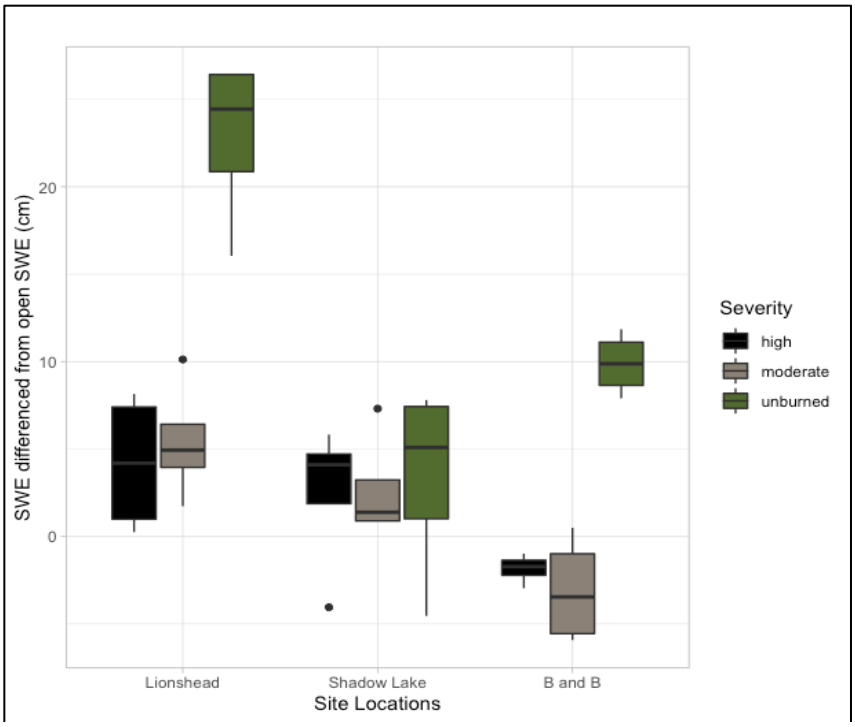

Figure 18: *Normalized SWE across landcover type: Normalized SWE shows the smallest differences from open compared to high severity at the 20-year-old B and B site with the smallest amount of variability. SWE was the most different between high severity and open immediately following burn. 10 years post burn had the most variable high severity storage capabilities.*

Table 6: *Mean peak SWE normalized against open region values across a 2-year-old fire, 10-year-old fire, and 20 year old fire following peak SWE survey winter collection year 2022.*

SWE Normalized by Open (cm-cm)	Lionshead Mean	Lionshead SD	Shadow Lake Mean	Shadow Lake SD	B and B Mean	B and B SD
High	4.19	4.03	2.49	4.44	-1.85	0.84
Moderate	5.43	3.48	2.74	3.08	-3.08	3.11
Unburned	22.83	4.89	3.35	5.71	9.87	1.80

4.3.6 Snow ablation using time-lapse photography derived snow depth in three burned forests 1, 2, 10, and 20 years following fire Snow melt rate, mean monthly depth, and snow disappearance day

Melt rates in high severity burn areas were twice the rate of the open meadows causing snow disappearance to occur 15 – 20 days earlier than the open meadows. The snow melt rate at the high severity site was the fastest at 6.61 cm/day and snow melt in the open was 5.11cm/day. Average snow depth remained the highest in the open meadow for the month of April (Depth = 161.12cm, $p<0.05$) and into the month of May when most

snow disappearance occurred (Depth = 15.06cm). Similar to 2021 snow survey results, snow depths in the forest and the high severity burn where equivalent on April 15th. Snow disappeared on April 29th in the high severity burn area and on May 15th in the open meadow (Figure 16). Snow in the forest melted off on May 12th, 3 days earlier than snow in the open meadow and about 17 days later than the snow in the high severity areas ($p=<0.05$).

4.3.7 Snow melt rate mean monthly depth, and disappearance date of a 2-year-old fire (2022)

Snow depth in the unburned forest was significantly lower than high and moderate burn areas (Figure 19a, $p<0.05$) making snow disappearance date almost two weeks later in both burned areas compared to the forested areas (ΔSDD = -13 days). The second accumulation period occurred near the middle of April and doubled the snow depth of the open, moderate, and high severity burn areas. The end of the season melt period from peak SWE (April 1st) to the site's snow disappearance date was more rapid in the high severity site (SMR = -1.83cm/d) than the open meadow (SMR = 1.77 cm/d). Average snow depth in April within the open meadow (Depth = 157.35cm) was approximately 25% greater than the high severity site (Depth = 118.04cm) and had 33% more snow than the moderate site (Depth = 91.15cm, $p<0.05$). In May, snow disappearance date was 10 days earlier in the burn regions than the open, but the snow in the forest melted off 14 and 24 days earlier than the burn and open meadows, respectively ($p<0.05$).

4.3.8 Snow melt rate mean monthly depth, and disappearance date of a 10-Year-Old Fire (2022)

Snow disappearance occurred within three days among all sites. In the 10-year-old fire, average snow depth at the beginning of melt was the highest for the moderate severity burn (Depth = 165.19 cm) with the high severity burn close enough to not have a significant relationship (Depth

= 154.21cm, Figure 19b). The forested areas (Depth =144.08cm) and the high (Depth = 154.21cm) and moderate severity areas (SMR = 165.19, $p<0.05$) all had average monthly snow depths that were greater than the open meadow (Depth =116.08cm). As melt progressed mean snow depth in the open (Depth = 84.72cm) did not differ from the high severity burn area (Depth = 92.25cm) and moderate severity burn area (Depth = 106.59). The forested region (Depth = 90.25cm) was irregular through this period and retained snow totals similar to the high severity burn area. Snow melt rate from peak SWE to the date of snow disappearance was highest in the moderate severity forests (4.39cm/day). So, despite a higher melt rate, snow disappeared in the high severity burn within 3 days of the other sites. Snow melt rate in the high severity and moderate severity areas was 4.01cm/day. Melt rate in the open meadow area was 3.22 cm/day. The snow disappearance dates for all sites spanned four days (Open 6/1, Moderate Severity 6/2, High Severity 6/2, Forest 6/4).

4.3.9 Snow Melt Rate Mean Monthly Depth, And Disappearance Date of a 20-Year-Old-Fire (2022)

Snow disappeared 4-5 days later in the burned areas compared to the open areas becoming less like the open meadow. Burned forests had the greatest average monthly snow depth 10-years post fire and 20–years post fire (Figure 19c). The average monthly snow depth at the start of ablation was highest in the open areas (Depth = 122.55cm) where depth dipped below the open for both for high severity (Depth = 113.41cm), and 110.04cm for moderate severity, while the average snow depth in the forested regions was 68.67cm ($p<0.05$). In the 20-year-old fire, during the midwinter drought, forested sites were the most susceptible to snow loss. During the end of season melt from peak SWE to SDD, the snow melt rate was highest in high severity burn (SMR = -3.74cm/d) and moderate severity burns (SMR = -3.62cm/d) compared to the forest (SMR = -3.35cm/d). However, snow totals before the final melt in April where on average 50% greater in the burn areas than the forests. This

helped the moderate (SDD = 05/23/2022) and high severity burn areas (SDD = 05/24/2022) have between a 4-5 day later snow disappearance dates than the forest (SDD = 05/19/2022).

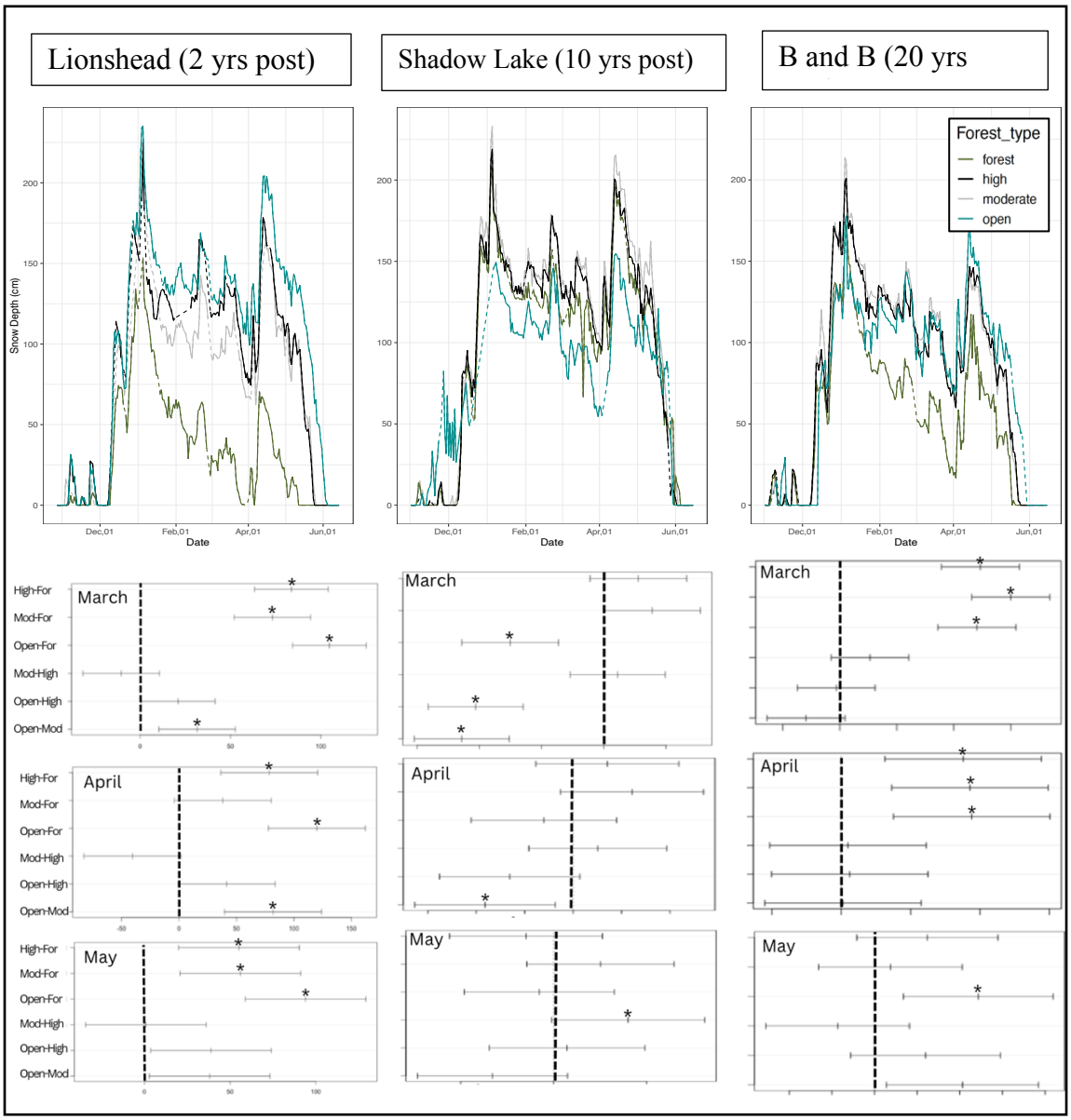

Figure 19: *Continuous snow depth timeseries (top) and Tukey significance plots (bottom) among three burn areas with respect to forest fire recovery derived via time-lapse photography (top). Far right is snow depth from the Lionshead fire immediately following burn, middle is snow depth following intermediate recovery via the Shadow Lake fire and 10 years from burn, and right is the B and B with advanced recovery following 20 years post burn. A * indicates a significant of <0.05.*

4.4 Spatial variability in the recovery of burned forest and effects on snow coverage

Objective 3: *Evaluate the spatial variability of the recovery of forest fire effects on snow covered area using remote sensing derived snow extent in the western Oregon Cascades.*

4.4.1 Snow accumulation

Immediately following fire, snow extent in March was greater in the burn region than the open meadow (Figure 20, 10%). Near intermediate recovery differences in snow extent between burn regions and the open became smaller. During intermediate recovery, snow cover area differences between the burn and the open regions where within 2% of each other and were constant up until advanced recovery in March. In advanced recovery the burn region had 5% greater snow extent in March. Advanced snow extent was higher in the burn region compared to the open meadow (Figure 13, +2%) for March 1st, but on March 15th, snow extent was 10% greater in the open meadow.

4.4.2 Snow Ablation

Immediately following fire, April snow cover area extended 5% more into the open are then the burn lower in the burn region than the open meadow (Figure 20). However, by intermediate recovery snow cover extended 3% more into the high severity burn area. At the start of the advanced recovery period, snow cover extended to be 2% greater in the high severity regions than the open. Immediately following the fire, snow extent was 11% higher in the open meadow compared to the burn region for the month of May (Figure 20). Over the next 5 years, snow extent during the month of May gradually got closer to having equal snow extent in the open and the burn. At intermediate recovery snow extent was 2% greater in the open region and was consistent for the entire intermediate period. Once in advanced recovery snow at 20 years following fire was slightly greater in the HS burn area then the open region, but this declined further into advanced recovery.

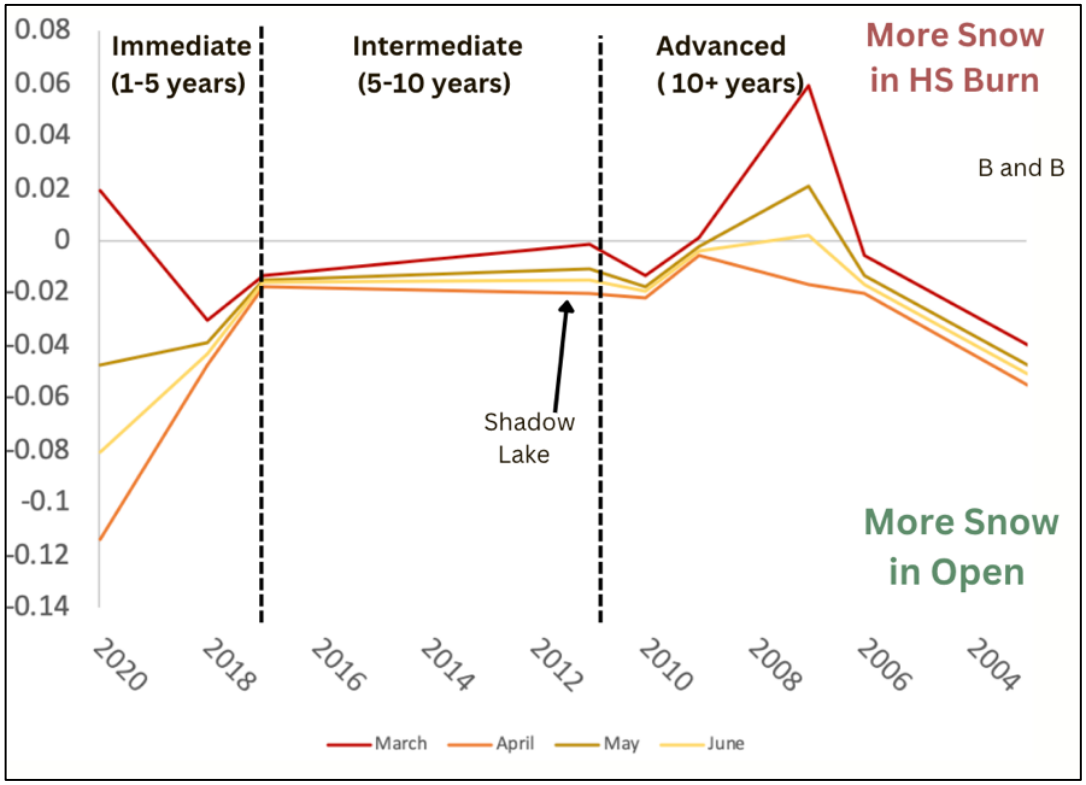

Figure 20: *Snow extent over time and recovery, each line represents a different snow extent for the date of the 2021 season snow extent. Variability decreasing around 2017 and then become more obscure around 15 years following fire. Where then snow extent variability levels out again. Above 0 on the horizontal characterizes more snow in the high severity region than the open buffer and below that line represents more snow in the open buffer as compared to the open. The vertical access is the percent difference normalized by area.*

4.4.3 Environmental Conditions Characterizing Snow Disappearance Date

We collected data from 12 distinct spatial datasets throughout 26 fires within the Willamette Watershed. The first 5 variables we describe as environmental predictors (i.e mean precipitation, mean temperature, canopy height, canopy bulk density, Figure 21). The largest variability of snow disappearance date among these variables is mean precipitation and mean temperature. Mean temperature shows the inverse, where snow disappearance decreases later with lower overall temperatures.

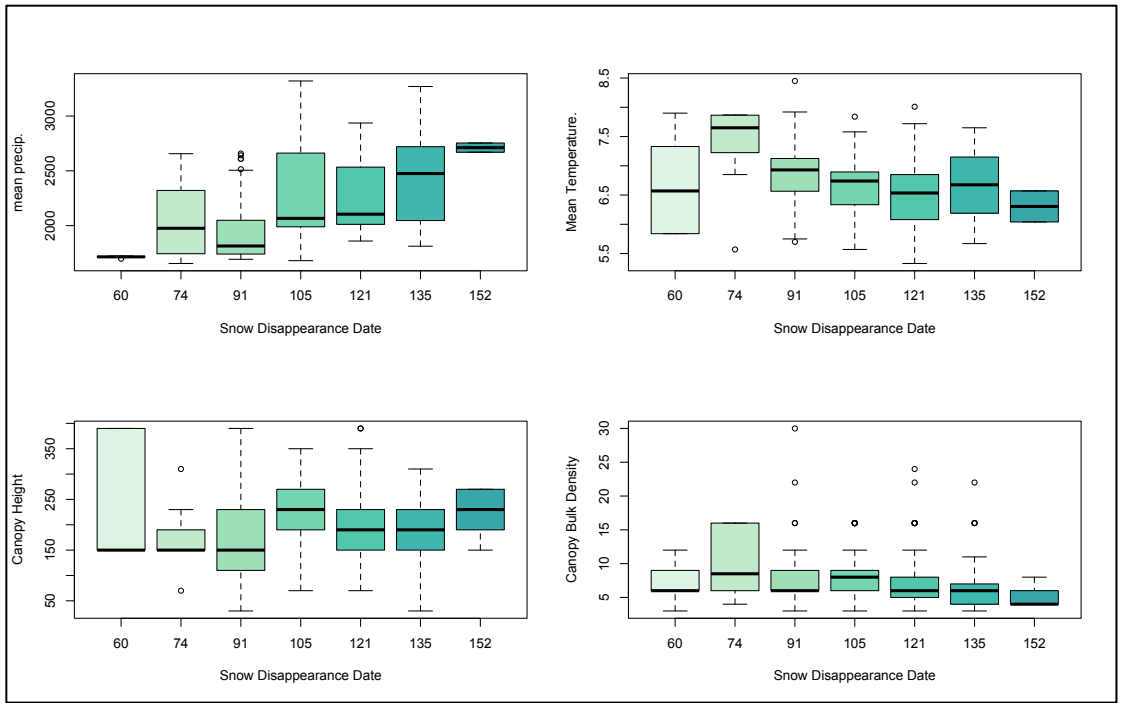

Figure 21: *Summary of raw data of Mean Precipitation (top left), mean temperature (top right), canopy height (bottom left) and canopy bulk density (bottom right) as they relate to snow disappearance date.*

Two sets of predictors collected as ecological datasets show four differing tree species (evergreen, grasslands/herbatious, shrub, and woody wetlands). In general grasslands produced the latest snow disappearance date with the greatest amount of variability. The sample size for wetlands is low and is therefore disregarded for the remainder of the study. Evergreen and shrublands have similar slightly earlier snow disappearance with distributions spread on the earlier side of snow disappearance for both datasets (Figure 22).

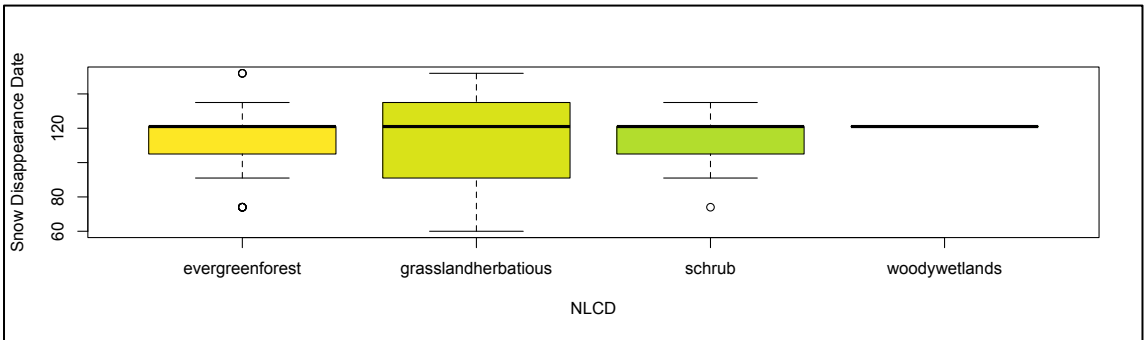

Figure 22: *Summary of raw data of vegetation derived from NLCD as it relates to snow disappearance date.*

Topographic predictors (i.e. latitude, longitude, slope, aspect, and elevation within the 13k-15k threshold) varied greatly with snow disappearance dates (Figure 23). Latitude and Longitude had the greatest variance in snow disappearance dates, where snow disappearance was earlier in higher latitude regions and had a greater variance, and snow disappearance was later among higher latitude regions and less variable. Snow disappearance with higher longitude disappeared both the earliest and the latest. Mid-longitude tended to have a more moderate snow disappearance date. Elevation and mean temperature are negatively correlated (r =-0.65) with each other, as are latitude and years since fire (r = -0.64), and canopy height and years since fire (r = -58).

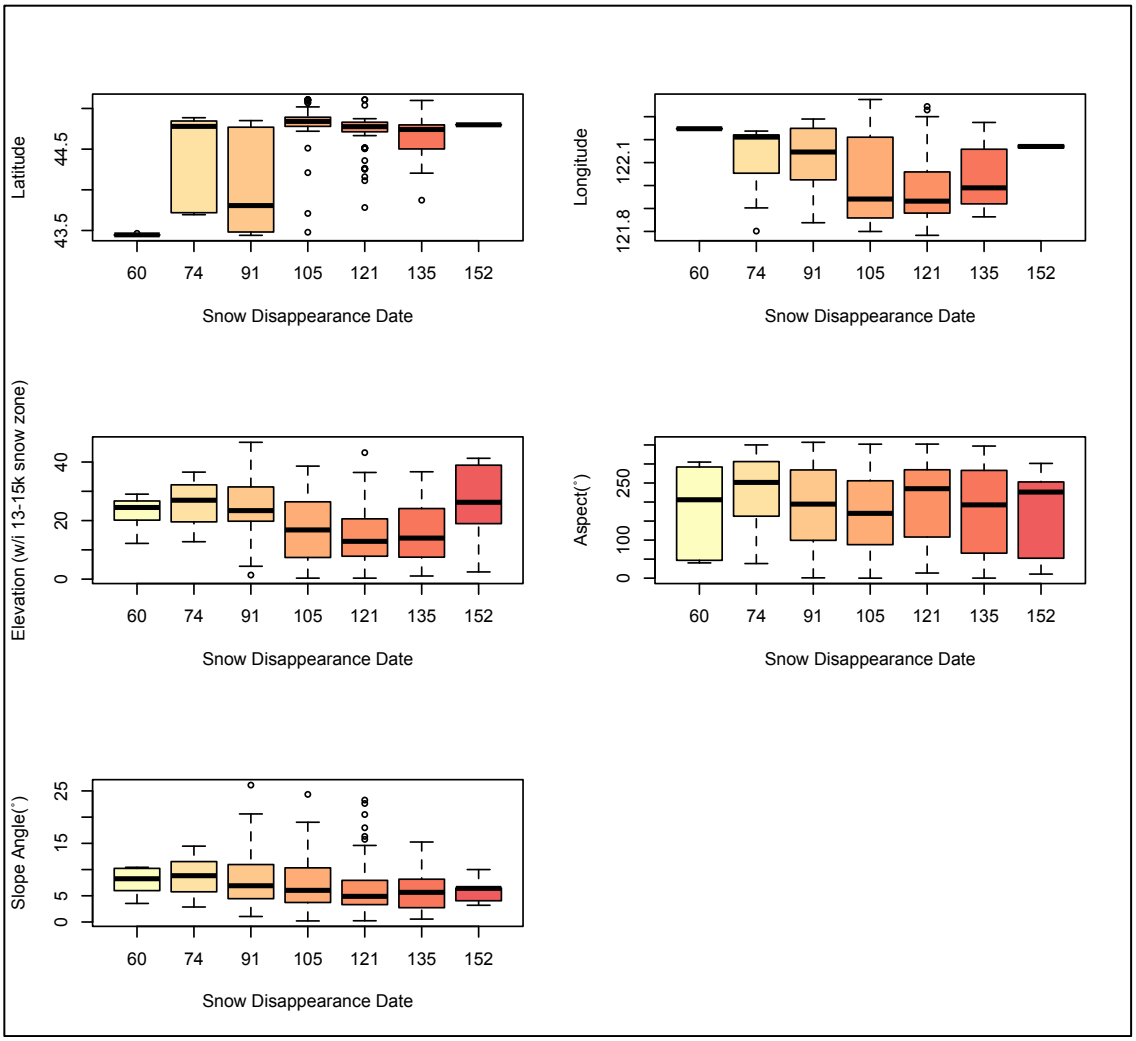

Figure 23: *Summary raw data of Slope Angle, Aspect, Elevation within the prime snow zone, Longitude and Latitude as they relate to snow disappearance date.*

4.5 Multivariate Analysis to Parse Out the Geographic, Topographic, and Environmental Variables Responsible for Snow Disappearance Date

4.5.1 PCA Feature Extraction

Environmental and topographic variables were used in a principal component analysis (PCA) to (1) identify dominant relationships within and between variables and (2) to reduce the number of strongly co-linear potential predictors for regression tree-based modeling framework exploring snow disappearance-fire recovery relationships. From the winter of 2021, PCA resulted in 11 principal components (PC1 – PC11) with 4 eigenvalues greater than one, capturing ~66% of the total variance across datasets (Appendix C). The

first two principal components alone account for almost half of the variance within the dataset (~46%, Figure 24).

PC1 is representative of geographic variables dependent on location. The largest 5 variables contributing to PC1 (r^2 = 78%) are years since fire, latitude, mean temperature, mean precipitation, and elevation (Appendix B, Appendix C). PC1 is positively correlated with years since fire, latitude, mean temperature, and elevation (r = 0.403, r = 0.473, r=0.327) and negatively correlated with mean precipitation (r = -0.328, Appendix C). One PC was found to be significant (Comp.1). PC1 alone makes up ~33% of the variance and is defined in scree/broken stick model as the only observed proportion of the variance that is higher than the corresponding broken stick model (Appendix B).

Through visual inspection we can draw qualitative conclusions from our PCA biplot based on the horizontal (PC1) axis (Figure 24). The plot compares all variables against categorical groupings based on NLCD data. Points associated with evergreen forests form a small cluster where we can deduce that higher latitudes, greater precipitation, higher canopy, and later snow disappearance are loosely associated with Evergreen abundance as well as more recent forest fires (Figure 24). Grasslands are associated with lower latitude, less precipitation and lower canopy height, as well as earlier snow disappearance and higher temperatures (Figure 24). Shrublands have a wide distribution and lower sample size and are challenging to interpret (Figure 24).

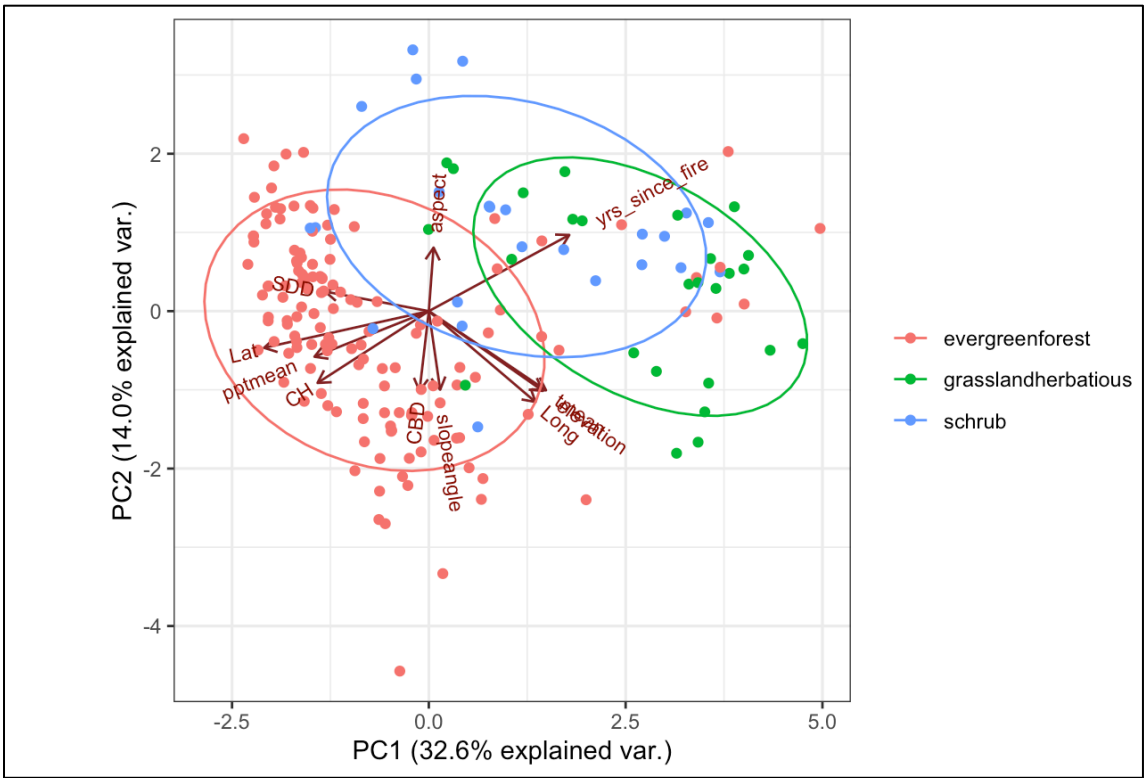

Figure 24: *PCA Biplot showing each site plotted according to its corresponding eigenvalue and significant PC axis. The eigenvectors of each value are plotted as arrows and titled in red. Categorical variables for NLCD where mapped and grouped providing some in-site concerning the distribution of the three land cover classifications. We can "drop" the 306 objects along the axis from the left to right. Along PC1 (from the left to the right), all specimen of evergreen (pink) are located on the left side of the axis and tend to form a cluster. The 'clustering' of these data points in the PCA space means the specimen are relatively similar to each other in terms all measured variables. Evergreen forests have a more tightly concentrated distribution of points. On the other hand, the specimen grasslands (green) are located further away from evergreens and intuitively are less similar. While shrubs are relatively more similar to grasslands than evergreen forests. Where grasslands are more present as years since fire increases. Shrubs have a larger range of distribution but is more centered around the axis.*

4.5.2 Classification Tree Split Decisions on Snow Extent

To reduce the complexity of the model and avoid overfitting the decision tree we applied dimensional reduction to our dataset through PCA feature extraction. Component 1 can be reduced by three variables (aspect, slope angle, and canopy bulk density). The remaining 8 variables are applied to a decision tree (canopy height, latitude, longitude, snow disappearance date, elevation, mean precipitation, mean temperature, and years since fire) where the differences in snow disappearance date are compared against the 7 variables. Up to 7 separate nodes were developed in the original decision tree, each node

representing a primary influence on snow disappearance. The order of nodes reflects the hypothesis that the snow disappearance date and extent increase with greater recovery periods. The resulting snow-years since fire are mapped to provide a visual representation of the hypothesized effect of forest recovery on snow extent across the landscape.

Node 1: Strong Influence of Latitudinal Location on snow disappearance date

Latitude exerts a strong control on the spatial distribution of snow with 4 times the influence of the secondary deciding variable (Appendix B, Latitude = 43). Latitude was the sole decider of snow disappearance date (n = 40, Appendix B). On latitudes under 43 degrees, 8 sites reported snow disappearance dates near March 13th (JD=72 days) and 32 of the sites at latitudes between 43 and 44 degrees were snow free around April 1st (JD=91 days). Snow disappearance at sites located at latitudes greater than 44 degrees north were dependent on years since fire (n = 265).

Node 2: Magnitude of forest fire recovery effect on snow disappearance date

Snow disappearance dates on average occur earlier immediately following fire (1-10 years, Figure 25) as compared to intermediate (10-20 years) and advanced recovery (20+years). Snow disappearance dates had greater variance immediately following fire with snow disappearance occurred anywhere from March 31st (JD=98 days, n=12) to May 5th (JD = 126 days, n=21). Following intermediate and into advanced recovery, (n =107) a few sites saw snow disappearance around April 17th (JD=107 days, n =11), while a majority of the sites disappeared near May 1st (JD =121 days, n =66) and near May 9th (JD = 129 days, n = 30)

Node2a: Environmental susceptibility of snow disappearance date immediately following fire

Immediately following fire, snow disappearance was more susceptible and responsive to environmental and geographic factors. Greater susceptibility to mean precipitation occurred below 1010m. Sites with less than 2107mm of mean precipitation disappeared on March 31st (JD = 90 days, n = 7) and sites with greater than 2107mm of precipitation disappeared 15 days later (JD = 105 days, n =19). When elevation was less than 1010m, canopy height decided snow disappearance. Snow disappeared near April 14th if canopy height was greater than 290m. If canopy height was less than 290m the canopy type and then latitude would decide disappearance. Shrubs caused earlier disappearance (JD =108 days, n = 18) than evergreens, and northern evergreens disappeared 12 days earlier (Latitude>=45, JD = 113 days, n = 40) than southern evergreens (Lat<45, JD=125 days, n = 15). If elevation was greater than or equal to 1017m, few other factors affected snow disappearance. Canopy height less than 210m melted snow around the 19th of April (JD = 109 days, n =18). Canopy greater than 210m saw snow disappear on April 16th and May 6th (Longitude +/-122).

Node2b: Snow disappearance date during intermediate (10-20 years following fire) and advanced (20 + years following fire) recovery.

Overall, snow disappears later 10 years following forest fire with variations dependent on latitude and then canopy height. Earliest disappearance occurring on the 17th of April for 11 sites where canopy height was greater than and equal to 210m in smaller canopy (<210m), 66 sites disappeared near May 1st (JD = 121days). Snow at sites with the latest snow disappearance date occurred the farthest north during intermediate and advanced recovery (Latitude > 44). Snow here disappeared near May 9th (JD= 129 days, n = 30).

4.5.3 Pruned Tree - Cross-validation plot

Cross validation was used to find the optimal pruning of the decision tree and to avoid overfitting. At current, the decision tree was over-fitted making it challenging to understand the magnitude of the influence of the different features. The appropriate depth of the tree found after averaging 5 tests, the Cp (Cp = 0.045, Appendix B) was determined based on the test decision tree that provided the greatest accuracy of the model (0.93). The pruned tree split the data into two separate nodes, where latitude less than 43.87 produced an average snow disappearance date on the 27th of March (JD = 86.28, Figure 25). All sites occurring at latitudes greater than 43.87 where primarily dependent on years since fire. Where if fire occurred immediately or within 2 years of the winter of 2021, then average snow disappearance date occurred on April 22nd (JD = 112 days, Figure 25). Snow within fires that occurred following the intermediate recovery period had disappearance dates around May 2nd (JD = 122 days, Figure 25), for the winter of 2021. Snow disappearance day occurred 11 days earlier immediately following fire than snow within sites with intermediate and advanced recovery.

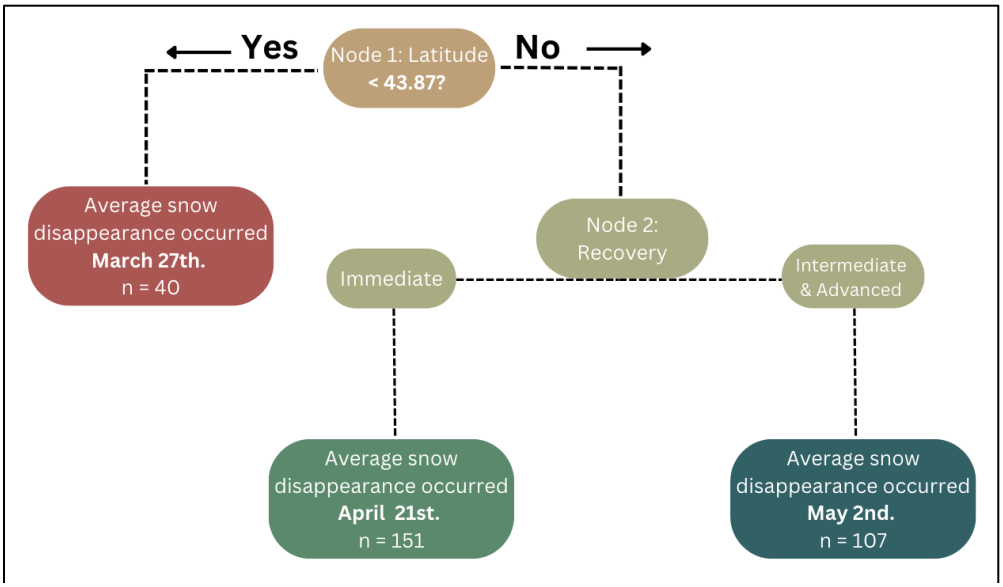

Figure 25: *Pruned decision tree, where 86.28 represents the mean snow disappearance date for snow located at latitudes less than 43.87˚. The next node represents the difference between years since fire, where immediately and two years following fire, snow disappears on a mean Julian date of 111.9 so where intermediate and advanced recovery sites disappear on average 10 days later.*

5. DISCUSSION

In this study we use a mix of methods to evaluate forest fire effects on snow hydrology as a function of forest recovery to complement previous research assessments. Our method draws on data generated from remote sensing-based open source data to compliment an in-depth analysis of *in situ* field testing. Additionally, forest fire recovery is analyzed as a function of scale, based on the assumption that the main challenge with varying data collection types, is a level of error associated with either environmental factors, data resolution, or availability. By considering a wide spectrum of data types and scales we are able draw more conclusions concerning post forest fire influence on snow immediately to years 20 + years following fire.

5.1 Objective 1: Quantify immediate post forest fire effects on snow storage potential and snowmelt using snow course transects in the western Oregon Cascades.

Wildfire is changing forested ecosystems (Westerling 2006), which has cascading impacts on watershed hydrology (Adams 2013). Maritime temperate domains of the Western Oregon Cascades affected by forest fire realize shifts in snow accumulation patterns. Accumulation rates and snowpack storage capacity increase in burn forests immediately following fire when compared to snow of the unburned forests. Illuminating the superior accrual of snowpack during individual snowfall events as a response to a loss of canopy cover, consequential of forest fire. Few distinguishing factors are responsible for differential snow accumulation within PNW watersheds following fire, first is that forest modifications through up to a 300% reduction of canopy density (Gleason 2013) decreases snow interception by approximately 60% of its previous state. Second, is the decrease of

energy input to the snowpack associated with lower longwave radiation inputs. Previous studies evaluated snowfall interception (Hedstrom and Pomeroy 1998; Essery 2003; Rutter 2009), insect defoliation (Boon 2012; Mikkelson 2013), clear cutting and silviculture (Lundquist and Dickerson-Lange 2013; Dickerson-Lange and Lutz 2015; Harpold 2020; Krogh 2020; Schneider 2019), and burn vs. unburned forests (Gleason 2013; Burles and Boon 2011; Winkler and Others 2011), identify reduced canopy density and foliage contributing to increased snowpack. Results from this study show a clear and consistent increase to snow storage and therefore water yield over the two years immediately following fire that are comparable to the yields of nearby open areas. Supported by the fact that a level of correlation is associated with tree mortality following forest fire and a deeper and more dense snowpack (Maxwell and St. Clair 2019). These patterns are consistent with findings found following the Las Conches fires in New Mexico (Harpold 2014) and the Cameron Peak fire in Colorado (McGrath 2023).

Moderate and high severity sites show a less dramatic response to the mid-winter snow melt then under forests during the winter of 2022 (Lundquist and Dickerson-Lange 2013). Midwinter, sloughing of burned woody debris and black carbon had not begun to concentrate on top of the snowpack to an extent that drives a significant decrease in snowpack reflectivity. Additionally, lower solar incidence angles in the winter diminished the energy inputs to the snowpack surface (DeWalle and Rango 2008). Indicating that sub-surface particulate matter during the mid-winter melt event had not absorbed enough incoming solar energy to drive early snow melt. Mid-winter snowmelt was less severe in the open, high severity, and moderately burned areas than in the forest, which lost 80% of its SWE and 70% of its depth between April sites visits. Disagreeing with previous research

which considers the influence of wildfire on mid-winter melt and saw declines of snowpack during the same winter (Hatchett 2023).

Following the vernal equinox, commonly falling around the end of March, a shift occurs where the days get longer, the sun gets higher, and the snow begins to absorb more energy. As the snow begins to melt, black carbon and other particulate matter more readily concentrates closer to the snowpack surface. This causes a 40% decrease in spectral albedo (Gleason 2013) and a combined 200% increase of net shortwave radiation (Gleason 2013) through reduced canopy cover. With the increase in solar energy comes higher rates of snowmelt in high severity burned forests. As a result, the benefits initially seen to snow storage during the accumulation phase quickly diminish and snow melt rates double provoking snow disappearance 24 days earlier in the burn region compared to the meadow. The initial increase of snowpack during accumulation in the burned forest supports our first hypothesis that snow storage in burn forests are more like open meadows. Indicating at their potential to increase water storage if snow albedo increases while forest canopy remains open.

5.2 Objective 2: Post forest fire effects on snow storage and snowmelt as a function of recovery using continuous in-situ snow time-lapse photography and peak SWE surveys in a 2-year old, 10-year old, and 20-year old burned forest relative to high severity, moderate severity, unburned and open areas using time-lapse photography and snow stakes in western Oregon cascades.

Distinctions become apparent in intermediate recovery, were the mass balance of the snowpack affected by trade-offs between increased net shortwave radiation due to LAP's and decreased canopy interception (Varhola 2010) begins to shift. Previous research identifies a period of 6-10 years post fire were post-fire snow albedo increases (Gleason 2019) as a result advanced SDD begins its decline after 8 years post ignition (Gleason

2019). Our research initially identified that snow accumulated at similar rates among all burn area's respective burn sites, exceeding snow accumulation of what is assumed in previously forested states. And through the progress of forest recovery, the moderate and high severity sites progressively outperform the storage capabilities of burn areas in earlier stages of recovery, were eventually the burned areas have higher peak accumulation than the open.

Snow in the moderate severity burn areas had the most noteworthy snow dynamics (greatest depth and SWE) indicating that the slight increase in canopy cover, may provide some influence on snowpack quantities. On one hand it can protect from wind (P. D. Broxton et al. 2015; Currier and Lundquist 2018) and direct solar radiation (Xue 2022) and increase snowpack, on the other hand, it can litter the snowpack surface with organic debris (Gleason 2013; Burles and Boon 2011; Wiscombe and Warren 1980) and increase the input of longwave radiation (Harding and Pomeroy 1996; Seyednasrollah 2013) decreasing snowpack. Moderate severity burn forests of intermediate and advanced recovery may have greater snow content as they are more closely related with the location identified as "cold and early" forest-snow class in Dickerson-Lange 2021. Here, a range of canopy gaps and thinning intensity is associated with greater snow in such regions. Opposing the "warm and early" snowpack which states that longer snow duration in larger forest gaps, which could be more closely associated to the Lionshead burn location.

In response to the mid-winter drought experienced in the winter of 2022, snow retention was maintained in high and moderate severity burned forests among all recovery periods while it was lost in most forested areas. This could be an important finding in our work suggesting that burned areas in warm Maritime climates could work to buffer the

influence of complex mid-winter climate effects. However, recent research in the Sierra Nevada Mountains, opposes this finding, stating that a 25 – 71% decline in broadband snow albedo at burned sites enhanced midwinter melt following the same multiweek dry spell in 2022 (Hatchett 2023), while also finding that minimal melt occurred following similar meteorological conditions in 2013. Indicating the need for further research to fully understand these present findings.

End of season snow melt rates were lowest in advanced recovery and highest immediately following fire. This noteworthy difference is potentially the result of lower snow surface debris concentrations in the burn forest with respect to recovery, where the mass of debris deposition was found in past research to be reduced by 62% from immediately following fire to near 15 years following fire (Gleason 2013). Snow disappearance date was 13 - 24 days later in burn regions compared to the open meadows immediately following fire. While in later stages of forest recovery snow disappearance date became synchronous among all forest types, being within just 2 or 3 days of each other in the intermediate recovery burn areas. Snow disappeared 11 days later in the 10-year-old fire compared to the 2 year old fire and 20 year old fire, 5 years earlier than the effective albedo decrease began to subside (Gleason 2019). Earlier snow disappearance in the advanced recovery burn area was unexpected and it could be considered that the 20-year old fire was beginning to return to its pre-fire state, due to the difference between snow disappearance dates from the forested site and the burn site decreasing from 11 days to 4 days in intermediate to advanced recovery, respectively. A potential theory is that melt rates at the bottom of the snowpack could have greater influence by the rise of net radiation due to canopy regrowth coupled with warmer ambient tempers and increased solar

radiation. Though not a quantity tested in this study, it has been found that more uniform snowpack, such as what is found in a burn area, are more sensitive to a shallower snow depth (Broxton 2021) and melts earlier due to greater energy exposure per unit SWE (Badger 2021).

Uncertainty caused by systematic errors, climate gaps, and complex snow factors, limit the usability of these fine scale results alone. As mentioned, the climate between the Shadow Lake, B and B and, and Lionshead burn areas had noteworthy distinctions. The Shadow Lake and the B and B burn areas, closer to the Cascade divide, ended up presenting as colder higher elevation snowpack's, with less dense canopy. Furthermore, the forested area in the Shadow lake burn had lower canopy and stem density, and the snow under this canopy had parallel character to the open and burned regions, opposing our expectations and past research. Finally, both the open meadow sites in the B and B and Shadow Lake were inundated with water at the start of accumulation, likely influencing SWE and snow depth measurements of our control sites, limiting their merit.

5.3 Objective 3: Evaluate the spatial and temporal variability of the recovery of forest fire effects on snow covered area using remote sensing derived snow extent in the western Oregon Cascades.

We observe several interesting relationships between vegetation, topography, precipitation, temperature, and snow extent across the Willamette Watershed. Fires burn in complex ways across landscapes due to variations in fuel loading, fire weather, and topography (Burles and Boon 2011). Parsing out the variability helped to distill the dominate factors related to snow disappearance within wildfire boundaries. The broad scale spatial analysis explained that snow cover area immediately following burn overall is greater in open meadows. Except for in March during peak accumulation. In intermediate

recovery snow extent is alike between the open and burned areas with little variability. We see similar trends with time-lapse imagery of the Shadow Lake fire and peak SWE surveys were the open meadows and burn areas are the most similar during intermediate recovery. It is during this period that the data supports our hypothesis that snow in the open and burn become more similar for all winter months following intermediate recovery.

Since fires burn and snow falls in complex ways across a landscape parsing out the variability helped to distill the dominate factors related to snow disappearance within wildfire boundaries. Throughout the seasonal snow zone forest recovery itself can vary greatly, and many of the sub-regions within the Willamette Watershed will see post-fire climate conditions shift. Surprisingly explicit factors most associated with the loss of snow on a point-based scale, such as aspect, slope and canopy density, had little to no input to the data within the wider reaches of the Willamette watershed. Geographic features, such as latitude, mean precipitation, and longitude, all have a strong influence on the controls of snow disappearance date.

An influential feature was the forest fire recovery factor were our analysis confined the dataset to two classes, immediate recovery, and intermediate and advanced recovery, where generally earlier snow disappearance dates are associated with more recent fires and later fires are associated with later snow disappearance dates. Immediately following fire, the relationships between the remaining factors is complicated. As mentioned throughout this study, snow immediately following fire and during the ablation period, have high concentrations of particulate matter (Gleason 2013), where we see snow melt rates indicating that the factors that influence melt are highly vulnerable to even small shifts in environmental change.

Snow in burn areas immediately following fire melted off on average 10 days before forests in intermediate and advanced recovery. Interestingly, our in-situ time-lapse study marked the difference in snow disappearance date between burns immediately following fire and in intermediate recovery as 11 days. Therefore, we see that comparing these modeled results to snow disappearance of more accurate in-situ data, we are able to derive consistencies between scale and temporal evaluation. Our simplified dataset identified three Julian dates for snow disappearance. One that was primarily dependent on the lowest values of northings and the second that was primarily dependent on the recovery period. Snow under forests immediately following fire melted off an average of 10 days before forests in intermediate and advanced recovery. Looking at the other pieces of this study, such as the snow disappearance date derived from the snow survey or time-lapse photography immediately following burn. Snow disappearance date also occurred on average 10 - 11 days earlier in the burn forest compared to the open area. Therefore, we see that comparing these modeled results to snow disappearance can help conclude that snow disappearance duration increases with respect to forest fire recovery, and increased recovery is associated with greater snow quantity and longer snow duration. The current broad scale spatial study was limited in that the data available is evaluated at a 30 m resolution, eliminating the possibility of understanding snow dynamics at a plot scale. Additionally, besides openings in trees snow cover cannot be analyzed under canopy for the present methods of remote sensing alone.

5.4 Broader Impacts for Watershed Management

Snowpack in the Western U.S. is declining while fire frequency, extent, and intensity are increasing (Westerling 2006) . Previous studies have evaluated possible implications of forest fire mitigation on surface water yields, but they have largely focused on burn areas immediately following fire verses treatments which have longer times since burn or have only conducted experiments leading to increased water yields in clear cut or other disturbance-based mitigation. This paper fills in a critical knowledge gap by directly comparing four different snow yields as forest recovers from a wildfire event. It could serve as a tool for hydrologists and resource managers to evaluate the potential of forest fire mitigation to decrease fire risk while also increasing snowpack in watersheds.

The prevailing narrative is that snowpack should increase once the flushing of burned woody debris and increase of snow surface albedo (Gleason 2019, Gersh 2020) gets farther from the burn event. Total snow yields up to peak SWE were largely positive relative to the pretreatment mean, and evidence suggests that this is likely due to changes brought on by the limited influence of opened canopy. Of the plot scale results snow in the burned areas increased in 4 of the 5 cases studied from their pretreatment forested plots. Indicating that there was greater snowpack yield following fire, though the runoff events occurring earlier in the season, likely limiting watershed and reservoir retention. There is a strong indication that intermediate recovery has the greatest potential to increase snow duration within a watershed, peak SWE surveys indicate increased SWE and snow depth, were time-lapse photography signified an 11-day prolonged snow depth as compared to immediately burned forest. Broad scale spatial analysis suggests consistent similarities between the open and the burned forest through the intermediate recovery phase and a 10

day increase in snow retention as compared to immediately following fire. However, results become confused when a forest enters advanced recovery, in some instances such as peak SWE surveys and snow extent relationships built by spatial analysis, snow depth and SWE exceed the retention capacity of the open meadows, though snow duration seemingly decreases as presented in time-lapse photography results, this could hint at forests beginning to return to their pre-fire state and snow retention based on evidence that local regrowth resulted in a 50% reduction in summer streamflow in a past study (Perry and Jones, 2016). Though this opposes the analysis of our broad spatial extent, which included advanced recovery in the prolonged snow extent results. It should then be the intention for future work to evaluate these same principles at broad and sub-basin scales to draw on more definitive results through the period of advanced recovery.

Overall, we see an increased potential for fires to increase snow and water retention as past studies have. One study specific to the Northwest (Jones and Post, 2004), noted an increase in discharge were 100% of the watershed had been cleared of vegetation and another noted that with a decrease of 75% of canopy significant changes were seen in runoff (Oda 2018). The prospect of controlled burn increasing watershed retention is an exciting idea, though the extent to which a forest would have to be cleared to make a significant difference is unknown, and the trade-offs between environmental impact and the potential benefits need to be studied in detail. Deeper studies into the understanding the mechanisms that drive hydrologic change due to landcover disturbance should be conducted over varying regions, vegetation, and forest remediation since the response is highly location dependent. The combination of the studies presented provides preliminary guidance and ideas to drive further research. By understanding underlying snow hydrologic

mechanics there is the potential to creating land management strategies that help facilitate climate resilience for the future of ecosystems and watersheds.

6. CONCLUSION

In this study we have used a combination of methods for evaluating forest fire effects on snow hydrology as a function of forest recovery. We draw on open-source remote sensing data in burn areas connected to an in-depth analysis of point based or in-situ experimentation all within the Willamette watershed. Using these methods, we were able to measure snow accumulation, extent, and melting at multiple scales as a function of forest recovery. Based on our analysis of these data, we conclude that forest fires result in increased snow accumulation and storage in a burn area post fire. Even though, forest fires result in increased melting immediately following fire they also showed increased resilience to mid-winter melt. Furthermore, snow disappearance date was prolonged 10 days following wildfire in intermediate recovery forests. The increased snow extent and advanced peak accumulation could provide benefits to abiotic and biotic species within watersheds. While simultaneously increasing water volume and increasing the extent of reflective surface later into the dry and warm summer months. These conclusions indicate that, from a human perspective, forest fires may result in some long-term benefits for water resources availability and snow retention in watersheds. However, we also found that snow extent in burn areas shows increased variability in advanced recovery, where it is quoted that forested watersheds become unpredictable with wildfire alteration (Vilà-Vilardelli 2023). It is challenging to definitively identify the long -term benefits and impacts that these ideas might have as the effects of forest fires on snow are still not yet fully understood. Our results hint at the ideology that controlled burns may be a method to increase snow retention in watersheds but given the increase in snow extent variability after forest fires, burns may not be a predictable tool for such alterations. Further studies are

needed to fully quantify the changes in snow melt timing and volume within a watershed as a result of wildfires, to evaluate the costs and benefits of this strategy. The research presented may be an essential first step in further studies that quantify water retention capabilities of forest fire.

7.0 REFERENCES

Aaro, Patti, and Bryant Becki. 2021. “Reclamation Announces 2022 Operating Conditions for Lake Powell and Lake Mead.” *Newsroom | Bureau of Reclamation.*, 2021.

Abatzoglou, John T., and Crystal A. Kolden. 2013. “Relationships between Climate and Macroscale Area Burned in the Western United States.” *International Journal of Wildland Fire* 22 (7): 1003–20.

Adam, Jennifer C., Alan F. Hamlet, and Dennis P. Lettenmaier. 2009. “Implications of Global Climate Change for Snowmelt Hydrology in the Twenty-First Century.” *Hydrological Processes* 23 (7): 962–72.

Adams, Mark A. 2013. “Mega-Fires, Tipping Points and Ecosystem Services: Managing Forests and Woodlands in an Uncertain Future.” *Forest Ecology and Management* 294 (April): 250–61.

Anghileri, D., N. Voisin, A. Castelletti, F. Pianosi, B. Nijssen, and D. P. Lettenmaier. 2016. “Value of Long-Term Streamflow Forecasts to Reservoir Operations for Water Supply in Snow-Dominated River Catchments.” *Water Resources Research* 52 (6): 4209–25.

Archer, Kellie J. 2010. “RpartOrdinal: An R Package for Deriving a Classification Tree for Predicting an Ordinal Response.” *Journal of Statistical Software* 34 (7): 7.

Atzet, Thomas, and Lisa A. McCrimmon. 1990. *Preliminary Plant Associations of the Southern Oregon Cascade Mountain Province*. Vol. 1990. [Portland, Or.?], U.S.D.A. Forest Service, Pacific Northwest Region, Siskiyou National Forest, 1990.

Avanzi, Francesco, Marco Caruso, Cristina Jommi, Carlo De Michele, and Antonio Ghezzi. 2014. “Continuous-Time Monitoring of Liquid Water Content in Snowpacks Using Capacitance Probes: A Preliminary Feasibility Study.” *Advances in Water Resources* 68 (June): 32–41.

Badger, Andrew M., Nels Bjarke, Noah P. Molotch, and Ben Livneh. 2021. “The Sensitivity of Runoff Generation to Spatial Snowpack Uniformity in an Alpine Watershed: Green Lakes Valley, Niwot Ridge Long-Term Ecological Research Station.” *Hydrological Processes* 35 (9). https://doi.org/10.1002/hyp.14331.

Bales, R. C., J. W. Hopmans, and A. T. O’Geen. 2011. “Soil Moisture Response to Snowmelt and Rainfall in a Sierra Nevada Mixed-Conifer ForestAll Rights Reserved. No Part of This Periodical May Be Reproduced or ….” *Vadose Zone Journal*. https://pubs.geoscienceworld.org/aeg/vzj/article/315933/Soil-Moisture-Response-to-Snowmelt-and-Rainfall-in.

Barnett, Jon, and W. Neil Adger. 2007. “Climate Change, Human Security and Violent Conflict.” *Political Geography* 26 (6): 639–55.

Barnett, T. P., J. C. Adam, and D. P. Lettenmaier. 2005. “Potential Impacts of a Warming Climate on Water Availability in Snow-Dominated Regions.” *Nature* 438 (7066): 303–9.

Barnhart, T. B., N. P. Molotch, and B. Livneh. 2016. “Snowmelt Rate Dictates Streamflow.” *Geophysical*. https://agupubs.onlinelibrary.wiley.com/doi/abs/10.1002/2016GL069690.

Bladon, Kevin D., Monica B. Emelko, Uldis Silins, and Micheal Stone. 2014. “Wildfire and the Future of Water Supply.” *Environmental Science & Technology* 48 (16): 8936–43.

Boisramé, Gabrielle, Sally Thompson, Brandon Collins, and Scott Stephens. 2017. “Managed Wildfire Effects on Forest Resilience and Water in the Sierra Nevada.” *Ecosystems (New York, N.Y.)* 20 (4): 717–32.

Boon, Sarah. 2012. “Snow Accumulation Following Forest Disturbance.” *Ecohydrology: Ecosystems, Land and Water Process Interactions, Ecohydrogeomorphology* 5 (3): 279–85.

Broxton, P. D., A. A. Harpold, J. A. Biederman, P. A. Troch, N. P. Molotch, and P. D. Brooks. 2015. “Quantifying the Effects of Vegetation Structure on Snow Accumulation and Ablation in Mixed-conifer Forests.” *Ecohydrology: Ecosystems, Land and Water Process Interactions, Ecohydrogeomorphology* 8 (6): 1073–94.

Broxton, Patrick D., C. David Moeser, and Adrian Harpold. 2021. “Accounting for Fine-scale Forest Structure Is Necessary to Model Snowpack Mass and Energy Budgets in Montane Forests.” *Water Resources Research* 57 (12). https://doi.org/10.1029/2021wr029716.

Bureau of Reclamation. 2022. “Lower Colorado River Operations.” Lower Colorado Region. November 1, 2022. https://www.usbr.gov/lc/region/g4000/hourly/mead-elv.html.

Burles, Katie, and Sarah Boon. 2011. “Snowmelt Energy Balance in a Burned Forest Plot, Crowsnest Pass, Alberta, Canada.” *Hydrological Processes*. https://doi.org/10.1002/hyp.8067.

Cansler, C. Alina, and Donald McKenzie. 2014. “Climate, Fire Size, and Biophysical Setting Control Fire Severity and Spatial Pattern in the Northern Cascade Range, USA.” *Ecological Applications: A Publication of the Ecological Society of America* 24 (5): 1037–56.

Carlowicz, M. 2022. “Lake Mead Keeps Dropping.” NASA Earth Observatory. July 22, 2022. https://earthobservatory.nasa.gov/images/150111/lake-mead-keeps-dropping.

Cess, R. D., G. L. Potter, M-H Zhang, J-P Blanchet, S. Chalita, R. Colman, D. A. Dazlich, et al. 1991. “Interpretation of Snow-Climate Feedback as Produced by 17 General Circulation Models.” *Science* 253 (5022): 888–92.

Clark, Martyn P., Jordy Hendrikx, Andrew G. Slater, Dmitri Kavetski, Brian Anderson, Nicolas J. Cullen, Tim Kerr, Einar Örn Hreinsson, and Ross A. Woods. 2011. “Representing Spatial Variability of Snow Water Equivalent in Hydrologic and Land-Surface Models: A Review.” *Water Resources Research* 47 (7). https://doi.org/10.1029/2011wr010745.

Collin Homer, Joyce A. Fry, and Christopher A. Barnes. 2012. “The National Land Cover Database.” Earth Resources Observation and Science (EROS) Center. 2012. https://doi.org/10.3133/fs20123020.

Contosta, Alexandra R., Alden Adolph, Denise Burchsted, Elizabeth Burakowski, Mark Green, David Guerra, Mary Albert, et al. 2017. “A Longer Vernal Window: The

Role of Winter Coldness and Snowpack in Driving Spring Transitions and Lags." *Global Change Biology* 23 (4): 1610–25.
Cooper, M. G., J. R. Schaperow, S. W. Cooley, S. Alam, L. C. Smith, and D. P. Lettenmaier. 2018. "Climate Elasticity of Low Flows in the Maritime Western U.s. Mountains." *Water Resources Research* 54 (8): 5602–19.
Currier, William Ryan, and Jessica D. Lundquist. 2018. "Snow Depth Variability at the Forest Edge in Multiple Climates in the Western United States." *Water Resources Research* 54 (11): 8756–73.
De Michele, C., F. Avanzi, A. Ghezzi, and C. Jommi. 2013. "Investigating the Dynamics of Bulk Snow Density in Dry and Wet Conditions Using a One-Dimensional Model." *The Cryosphere* 7 (2): 433–44.
De Noblet-Ducoudré R. Houghton J. House K. Kitajima C. Lennard A. Popp A. Sirin R. Sukumar L. Verchot Jia G E Shevliakova P Artaxo, N. 2019. "Land-Climate Interactions." In *Climate Change and Land: An IPCC Special Report on Climate Change, Desertification, Land Degradation, Sustainable Land Management, Food Security, and Greenhouse Gas Fluxes in Terrestrial Ecosystems*, edited by R. van Diemen M. Ferrat E. Haughey S. Luz S. Neogi M. Pathak J. Petzold J. Portugal Pereira P. Vyas E. Huntley K. Kissick M Belkacemi J. Malley (eds.) P R Shukla J Skea E Calvo Buendia V Masson-Delmotte H-O Pörtner D C Roberts P Zhai R Slade S Connors.
Dennison, Philip E., Simon C. Brewer, James D. Arnold, and Max A. Moritz. 2014. "Large Wildfire Trends in the Western United States, 1984-2011." *Geophysical Research Letters* 41 (8): 2928–33.
Deschutes and Ochoco National Forests. 2005. *B & B Complex*. Bend, Oregon.
DeWalle, David R., and Albert Rango. 2008. *Principles of Snow Hydrology*. Cambridge University Press.
Dickerson-Lange, S. E., and R. F. Gersonde. 2017. "Snow Disappearance Timing Is Dominated by Forest Effects on Snow Accumulation in Warm Winter Climates of the Pacific Northwest, United States." *Hydrological*. https://onlinelibrary.wiley.com/doi/abs/10.1002/hyp.11144.
Dickerson-Lange, S. E., and J. A. Lutz. 2015. "Observations of Distributed Snow Depth and Snow Duration within Diverse Forest Structures in a Maritime Mountain Watershed." *Water Resources*. https://agupubs.onlinelibrary.wiley.com/doi/abs/10.1002/2015WR017873.
Dickerson-Lange, S. E., and J. A. Vano. 2021. "Ranking Forest Effects on Snow Storage: A Decision Tool for Forest Management." *Water Resources*. https://agupubs.onlinelibrary.wiley.com/doi/abs/10.1029/2020WR027926.
Donel Lane, Henry Stewart, John Mangan, Oke Eckholm, David Bauman, Allan Meadowcroft, Horace Harding, Francis Nelson. 1969. "Willamette Basin Comprehensive Study." Willamette Basin Task Force - Pacific Norhtwest River Basincs Commision.
Dozier, Jeff. 1989. "Spectral Signature of Alpine Snow Cover from the Landsat Thematic Mapper." *Remote Sensing of Environment* 28 (April): 9–22.

Dozier, Jeff, Robert O. Green, Anne W. Nolin, and Thomas H. Painter. 2009. "Interpretation of Snow Properties from Imaging Spectrometry." *Remote Sensing of Environment* 113 (September): S25–37.
Dyer, Jamie L., and Thomas L. Mote. 2006. "Spatial Variability and Trends in Observed Snow Depth over North America." *Geophysical Research Letters* 33 (16). https://doi.org/10.1029/2006gl027258.
Ebel, Brian A., John A. Moody, and Deborah A. Martin. 2012. "Hydrologic Conditions Controlling Runoff Generation Immediately after Wildfire." *Water Resources Research* 48 (3). https://doi.org/10.1029/2011wr011470.
Eidenshink, Jeff, Brian Schwind, Ken Brewer, Zhi-Liang Zhu, Brad Quayle, and Stephen Howard. 2007. "A Project for Monitoring Trends in Burn Severity." *Fire Ecology* 3 (1): 3–21.
Ellis, C. R., J. W. Pomeroy, R. L. H. Essery, and T. E. Link. 2011. "Effects of Needleleaf Forest Cover on Radiation and Snowmelt Dynamics in the Canadian Rocky Mountains." *Canadian Journal of Forest Research* 41 (3): 608–20.
Essery, Richard, John Pomeroy, Jason Parviainen, and Pascal Storck. 2003. "Sublimation of Snow from Coniferous Forests in a Climate Model." *Journal of Climate* 16 (11): 1855–64.
"Existing Vegetation Height." 2022. Landfire. 2022. https://landfire.gov/evh.php.
Flanner, M. G., C. S. Zender, P. G. Hess, N. M. Mahowald, T. H. Painter, V. Ramanathan, and P. J. Rasch. 2009. "Springtime Warming and Reduced Snow Cover from Carbonaceous Particles." *Atmospheric Chemistry and Physics* 9 (7): 2481–97.
Frei, A., M. Tedesco, S. Lee, J. Foster, and D. K. Hall. 2012. "A Review of Global Satellite-Derived Snow Products." *Advances in Space*. https://www.sciencedirect.com/science/article/pii/S0273117711008611.
Freitas, Letícia de, Jener de Moraes, Adriana da Costa, Letícia Martins, Bruno Silva, Junior Avanzi, and Alexandre Uezu. 2022. "How Far Can Nature-Based Solutions Increase Water Supply Resilience to Climate Change in One of the Most Important Brazilian Watersheds?" *Earth (Basel, Switzerland)* 3 (3): 748–67.
Gersh, Max, Kelly E. Gleason, and Anton Surunis. 2022. "Forest Fire Effects on Landscape Snow Albedo Recovery and Decay." *Remote Sensing* 14 (16): 4079.
Gilliam, Frank S. 2016. "Forest Ecosystems of Temperate Climatic Regions: From Ancient Use to Climate Change." *The New Phytologist* 212 (4): 871–87.
Gleason, K. E., and A. W. Nolin. 2016. "Charred Forests Accelerate Snow Albedo Decay: Parameterizing the Post-fire Radiative Forcing on Snow for Three Years Following Fire." *Hydrological Processes*. https://onlinelibrary.wiley.com/doi/abs/10.1002/hyp.10897.
Gleason, K. E., A. W. Nolin, and T. R. Roth. 2017. "Developing a Representative Snow-Monitoring Network in a Forested Mountain Watershed." *Hydrology and Earth System Sciences*. https://hess.copernicus.org/articles/21/1137/2017/.
Gleason, Kelly. 2015. "Forest Fire Effects on Radiative and Turbulent Fluxes over Snow: Implications for Snow Hydrology."

Gleason, Kelly, Joseph R. McConnell, Monica M. Arienzo, Nathan Chellman, and Wendy M. Calvin. 2019. “Four-Fold Increase in Solar Forcing on Snow in Western U.S. Burned Forests since 1999.” *Nature Communications* 10 (1): 2026.

Gleason, Kelly, Anne Nolin, and Travis R. Roth. 2013. “Charred Forests Increase Snowmelt: Effects of Burned Woody Debris and Incoming Solar Radiation on Snow Ablation.” *Geophysical Research Letters* 40 (17): 4654–61.

Golding, D. L., and R. H. Swanson. 1978. “Snow Accumulation and Melt in Small Forest Openings in Alberta.” *Canadian Journal of Forest Research* 8 (4): 380–88.

———. 1986. “Snow Distribution Patterns in Clearings and Adjacent Forest.” *Water Resources Research*. https://doi.org/10.1029/WR022i013p01931.

Goodell goodell, B. 1952. “Watershed-Management Aspects of Thinned Young Lodgepole Pine Stands.” *CrossRef Full Text | Google Scholar* 50: 374–78.

Gordon, A. D., L. Breiman, J. H. Friedman, R. A. Olshen, and C. J. Stone. 1984. “Classification and Regression Trees.” *Biometrics* 40 (3): 874.

Hamlet, Alan F., and Dennis P. Lettenmaier. 1999. “Effects of Climate Change on Hydrology and Water Resources in the Columbia River Basin.” *Journal of the American Water Resources Association* 35 (6): 1597–1623.

Harding, R. J., and J. W. Pomeroy. 1996. “The Energy Balance of the Winter Boreal Landscape.” *Journal of Climate*. https://journals.ametsoc.org/view/journals/clim/9/11/1520-0442_1996_009_2778_tebotw_2_0_co_2.xml.

Hardy, J. P., R. Melloh, G. Koenig, D. Marks, A. Winstral, J. W. Pomeroy, and T. Link. 2004. “Solar Radiation Transmission through Conifer Canopies.” *Agricultural and Forest Meteorology* 126 (3–4): 257–70.

Hardy, J. P., R. Melloh, P. Robinson, and R. Jordan. 2000. “Incorporating Effects of Forest Litter in a Snow Process Model.” *Hydrological Processes* 14 (18): 3227–37.

Harley, Grant L., R. Stockton Maxwell, Bryan A. Black, and Matthew F. Bekker. 2020. “A Multi-Century, Tree-Ring-Derived Perspective of the North Cascades (USA) 2014–2016 Snow Drought.” *Climatic Change* 162 (1): 127–43.

Harpold, A. A., S. Rajagopal, J. B. Crews, T. Winchell, and R. Schumer. 2017. “Relative Humidity Has Uneven Effects on Shifts from Snow to Rain over the Western U.s.” *Geophysical Research Letters* 44 (19): 9742–50.

Harpold, Adrian A., Joel A. Biederman, Katherine Condon, Manuel Merino, Yoganand Korgaonkar, Tongchao Nan, Lindsey L. Sloat, Morgan Ross, and Paul D. Brooks. 2014. “Changes in Snow Accumulation and Ablation Following the Las Conchas Forest Fire, New Mexico, USA.” *Ecohydrology* 7 (2): 440–52.

Harpold, Adrian A., Sebastian A. Krogh, Mackenzie Kohler, Devon Eckberg, Jonathan Greenberg, Gary Sterle, and Patrick D. Broxton. 2020. “Increasing the Efficacy of Forest Thinning for Snow Using High-resolution Modeling: A Proof of Concept in the Lake Tahoe Basin, California, USA.” *Ecohydrology: Ecosystems, Land and Water Process Interactions, Ecohydrogeomorphology* 13 (4). https://doi.org/10.1002/eco.2203.

Harpold, Adrian A., and Noah P. Molotch. 2015. “Sensitivity of Soil Water Availability to Changing Snowmelt Timing in the Western U.S.” *Geophysical Research Letters* 42 (19): 8011–20.

Hatchett, Benjamin J., Arielle L. Koshkin, Kristen Guirguis, Karl Rittger, Anne W. Nolin, Anne Heggli, Alan M. Rhoades, et al. 2023. “Midwinter Dry Spells Amplify Post-fire Snowpack Decline.” *Geophysical Research Letters* 50 (3). https://doi.org/10.1029/2022gl101235.

Hedstrom, N. R., and J. W. Pomeroy. 1998. “Measurements and Modelling of Snow Interception in the Boreal Forest.” *Hydrological Processes* 12 (10–11): 1611–25.

Heeswijk, Marijke van, John S. Kimball, and Danny Marks. 1996. *Simulation of Water Available for Runoff in Clearcut Forest Openings During Rain-on-Snow Events in the Western Cascade Range of Oregon and Washington*. U.S. Department of the Interior, Geological Survey.

Henderson, Gina R., Yannick Peings, Jason C. Furtado, and Paul J. Kushner. 2018. “Snow–Atmosphere Coupling in the Northern Hemisphere.” *Nature Climate Change* 8 (11): 954–63.

Hoover, Katie, Laura A. Hanson, and Congressional Research Service. 2021. “Wildfire Statistics.” Congressional Research Service. https://apps.dtic.mil/sti/citations/AD1143321.

Hopkinson, Chris, Mike Sitar, Laura Chasmer, Chris Gynan, David Agro, Robert Enter, James Foster, et al. 2001. “Mapping the Spatial Distribution of Snowpack Depth beneath a Variable Forest Canopy Using Airborne Laser Altimetry.” In *Proceedings of the 58th Eastern Snow Conference, Ottawa, Ontario, Canada: USA, Eastern Snow Conference*, 253–64. academia.edu.

Houze, Robert A., Jr. 2012. “Orographic Effects on Precipitating Clouds.” *Reviews of Geophysics* 50 (1). https://doi.org/10.1029/2011rg000365.

Huang, Shengzhi, Jianxia Chang, Qiang Huang, Yutong Chen, and Guoyong Leng. 2016. “Quantifying the Relative Contribution of Climate and Human Impacts on Runoff Change Based on the Budyko Hypothesis and SVM Model.” *Water Resources Management* 30 (7): 2377–90.

Huntington, Justin L., and Richard G. Niswonger. 2012. “Role of Surface-Water and Groundwater Interactions on Projected Summertime Streamflow in Snow Dominated Regions: An Integrated Modeling Approach.” *Water Resources Research* 48 (11). https://agupubs.onlinelibrary.wiley.com/doi/abs/10.1029/2012WR012319.

Hutchison, Boyd A., and Detlef R. Matt. 1977. “The Distribution of Solar Radiation within a Deciduous Forest.” *Ecological Monographs* 47 (2): 185–207.

“Hydrologic Modeling System.” 2002. HEC HMS Applications Guide. 2002.

“Incident Information System.” 2021. National Wildfire Coordinating Group.

Intergovernmental Panel on Climate Change. 2007. *Climate Change 2007 - The Physical Science Basis: Working Group I Contribution to the Fourth Assessment Report of the IPCC*. Cambridge University Press.

Jefferson, Anne, Anne Nolin, Sarah Lewis, and Christina Tague. 2008. “Hydrogeologic Controls on Streamflow Sensitivity to Climate Variation.” *Hydrological Processes* 22 (22): 4371–85.

Jennings, Tori L. 2011. “Transcending the Adaptation/Mitigation Climate Change Science Policy Debate: Unmasking Assumptions about Adaptation and Resilience.” *Weather, Climate, and Society* 3 (4): 238–48.

Jeong, Su-Jong, David Medvigy, Elena Shevliakova, and Sergey Malyshev. 2012. “Uncertainties in Terrestrial Carbon Budgets Related to Spring Phenology.” *Journal of Geophysical Research: Biogeosciences* 117 (G1). https://doi.org/10.1029/2011JG001868.

Jimmy Kagan, Kyla Zaret, Joe Bernert and Emilie Henderson. 2018. “Methodology for Creating the 2018 Oregon Habitat Map.”

Jin, Zhonghai, Thomas P. Charlock, Ping Yang, Yu Xie, and Walter Miller. 2008. “Snow Optical Properties for Different Particle Shapes with Application to Snow Grain Size Retrieval and MODIS/CERES Radiance Comparison over Antarctica.” *Remote Sensing of Environment* 112 (9): 3563–81.

Jost, Georg, Markus Weiler, David R. Gluns, and Younes Alila. 2007. “The Influence of Forest and Topography on Snow Accumulation and Melt at the Watershed-Scale.” *Journal of Hydrology* 347 (1–2): 101–15.

Kanyongo, Gibbs Y. 2005. “The Influence of Reliability on Four Rules for Determining the Number of Components to Retain.” *Journal of Modern Applied Statistical Methods: JMASM* 5 (2): 332–43.

Kapnick, Sarah, and Alex Hall. 2012. “Causes of Recent Changes in Western North American Snowpack.” *Climate Dynamics* 38 (9–10): 1885–99.

Kenyon, Kathleen M. 1956. “Jericho and Its Setting in Near Eastern History.” *Antiquity* 30 (120): 184–97.

Kittredge, Joseph. 1953. “Influences of Forests on Snow in the Ponderosa-Sugar Pine-Fir Zone of the Central Sierra Nevada.” *Hilgardia* 22 (1): 1–96.

Kitzberger, Thomas, Donald A. Falk, Anthony L. Westerling, and Thomas W. Swetnam. 2017. “Direct and Indirect Climate Controls Predict Heterogeneous Early-Mid 21st Century Wildfire Burned Area across Western and Boreal North America.” *PloS One* 12 (12): e0188486.

Klos, P. Zion, Timothy E. Link, and John T. Abatzoglou. 2014. “Extent of the Rain-Snow Transition Zone in the Western U.S. under Historic and Projected Climate.” *Geophysical Research Letters* 41 (13): 4560–68.

Krogh, Sebastian A., Patrick D. Broxton, Patricia N. Manley, and Adrian A. Harpold. 2020. “Using Process Based Snow Modeling and Lidar to Predict the Effects of Forest Thinning on the Northern Sierra Nevada Snowpack.” *Frontiers in Forests and Global Change* 3 (March). https://doi.org/10.3389/ffgc.2020.00021.

Lang, Dengxiao, Jiangkun Zheng, Jiaqi Shi, Feng Liao, Xing Ma, Wenwu Wang, Xuli Chen, and Mingfang Zhang. 2017. “A Comparative Study of Potential Evapotranspiration Estimation by Eight Methods with FAO Penman–Monteith Method in Southwestern China.” *Water* 9 (10): 734.

Lawler, Robert R., and Timothy E. Link. 2011. “Quantification of Incoming All-Wave Radiation in Discontinuous Forest Canopies with Application to Snowmelt Prediction.” *Hydrological Processes* 25 (21): 3322–31.

Lee, Xuhui, William Massman, and Beverly Law. 2004. *Handbook of Micrometeorology: A Guide for Surface Flux Measurement and Analysis*. Springer Science & Business Media.

Li, Dongyue, Melissa L. Wrzesien, Michael Durand, Jennifer Adam, and Dennis P. Lettenmaier. 2017. "How Much Runoff Originates as Snow in the Western United States, and How Will That Change in the Future?" *Geophysical Research Letters* 44 (12): 6163–72.

Link, Timothy E., and Danny Marks. 1999. "Point Simulation of Seasonal Snow Cover Dynamics beneath Boreal Forest Canopies." *Journal of Geophysical Research* 104 (D22): 27841–57.

Link, Timothy E., Danny Marks, and Janet P. Hardy. 2004. "A Deterministic Method to Characterize Canopy Radiative Transfer Properties." *Hydrological Processes* 18 (18): 3583–94.

Littell, Jeremy S., David L. Peterson, Karin L. Riley, Yongquiang Liu, and Charles H. Luce. 2016. "A Review of the Relationships between Drought and Forest Fire in the United States." *Global Change Biology* 22 (7): 2353–69.

López-Moreno, J. I., S. Gascoin, J. Herrero, E. A. Sproles, M. Pons, E. Alonso-González, L. Hanich, et al. 2017. "Different Sensitivities of Snowpacks to Warming in Mediterranean Climate Mountain Areas." *Environmental Research Letters: ERL [Web Site]* 12 (7): 074006.

López-Moreno, J. I., Jean Michel Soubeyroux, Simon Gascoin, E. Alonso-Gonzalez, Nuria Durán-Gómez, Matthieu Lafaysse, Matthieu Vernay, Carlo Carmagnola, and Samuel Morin. 2020. "Long-term Trends (1958–2017) in Snow Cover Duration and Depth in the Pyrenees." *International Journal of Climatology* 40 (14): 6122–36.

Luce, Charles, Brian Staab, Marc Kramer, Seth Wenger, Dan Isaak, and Callie McConnell. 2014. "Sensitivity of Summer Stream Temperatures to Climate Variability in the Pacific Northwest." *Water Resources Research* 50 (4): 3428–43.

Lundberg, Angela, Nils Granlund, and David Gustafsson. 2010. "Towards Automated 'Ground Truth' Snow Measurements-a Review of Operational and New Measurement Methods for Sweden, Norway, and Finland." *Hydrological Processes*. https://doi.org/10.1002/hyp.7658.

Lundquist, J. D., and D. R. Cayan. 2007. "Surface Temperature Patterns in Complex Terrain: Daily Variations and Long-term Change in the Central Sierra Nevada, California." *Journal of Geophysical Research*. https://agupubs.onlinelibrary.wiley.com/doi/abs/10.1029/2006JD007561.

Lundquist, J. D., and S. E. Dickerson-Lange. 2013. "Lower Forest Density Enhances Snow Retention in Regions with Warmer Winters: A Global Framework Developed from Plot-scale Observations and Modeling." *Water Resources*. https://agupubs.onlinelibrary.wiley.com/doi/abs/10.1002/wrcr.20504.

Lyon, Steve W., Peter A. Troch, Patrick D. Broxton, Noah P. Molotch, and Paul D. Brooks. 2008. "Monitoring the Timing of Snowmelt and the Initiation of Streamflow Using a Distributed Network of Temperature/Light Sensors." *Ecohydrology: Ecosystems, Land and Water Process Interactions, Ecohydrogeomorphology* 1 (3): 215–24.

Male, D. H., and R. J. Granger. 1981. “Snow Surface Energy Exchange.” *Water Resources Research* 17 (3): 609–27.
Marks, Danny, and Jeff Dozier. 1992. “Climate and Energy Exchange at the Snow Surface in the Alpine Region of the Sierra Nevada: 2. Snow Cover Energy Balance.” *Water Resources Research* 28 (11): 3043–54.
Marks, Danny, John Kimball, Dave Tingey, and Tim Link. 1998. “The Sensitivity of Snowmelt Processes to Climate Conditions and Forest Cover during Rain-on-Snow: A Case Study of the 1996 Pacific Northwest Flood.” *Hydrological Processes* 12 (10–11): 1569–87.
Massman, W. J., R. A. Sommerfeld, A. R. Mosier, K. F. Zeller, T. J. Hehn, and S. G. Rochelle. 1997. “A Model Investigation of Turbulence-Driven Pressure-Pumping Effects on the Rate of Diffusion of CO2, N2O, and CH4through Layered Snowpacks.” *Journal of Geophysical Research* 102 (D15): 18851–63.
Mastrotheodoros, Theodoros, Christoforos Pappas, Peter Molnar, Paolo Burlando, Gabriele Manoli, Juraj Parajka, Riccardo Rigon, et al. 2020. “More Green and Less Blue Water in the Alps during Warmer Summers.” *Nature Climate Change* 10 (2): 155–61.
Maxwell, Jordan, and Samuel B. St Clair. 2019. “Snowpack Properties Vary in Response to Burn Severity Gradients in Montane Forests.” *Environmental Research Letters* 14 (12): 124094.
Mazzotti, Giulia, William Ryan Currier, Jeffrey S. Deems, Justin M. Pflug, Jessica D. Lundquist, and Tobias Jonas. 2019. “Revisiting Snow Cover Variability and Canopy Structure within Forest Stands: Insights from Airborne Lidar Data.” *Water Resources Research* 55 (7): 6198–6216.
McGrath, Daniel, Lucas Zeller, Randall Bonnell, Wyatt Reis, Stephanie Kampf, Keith Williams, Marianne Okal, et al. 2023. “Declines in Peak Snow Water Equivalent and Elevated Snowmelt Rates Following the 2020 Cameron Peak Wildfire in Northern Colorado.” *Geophysical Research Letters* 50 (6): e2022GL101294.
McLaughlin, Daniel L., David A. Kaplan, and Matthew J. Cohen. 2013. “Managing Forests for Increased Regional Water Yield in the Southeastern U.s. Coastal Plain.” *Journal of the American Water Resources Association* 49 (4): 953–65.
Meromy, Leah, Noah P. Molotch, Timothy E. Link, Steven R. Fassnacht, and Robert Rice. 2013. “Subgrid Variability of Snow Water Equivalent at Operational Snow Stations in the Western USA.” *Hydrological Processes* 27 (17): 2383–2400.
Mikkelson, K. M., R. M. Maxwell, I. Ferguson, J. D. Stednick, J. E. McCray, and J. O. Sharp. 2013. “Mountain Pine Beetle Infestation Impacts: Modeling Water and Energy Budgets at the Hill-Slope Scale.” *Ecohydrology* 6 (1): 64–72.
Molotch, Noah P., Peter D. Blanken, Mark W. Williams, Andrew A. Turnipseed, Russell K. Monson, and Steven A. Margulis. 2007. “Estimating Sublimation of Intercepted and Sub-Canopy Snow Using Eddy Covariance Systems.” *Hydrological Processes* 21 (12): 1567–75.
Morris, E. M. 1989. “Turbulent Transfer over Snow and Ice.” *Journal of Hydrology* 105: 205–23.

Mote, P. W., S. Li, D. P. Lettenmaier, and M. Xiao. 2018. “Dramatic Declines in Snowpack in the Western US.” *Npj Climate And*. https://www.nature.com/articles/s41612-018-0012-1.

Mote, Philip W., Alan F. Hamlet, Martyn P. Clark, and Dennis P. Lettenmaier. 2005. “Declining Mountain Snowpack in Western North America.” *Bulletin of the American Meteorological Society* 86 (1): 39–50.

Mott, R., D. Scipión, M. Schneebeli, N. Dawes, A. Berne, and M. Lehning. 2014. “Orographic Effects on Snow Deposition Patterns in Mountainous Terrain.” *Journal of Geophysical Research* 119 (3): 1419–39.

Mueller, Rebecca C., Crescent M. Scudder, Marianne E. Porter, R. Talbot Trotter III, Catherine A. Gehring, and Thomas G. Whitham. 2005. “Differential Tree Mortality in Response to Severe Drought: Evidence for Long-Term Vegetation Shifts.” *The Journal of Ecology* 93 (6): 1085–93.

Musselman, Keith N., Nans Addor, Julie A. Vano, and Noah P. Molotch. 2021. “Winter Melt Trends Portend Widespread Declines in Snow Water Resources.” *Nature Climate Change* 2021 (April). https://doi.org/10.1038/s41558-021-01014-9.

Musselman, Keith N., John W. Pomeroy, and Timothy E. Link. 2015. “Variability in Shortwave Irradiance Caused by Forest Gaps: Measurements, Modelling, and Implications for Snow Energetics.” *Agricultural and Forest Meteorology* 207 (July): 69–82.

Niknami, Kimberly Jones And. 2012. “Watershed Boundary Dataset.” USGS National Hydrography. 2012. https://www.usgs.gov/publications/federal-standards-and-procedures-national-watershed-boundary-dataset-wbd.

Nolin, Anne W. 2010. “Recent Advances in Remote Sensing of Seasonal Snow.” *Journal of Glaciology* 56 (200): 1141–50.

Nolin, Anne W., and Christopher Daly. 2006. “Mapping ‘at Risk’ Snow in the Pacific Northwest.” *Journal of Hydrometeorology* 7 (5): 1164–71.

Oregon State University data created 4 Feb 2014, accessed 16 Dec 2020. 2014. “30-Year Normals.” PRISM Climate Group. February 4, 2014. https://prism.oregonstate.edu.

Painter, Thomas H., Andrew P. Barrett, Christopher C. Landry, Jason C. Neff, Maureen P. Cassidy, Corey R. Lawrence, Kathleen E. McBride, and G. Lang Farmer. 2007. “Impact of Disturbed Desert Soils on Duration of Mountain Snow Cover.” *Geophysical Research Letters* 34 (12). https://doi.org/10.1029/2007gl030284.

Painter, Thomas H., Ann C. Bryant, and S. Mckenzie Skiles. 2012. “Radiative Forcing by Light Absorbing Impurities in Snow from MODIS Surface Reflectance Data.” *Geophysical Research Letters* 39 (17). https://doi.org/10.1029/2012gl052457.

Pickett, Evelyne Stitt. 1995. “James Edward Church, Jr., and the Development of Snow Surveying for Runoff Forecasting.” *Yearbook of the Association of Pacific Coast Geographers* 57: 57–75.

Pomeroy, J. W., and K. Dion. 1996. “WINTER RADIATION EXTINCTION AND REFLECTION IN A BOREAL PINE CANOPY: MEASUREMENTS AND MODELLING.” *Hydrological Processes* 10 (12): 1591–1608.

Pomeroy, John, Chad Ellis, Aled Rowlands, Richard Essery, Janet Hardy, Tim Link, Danny Marks, and Jean Emmanuel Sicart. 2008. “Spatial Variability of

Shortwave Irradiance for Snowmelt in Forests." *Journal of Hydrometeorology* 9 (6): 1482–90.
Pomeroy, John W., and R. A. Schmidt. 1993. "The Use of Fractal Geometry in Modelling Intercepted Snow Accumulation and Sublimation." In *Proceedings of the Eastern Snow Conference*, 50:1–10. westernsnowconference.org.
Portland Environmental Services. 2017. "Willamette Watershed." City of Portland Environmental Services. 2017. https://www.portlandoregon.gov/bes/30938#:~:text=The%20Willamette%20River%20stretches%20nearly,more%20than%2011%2C500%20square%20miles.
Prism Climate Group, OSU, USDA. 2022. "Recent Years (Jan 1981 - Apr 2022)." Prism Climate Group. 2022. https://prism.oregonstate.edu/.
R Core Team. 2023. "R: A Language and Environemetn for Statistisical Computing. R Foundation for Statistical Computing, Vienna, Austria." https://www.R-project.org/.
Ross, Robert T., and Arthur J. Nozik. 1982. "Efficiency of Hot-carrier Solar Energy Converters." *Journal of Applied Physics* 53 (May).
Roth, Travis R., and Anne W. Nolin. 2017. "Forest Impacts on Snow Accumulation and Ablation across an Elevation Gradient in a Temperate Montane Environment." *Hydrology and Earth System Sciences* 21 (11): 5427–42.
Rowse, John, and Calum J. Center. 1998. "Forest Harvesting to Optimize Timber Production and Water Runoff." *Socio-Economic Planning Sciences* 32 (4): 277–93.
Rutter, Nick, Richard Essery, John Pomeroy, Nuria Altimir, Kostas Andreadis, Ian Baker, Alan Barr, et al. 2009. "Evaluation of Forest Snow Processes Models (SnowMIP2)." *Journal of Geophysical Research* 114 (D6). https://doi.org/10.1029/2008jd011063.
Saksa, P. C., M. H. Conklin, J. J. Battles, C. L. Tague, and R. C. Bales. 2017. "Forest Thinning Impacts on the Water Balance of Sierra Nevada Mixed-Conifer Headwater Basins." *Water Resources Research* 53 (7): 5364–81.
Saydi, Muattar, and Jian-Li Ding. 2020. "Impacts of Topographic Factors on Regional Snow Cover Characteristics." *Water Science and Engineering* 13 (3): 171–80.
Schneider, Eryn E., David L. R. Affleck, and Andrew J. Larson. 2019. "Tree Spatial Patterns Modulate Peak Snow Accumulation and Snow Disappearance." *Forest Ecology and Management* 441 (June): 9–19.
Schnorbus, Markus, and Younes Alila. 2004. "Forest Harvesting Impacts on the Peak Flow Regime in the Columbia Mountains of Southeastern British Columbia: An Investigation Using Long-Term Numerical Modeling." *Water Resources Research* 40 (5). https://doi.org/10.1029/2003wr002918.
Schweizer, Jürg, Kalle Kronholm, J. Bruce Jamieson, and Karl W. Birkeland. 2008. "Review of Spatial Variability of Snowpack Properties and Its Importance for Avalanche Formation." *Cold Regions Science and Technology* 51 (2): 253–72.
Selkowitz, D. J., T. H. Painter, and K. E. Rittger. 2017. "The USGS Landsat Snow Covered Area Products: Methods and Preliminary Validation." *Approaches for Snow* .... https://www.researchgate.net/profile/David-Selkowitz/publication/331024289_The_USGS_Landsat_Snow_Covered_Area_Pr

oducts_Methods_and_Preliminary_Validation/links/5c61d08092851c48a9cd3d7a/The-USGS-Landsat-Snow-Covered-Area-Products-Methods-and-Preliminary-Validation.pdf.
Seyednasrollah, Bijan, Mukesh Kumar, and Timothy E. Link. 2013. "On the Role of Vegetation Density on Net Snow Cover Radiation at the Forest Floor." *Journal of Geophysical Research* 118 (15): 8359–74.
Sicart, J. E., J. W. Pomeroy, R. L. H. Essery, and D. Bewley. 2006. "Incoming Longwave Radiation to Melting Snow: Observations, Sensitivity and Estimation in Northern Environments." *Hydrological Processes* 20 (17): 3697–3708.
Skiles, S. Mckenzie, Thomas H. Painter, Jeffrey S. Deems, Ann C. Bryant, and Christopher C. Landry. 2012. "Dust Radiative Forcing in Snow of the Upper Colorado River Basin: 2. Interannual Variability in Radiative Forcing and Snowmelt Rates." *Water Resources Research* 48 (7). https://doi.org/10.1029/2012wr011986.
Smoot, Emily E., and Kelly E. Gleason. 2020. "Forest Fire Effects on Snow Storage and Melt."
St Denis Amanda Lee Hughes Leysia Palen, Lise. 2012. "The Deployment of Trusted Digital Volunteers in the 2011 Shadow Lake Fire." In *Trial by Fire: The Deployment of Trusted Digital Volunteers in the 2011 Shadow Lake Fire*.
State of California. 2022. "Challenges of Forecasting Water Supply in a Hotter Climate." California Department of Water Resources. April 11, 2022. https://water.ca.gov/News/Blog/2022/April-22/Forecasting-Water-Supply-Hotter-Climate.
Stavros, E. Natasha, John Abatzoglou, Narasimhan K. Larkin, Donald McKenzie, and E. Ashley Steel. 2014. "Climate and Very Large Wildland Fires in the Contiguous Western USA." *International Journal of Wildland Fire* 23 (7): 899.
Stewart, Iris T. 2009. "Changes in Snowpack and Snowmelt Runoff for Key Mountain Regions." *Hydrological Processes* 23 (1): 78–94.
Stewart, Iris T., Daniel R. Cayan, and Michael D. Dettinger. 2004. "Changes in Snowmelt Runoff Timing in Western North America under a `business as Usual' Climate Change Scenario." *Climatic Change* 62 (1–3): 217–32.
Stillinger, Timbo, Christopher Costello, Roger C. Bales, and Jeff Dozier. 2021. "Reservoir Operators React to Uncertainty in Snowmelt Runoff Forecasts." *Journal of Water Resources Planning and Management* 147 (10): 06021010.
Storck, Pascal, Dennis P. Lettenmaier, and Susan M. Bolton. 2002. "Measurement of Snow Interception and Canopy Effects on Snow Accumulation and Melt in a Mountainous Maritime Climate, Oregon, United States." *Water Resources Research* 38 (11): 5-1-5–16.
Sturm, M., J. Holmgren, and G. E. Liston. 1995. "A Seasonal Snow Cover Classification System for Local to Global Applications." *Journal of Climate*. https://journals.ametsoc.org/view/journals/clim/8/5/1520-0442_1995_008_1261_asscc s_2_0_co_2.xml.
Sun, N., H. Yan, and M. S. Wigmosta. 2022. "Forest Canopy Density Effects on Snowpack across the Climate Gradients of the Western United States Mountain

Ranges." *Water Resources*. https://agupubs.onlinelibrary.wiley.com/doi/abs/10.1029/2020WR029194.
Tague, Christina, and Gordon E. Grant. 2004. "A Geological Framework for Interpreting the Low-Flow Regimes of Cascade Streams, Willamette River Basin, Oregon." *Water Resources Research* 40 (4). https://doi.org/10.1029/2003wr002629.
Taylor, G., and C. Hannan. 1999. *The Climate of Oregon: From Rain Forest to Desert*. Corvallis, Oregon: Oregon State University Press.
Thackeray, Chad W., and Christopher G. Fletcher. 2016. "Snow Albedo Feedback: Current Knowledge, Importance, Outstanding Issues and Future Directions." *Progress in Physical Geography: Earth and Environment* 40 (3): 392–408.
Trouet, Valerie, Alan H. Taylor, Andrew M. Carleton, and Carl N. Skinner. 2006. "Fire-Climate Interactions in Forests of the American Pacific Coast." *Geophysical Research Letters* 33 (18). https://doi.org/10.1029/2006gl027502.
Uecker, Ted M., Susan D. Kaspari, Keith N. Musselman, and S. McKenzie Skiles. 2020. "The Post-Wildfire Impact of Burn Severity and Age on Black Carbon Snow Deposition and Implications for Snow Water Resources, Cascade Range, Washington." *Journal of Hydrometeorology* 21 (8): 1777–92.
Us Epa, Oar. 2016. "Climate Change Indicators: Snowpack," July. https://www.epa.gov/climate-indicators/climate-change-indicators-snowpack.
Varhola, Andrés, Nicholas C. Coops, Markus Weiler, and R. Dan Moore. 2010. "Forest Canopy Effects on Snow Accumulation and Ablation: An Integrative Review of Empirical Results." *Journal of Hydrology* 392 (3): 219–33.
Vilà-Vilardell, Lena, Miquel De Cáceres, Míriam Piqué, and Pere Casals. 2023. "Prescribed Fire after Thinning Increased Resistance of Sub-Mediterranean Pine Forests to Drought Events and Wildfires." *Forest Ecology and Management* 527 (January): 120602.
Walsh, Megan Kathleen. 2008. "Natural and Anthropogenic Influences on the Holocene Fire and Vegetation History of the Willamette Valley, Northwest Oregon and Southwest Washington." http://www.worldcat.org/title/449187260.
Warren, Stephen G., and Warren J. Wiscombe. 1980. "A Model for the Spectral Albedo of Snow. II: Snow Containing Atmospheric Aerosols." *Journal of the Atmospheric Sciences* 37 (12): 2734–45.
Westerling, A. L., H. G. Hidalgo, D. R. Cayan, and T. W. Swetnam. 2006. "Warming and Earlier Spring Increase Western U.S. Forest Wildfire Activity." *Science* 313 (5789): 940–43.
Westerling, Anthony Leroy. 2016. "Increasing Western US Forest Wildfire Activity: Sensitivity to Changes in the Timing of Spring." *Philosophical Transactions of the Royal Society of London. Series B, Biological Sciences* 371 (1696): 20150178.
Wheeler, Tim, and Joachim von Braun. 2013. "Climate Change Impacts on Global Food Security." *Science (New York, N.Y.)* 341 (6145): 508–13.
Williams, A. Park, Ben Livneh, Karen A. McKinnon, Winslow D. Hansen, Justin S. Mankin, Benjamin I. Cook, Jason E. Smerdon, et al. 2022. "Growing Impact of Wildfire on Western US Water Supply." *Proceedings of the National Academy of Sciences of the United States of America* 119 (10). https://doi.org/10.1073/pnas.2114069119.

Winkler, Rita D., and Others. 2011. “Changes in Snow Accumulation and Ablation after a Fire in South-Central British Columbia.” *Streamline Watershed Management Bulletin* 14 (2): 1–7.
Winstral, Adam, and Danny Marks. 2014. “Long-Term Snow Distribution Observations in a Mountain Catchment: Assessing Variability, Time Stability, and the Representativeness of an Index Site.” *Water Resources Research* 50 (1): 293–305.
Wiscombe, Warren J., and Stephen G. Warren. 1980. “A Model for the Spectral Albedo of Snow. I: Pure Snow.” *Journal of the Atmospheric Sciences* 37 (12): 2712–33.
Xue, Xinbo, Shichao Jin, Feng An, Huaiqing Zhang, Jiangchuan Fan, Markus P. Eichhorn, Chengye Jin, Bangqian Chen, Ling Jiang, and Ting Yun. 2022. “Shortwave Radiation Calculation for Forest Plots Using Airborne LiDAR Data and Computer Graphics.” *Plant Phenomics (Washington, D.C.)* 2022 (July): 9856739.
Yan, Hongxiang, Ning Sun, Aimee Fullerton, and Matthew Baerwalde. 2021. “Greater Vulnerability of Snowmelt-Fed River Thermal Regimes to a Warming Climate.” *Environmental Research Letters: ERL [Web Site]* 16 (5): 054006.
Yang, Chao, Guofeng Wu, Kai Ding, Tiezhu Shi, Qingquan Li, and Jinliang Wang. 2017. “Improving Land Use/Land Cover Classification by Integrating Pixel Unmixing and Decision Tree Methods.” *Remote Sensing* 9 (12): 1222.
Yarnell, Sarah M., Joshua H. Viers, and Jeffrey F. Mount. 2010. “Ecology and Management of the Spring Snowmelt Recession.” *Bioscience* 60 (2): 114–27.
Zheng, Zeshi, Qin Ma, Shichao Jin, Yanjun Su, Qinghua Guo, and Roger C. Bales. 2019. “Canopy and terrain interactions affecting snowpack spatial patterns in the Sierra Nevada of California.” *Water resources research* 55 (11): 8721–39.
Zybach, Lapham. 2011. “B&B Complex Forest and Fire History.” *Oregon Websites and Watersheds Project*.

APPENDIX A: LITERATURE REVIEW OF THE SNOWPACK ENERGY BALANCE

Snowpack Energy Balance within forested watersheds

Snow goes through a natural maturation process that is dependent on the physical landscape it is deposited upon, as well as gross and micro-scale climate variation over its period of melt. The inputs and outputs in the snowpack's energy balance control the ripening of the snowpack and resulting preferential flow. Snow retention is heterogeneous under diverse ecosystems and canopy types (Sun, Yan, and Wigmosta 2022; Male and Granger 1981; J. Pomeroy et al. 2008; Ellis et al. 2011; Mazzotti et al. 2019; Burles and Boon 2011). Other factors include the rates of canopy interception, sublimation efficiency and sub-canopy snowpack (Sun, Yan, and Wigmosta 2022; Burles and Boon 2011; John W. Pomeroy and Schmidt 1993).

Accumulation and ablation of a snowpack are measured by physical metrics that vary with scale, seasonality, and diurnal metamorphism. Energy exchange that is absorbed or reflected is critical to the melting potential of a snowpack. The basic energy balance equation:

$$\Delta Q = S_{net} + L_{net} + H + LE + R + G$$

Where ΔQ is the change in snowpack energy storage, S_{net} and L_{net} are net shortwave and bi-lateral net longwave effects, respectively (Marks and Dozier 1992). Turbulent transport can be partitioned into the sensible heat (H) flux and latent heat transfer (LE). These two components govern the majority of the energy exchange that occurs within forested regions (Marks and Dozier 1992; John W. Pomeroy and Schmidt 1993; Sicart et al. 2006; Link, Marks, and Hardy 2004; J. W. Pomeroy and Dion 1996; J. Pomeroy et al. 2008; Hutchison and Matt 1977).

Net Radiation

Forests have wide reaching effects on the snowpack energy balance where net radiation accounts for 60 – 90% of snowmelt energy within forested watersheds (Marks and Dozier 1992; John W. Pomeroy and Schmidt 1993; Link and Marks 1999; Male and Granger 1981). For the 11 states that make up the Western U.S., 65% of their water supply originates on forested land (DeWalle and Rango 2008) making it one of the most temporally dynamic and spatially variable of all water metrics.

Shortwave Radiation

Downwelling shortwave radiation originates from the sun where incident spectral irradiance subtracted by the spectral exitance is dependent on the reflectivity of the snows surface. These values are integrated over the visible and near-infrared wavelengths and source positive energy onto the snowpack surface (Marks and Dozier 1992).

$$S_{net}=(1-\alpha)QSW\downarrow$$

α is albedo and is the ratio of reflected shortwave radiation to the downwelling shortwave radiation. Albedo varies from wavelength to wavelength and is a function of the crystalline structure of the snowpack surface, solar zenith angle, and concentrations of light-absorbing impurities (Wiscombe and Warren 1980; Warren and Wiscombe 1980). Pure snow is one of the most reflective naturally occurring substances on the earth's surface and can reflect up to 95% of solar energy in the visible wavelengths, having a significant cooling effect to global climate (Jin et al. 2008).

Forests alter spectral broadband albedo by influencing radiation and convective heat exchange (DeWalle and Rango 2008) first, by modifying the intensity and spectral composition of incident spectral irradiance as a function of forest transmissivity (Hardy et al. 2004). Then by littering organic debris onto the snow surface decreasing the snows albedo. Snow beneath the canopy of trees experiences some direct irradiance as well as diffuse incoming shortwave radiation. Key parameters are the sky view fraction, solar zenith angle, and canopy transmissivity for each component (Hutchison and Matt 1977; J. W. Pomeroy and Dion 1996; J. Pomeroy et al. 2008).

Forests of the PNW have densely littered floors comprised of decomposing bryophytes, small herbaceous plants, needles and branches (Burles and Boon 2011; Boon 2012). Forest litter and organic deposits on the snow surface reduce snowpack albedo (Hardy et al. 2000) increasing melt behavior. The snowpack and the energy balance are also subject to sub-canopy obstruction of net radiation through shading from direct sunlight (Fig.1). The flux density of shortwave that reaches the snow is the result of reflection, transmission, and absorption through foliage, wood, and the ground (Ross and Nozik 1982). Forest cover can reduce shortwave radiation on the snowpack surface and decrease melt rates (Ellis et al. 2011; Musselman, Pomeroy, and Link 2015). The fraction of shortwave radiation that penetrates through the forest canopy can be represented as a function of canopy density (Fig.1, Seyednasrollah et al., 2013).

Longwave Radiation (L_{net})

Shortwave loss due to canopy cover can be offset by advances of longwave radiation (Fig.1) under canopy where increases in net longwave from trees and trunks

amplify energy inputs (Sicart et al. 2006; Rutter et al. 2009) and ultimately alter the timing of snowmelt (Lundquist and Dickerson-Lange 2013; Roth and Nolin 2017). Net longwave flux is electromagnetic radiation emitted by a body at infrared wavelengths. The quantity of radiation emitted by a body is a function of the temperature of the surface of the body according to Plank's law.

Snow and vegetation are considered perfect emitters, also called blackbodies. Their emissivity is at or is close to 1 on a scale between 1 and 0 ("Hydrologic Modeling System" 2002). Upwelling longwave is emitted by the snow surface as energy is lost from the snow, cooling the surface. Downwelling or incoming longwave is emitted by the atmosphere and other entities surrounding the snow and is energy that warms the snow ("Hydrologic Modeling System" 2002). Direct longwave radiation makes its way through the atmosphere through gaps and openings in the forest canopy, however, nearly all longwave is exchanged beneath the forest canopy (Fig.1) and a small proportion is emitted back into the atmosphere (DeWalle and Rango 2008). Longwave increases the energy gained by the snow ("Hydrologic Modeling System" 2002).

Montane forests influence the proportion of incoming longwave radiation. Longwave from the atmosphere and the canopy combine as inputs into the snowpack surface in addition to direct shortwave absorption from trees and consequent heating during the day (Lundquist and Dickerson-Lange 2013; Sicart et al. 2006), (Hardy et al. 2004). If changes are made to the forest canopy, the energy available for snow melt will be altered (J. Pomeroy et al. 2008; Link, Marks, and Hardy 2004; Link and Marks 1999; Lundquist and Dickerson-Lange 2013). The intensity at which thermal irradiance transmits is a

function of forest structure, canopy, trunk temperature, and the Stephan's Law (Lawler and Link 2011). Reduction in the forest canopy leads to reductions in emissivity of longwave radiation (Fig.1), canopy interception (Fig.1), and the accumulation of particulate matter on the snowpack surface (Lundquist and Dickerson-Lange 2013). It is this balance between reduced accumulation and enhanced or decreased melting that determines snowpack retention under varying forest types (Dickerson-Lange and Gersonde 2017).

Turbulent Energy Transport

Melt occurring in open forest groves or meadows is driven by both turbulent and radiative flux through reduced canopy interception (Fig.1), increased light transmission, and modified surface energy balance. Turbulent transport can be partitioned into the sensible heat (H) flux and latent heat transfer (LE). Both H and LE strongly relate to boundary layer turbulence and wind speeds that drive air exchange between snowpack and the overlying atmosphere (Massman et al. 1997; Lee, Massman, and Law 2004). They are the second most important factor in their impact to the snowpack energy balance after S_{net} and L_{net}, the net shortwave and bi-lateral net longwave effects (Morris 1989). Sensible heat is energy transferred from warmer objects to a colder, (Morris 1989) while latent heat transfer occurs due to phase changes from ice to water to vapor in the atmosphere. Sublimation absorbs heat energy whereas condensation releases heat into the snowpack.

The forest acts as a buffer for wind, so protection from wind driven changes in the snowpack energy balance obscure temperature variations caused by sensible heat exchange (Dickerson-Lange and Vano 2021) and sublimation through latent heat exchange (J. Pomeroy et al. 2008). Forest canopies alter heat fluxes by intercepting falling snow in a space were the wind is more severe and sublimation rates are higher (Molotch et al. 2007).

The forest intercepts falling snow and stores it high above snowpack where large proportions are blow into the atmosphere and are either redistributed or sublimate (Molotch et al. 2007).

The final pieces of the energy exchange have a small to insignificant influence on snow in forested ecosystems. G is small net conductive energy flux (soil), generally through heat from the ground in the form of convective exchange of sensible heat [W m^{-2}]. R is net advective energy flux typically through melt water loss input from rain [W m^{-2}]. Many times, R and G have very limited influence on the snowpack energy balance and can be counted as negligible as will be in the case of this study (Marks and Dozier 1992).

APPENDIX B: SUPPLEMENTAL FIGURES

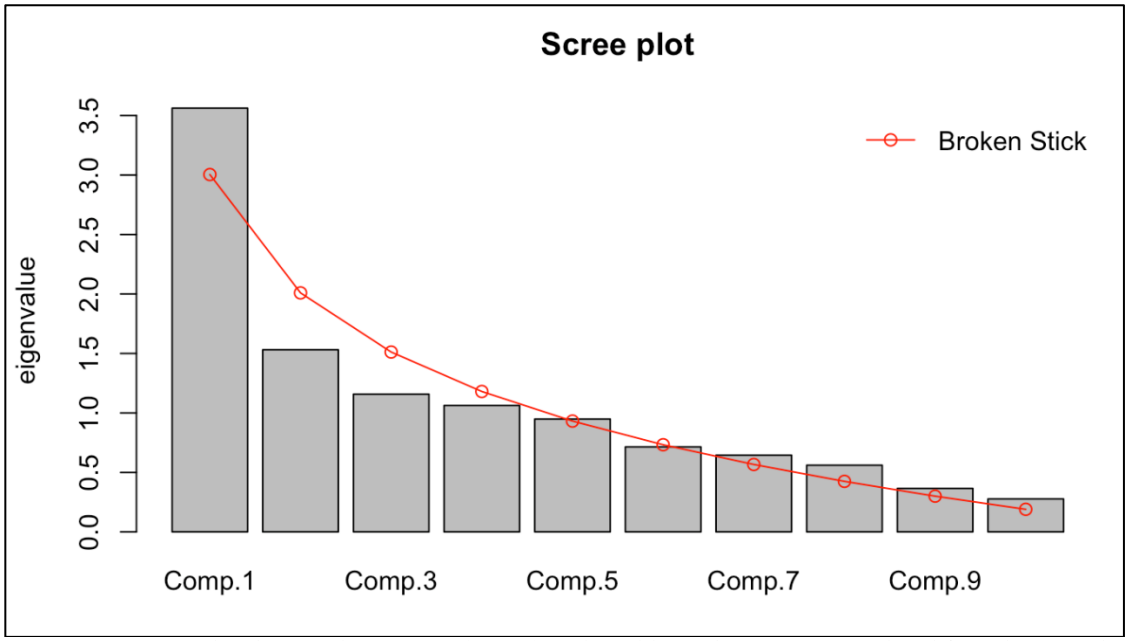

Figure A. B1: *Scree plot showing the variance (inertia) explained by each component produced from the PCA along with the level of variance expected by random change (Broken Stick). Component 1 (Comp. 1) is the only PC value that is kept because only the first observed proportion of variance (bar plot) is higher than the corresponding broken-stick proportion (red line).*

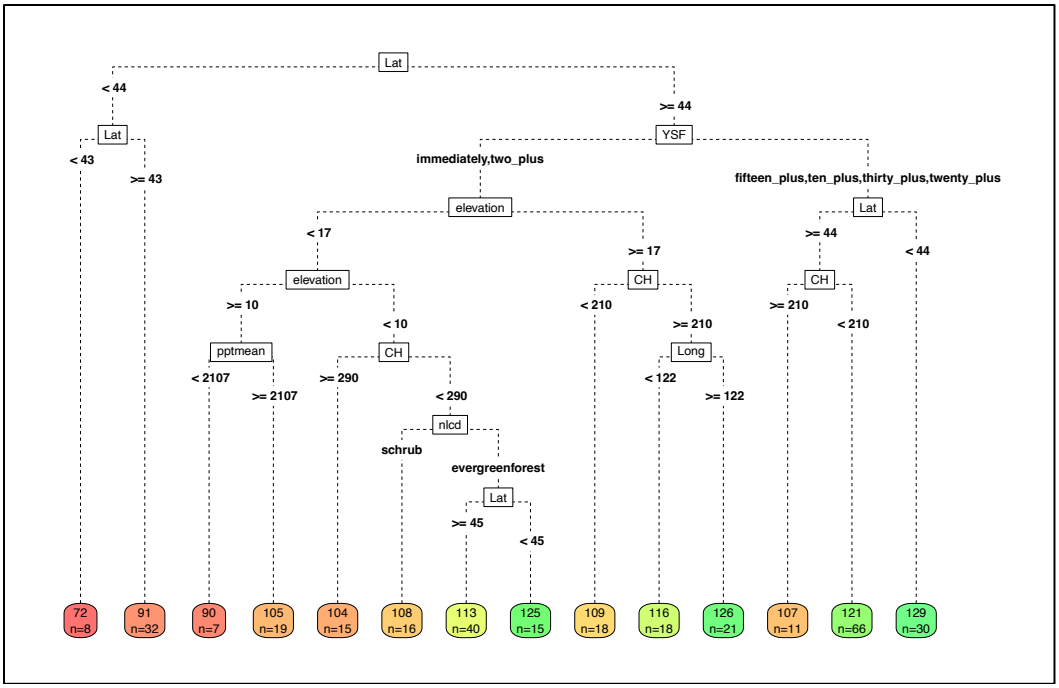

Figure A.B2: *The classification/regression tree plot displays a series of decision rules predicting Snow Disappearance (SDD) in each terminal node. Lat represents latitude which is the first node, with the greatest difference between below 44˚ and greater then 44˚. If greater then 44˚ other factors play into snow disappearance date, the most influential being years since fire were immediately following fire and intermediate and advanced fire are split into two sub groups. Immediately following fire, elevation, canopy height, mean precipitation and species determined via NLCD all influence*

snow disappearance date. Where generally the highest longitudes and canopy heights have the latest disappearance dates in immediately burned fires above 1317m, below 1310m lower precipitation is primarily responsible for the earliest snow disappearance dates, while above 1310m to 1317m greater canopy height is associated with earlier snow disappearance and later snow disappearance is attributed to pre-fire vegetation being evergreen forest rather than shrub with the latest dates in evergreen forests at latitude greater than 45˚.

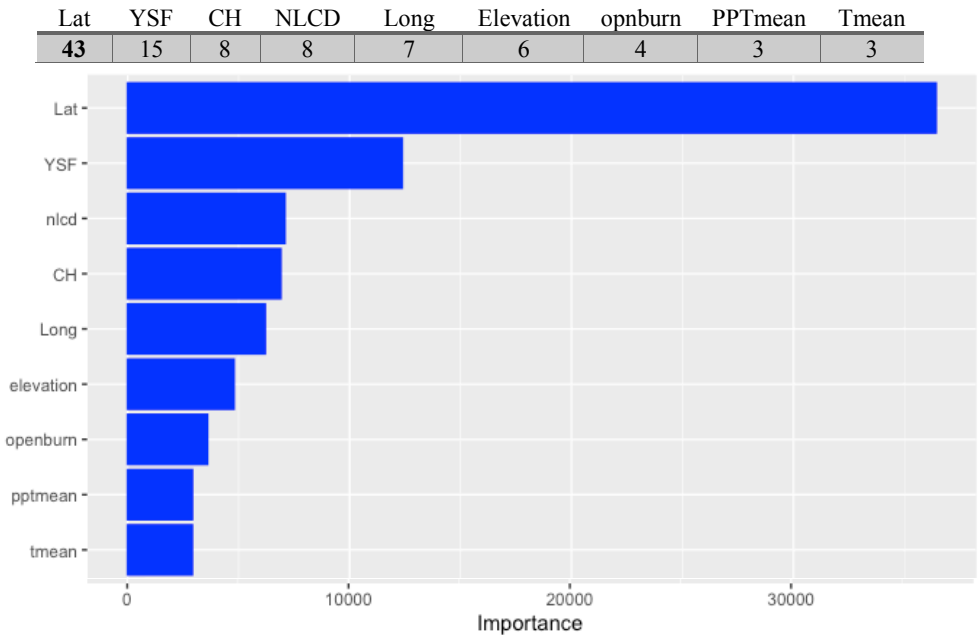

Figure A.B3: *Variable Importance Plot- ranking the importance of each predictor with relation to the model performance. The larger values, Latitude and YSF, are the more important predictors. This is based on randomly sampling half of the dataset.*

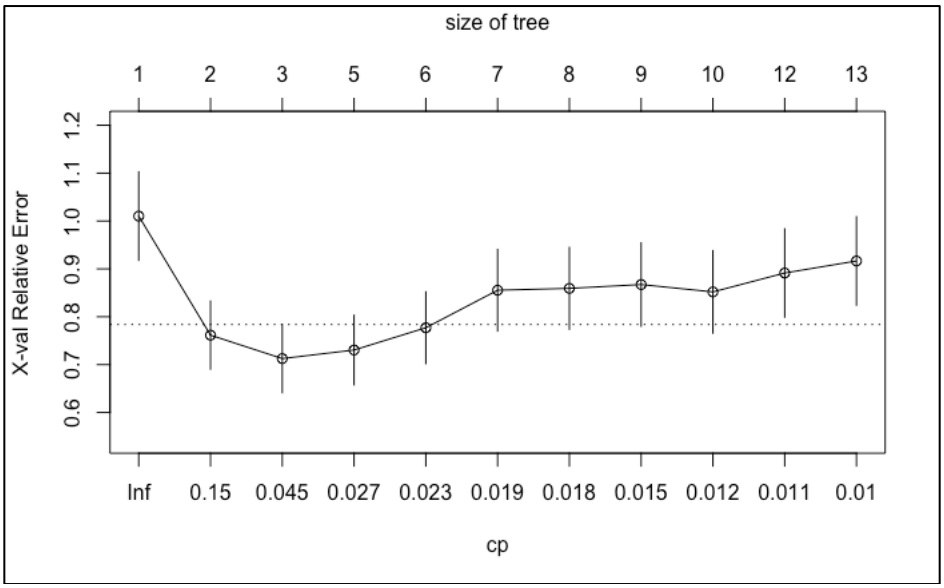

Figure A.B4: *Cross-validation plot, where 0.045 is the lowest accepted Cp value. This value is used to develop the pruned decisions tree, representing the final optimal model for the data presented.*

APPENDIX C: SUPPLEMENTAL TABLES AND STATISTICS

Lionshead 2020/2021 – TIMELAPSE SNOW DEPTH

Table A.C1: *Peak snow metrics derived via time-lapse photography dataset of the winter of 2020 - 2021 Lionshead burn area. Snow metrics calculated for the winter of 2021: PSWE is the day from which snow is at its peak snow depth during the 2021 winter season. MSWE is the date of peak SWE, historically April 1st SWE snow metrics. PSD is the date in which that peak snow for the season is achieved. Peak Snow (cm) is the value in centimeters by which that peak is recorded. SDD is the snow disappearance date because there is no mid-winter melt event SDD. SMR for PSWE is calculated as the total snow melt rate (TSMR) from peak snow to the SDD. SMR for MSWE is the SMR from peak SWE date to SDD.*

FOREST TYPE	PEAK SNOW DEPTH (DAY)	PEAK SNOW DEPTH (CM)	DISAPPEARANCE DAY	SNOW MELT RATE (CM/D)
FORESTED (PEAK SWE)	Feb 29, 2021	209.41	April 1st, 2021	2.86
HIGH (PEAK SWE)	Feb 27, 2021	248.74	April 1st, 2021	4.14
MODERATE (PEAK SWE)	Feb 28, 2021	174.59	April 1st, 2021	3.23
OPEN (PEAK SWE)	Feb 27, 2021	278.65	April 1st, 2021	2.23
FORESTED (MID-WINTER)	Mar 29, 2021	177.17	May 12, 2021	4.12
HIGH (MID-WINTER)	April 1, 2021	178.57	April 29, 2021	6.61
MODERATE (MID-WINTER)	April 1, 2021	137.53	April 24, 2021	6.25
OPEN (MID-WINTER)	April 1, 2021	220.84	May 15, 2021	5.11

Table A.C2: *Summary statistics and ANOVA results (Pr). Showing the mean snow depth of each ablation month and significance testing where *** or P<0.05 indicates significance*

Date	Mean	Standard Deviation	Forested	High	Open	Moderate	Pr(>)F
March	183.15	38.57	159.55	194.05	233.38	138.87	<0.05***
April	110.755	56.36	114.24	110.61	161.12	57.27	<0.05***
May	6.71	15.93	011.77	0	15.06	0	<0.05***

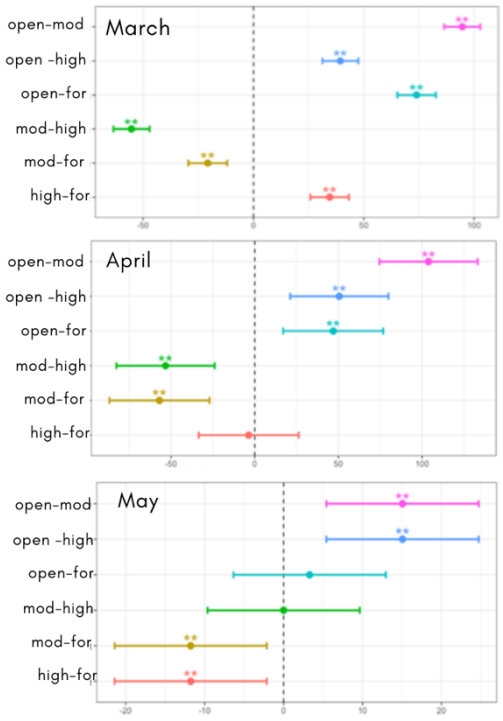

MARCH - 2021	**P-VALUE**
Open-Moderate	<0.05**
Open-High	<0.05**
Open-Forested	<0.05**
Moderate-High	<0.05**
Moderate-forested	<0.05**
High-forested	<0.05**

APRIL - 2021	**P-VALUE**
High-Forested	0.98
Moderate-Forested	<0.05**
Open-Forested	<0.05**
Moderate-High	<0.05**
Open-High	<0.05**
Open-Moderate	<0.05**

MAY - 2021	P-VALUE
High-forested	<0.05**
Moderate-forested	<0.05**
Open-Forested	0.81
Moderate-High	1
Open-High	<0.05**
Open-Moderate	<0.05**

Lionshead 2021/2022 – TIMELAPSE SNOW DEPTH

Table A. C3 Peak snow metrics derived via time-lapse photography dataset of the winter of 2021 - 2022 Lionshead burn area

Forest Type	Peak Snow Depth (day)	Peak Snow Depth (cm)	Disappearance Day	Snow Melt Rate (cm/d)
Forested (PSWE)	April 10, 2022	70.31	May 11, 2022	-2.27
High (PSWE)	April 13, 2022	178.57	May 24, 2022	-4.35
Moderate (PSWE)	April 17, 2022	159.36	May 25, 2022	-4.37
Open (PSWE)	April 13, 2022	204.31	June 4, 2022	-3.93
Forested (MSWE)	Jan. 5, 2022	153.58	April 1, 2022	-1.94
High (MSWE)	Jan. 5, 2022	225.13	April 1, 2022	-1.83
Moderate (MSWE)	Jan. 5, 2022	200.00	April 1, 2022	-1.62
Open (MSWE)	Jan. 5, 2022	235.11	April 1, 2022	-1.77

Table A.C4: *Summary statistics and results from ANOVA statistical analysis. Showing the mean snow depth of each ablation month and significance testing where ** (P<0.05) indicates significance.*

Date	**Mean**	**Standard Deviation**	**Forested**	**High**	**Open**	**Moderate**	**Pr(>)F**
March	114.65	23.58	111.50	128.31	85.80	132.31	<0.05**
April	100.79	58.97	36.62	118.04	157.35	91.15	<0.05**
May	53.32	49.40	3.71	55.36	102.33	51.87	<0.05**

MARCH -2022	**P-VALUE**
High-forested	<0.05***
Moderate-forested	<0.05***
Open-Forested	<0.05***
Moderate-High	0.55
Open-High	0.04*
Open-Moderate	<0.05***
ARIL -2022	**P-VALUE**
High-Forested	<0.05**
Moderate-forested	0.09*
Open-Forested	<0.05**
Moderate-High	0.06*
Open-High	0.06*
Open-Moderate	<0.05**
MAY -2022	**P-VALUE**
High-forested	<0.05**
Moderate-forested	<0.05**
Open-Forested	<0.05**
Moderate-High	0.99
Open-High	0.02*
Open-Moderate	0.03*

SHADOW LAKE 2021/2022 – TIMELAPSE SNOW DEPTH

Table A. C5: Peak snow metrics derived via time-lapse photography dataset of the winter of 2021 - 2022 Shadow Lake burn area.

Forest Type	Peak Snow Depth (day)	Peak Snow Depth (cm)	Disappearance Day	Snow Melt Rate (cm/d)
Forested (PSWE)	4/13/22	195.77	6/04/22	-3.76
High (PSWE)	4/13/22	200.62	6/02/22	-4.01
Moderate(PSWE	4/14/22	215.24	6/02/22	-4.39
Open (PSWE)	4/14/22	154.62	6/01/22	-3.22
Forested(MSWE)	1/05/22	207.71	04/01/22	-0.67
High (MSWE)	1/05/22	218.62	04/01/22	-0.55
Moderate(MSW	1/05/22	233.97	04/01/22	-0.57
Open (MSWE)	1/08/22	149.32	04/01/22	-1.05

Table A. C6: *Summary statistics and results from ANOVA statistical analysis. Showing the mean snow depth of each ablation month and significance testing where *** (P<0.05).*

Date	Mean	Standard Deviation	Forested	High	Open	Moderate	Pr(>)F
March	114.65	23.58	111.50	128.31	85.80	132.31	<0.05**
April	145.71	35.20	144.08	154.21	116.08	165.19	<0.05**
May	93.70	38.72	90.25	92.91	84.72	106.59	0.06*

MARCH -2022	P-VALUE
High-forested	0.24
Moderate-forested	0.04*
Open-Forested	<0.05**
Moderate-High	0.86
Open-High	<0.05**
Open-Moderate	<0.05**
ARIL -2022	**P-VALUE**
Open -Moderate	0.59
Moderate-forested	0.14
Open-Forested	0.71
Moderate-High	0.78
Open-High	0.09*
Open-Moderate	<0.05**
MAY -2022	**P-VALUE**
High-forested	0.77
Moderate-forested	0.34
Open-Forested	0.95
Moderate-High	<0.05**
Open-High	0.96
Open-Moderate	0.14

B AND B 2021/2022 – TIMELAPSE SNOW DEPTH

Table A.C7: *Peak snow metrics derived via time-lapse photography dataset of the winter of 2021 - 2022 B and B burn area.*

Forest Type	Peak Snow Depth (day)	Peak Snow Depth (cm)	Disappearance Day	Snow Melt Rate (cm/d)
Forested (PSWE)	4/15/22	117.45	05/20/22	-3.35
High (PSWE)	4/14/22	146.79	05/24/22	-3.74
Moderate (PSWE	4/14/22	144.65	05/23/22	-3.62
Open (PSWE)	4/14/22	171.43	05/26/22	-4.08
Forested (MSWE)	1/05/22	172.74	04/01/22	-1.72
High (MSWE)	1/05/22	200.96	04/01/22	-1.55
Moderate (MSWE)	1/04/22	211.95	04/01/22	-1.60
Open (MSWE)	1/05/22	176.73	04/01/22	-1.16

Table A. C8: *Summary statistics and results from ANOVA statistical analysis. Showing the mean snow depth of each ablation month and significance testing where *** (P<0.05).*

Date	**Mean**	**Standard Devetion**	**Forested**	**High**	**Open**	**Moderate**	**Pr(>)F**
March	86.62	26.29	NA	96.178	96.95	103.46	2.2e-16***
April	103.2	32.86	68.67	111.82	122.55	110.04	4.507e-05***
May	47.62	37.53	23.76	49.82	77.03	44.26	0.003707***

MARCH -2022	**P-VALUE**
High-forested	<0.05**
Moderate-forested	<0.05**
Open-Forested	<0.05**
Moderate-High	0.178
Open-High	0.99
Open-Moderate	0.11
ARIL -2022	**P-VALUE**
High-Forested	<0.05**
Moderate-Forested	<0.05**
Open-Forested	<0.05**
Moderate-High	0.99
Open-High	0.99
Open-Moderate	0.99
MAY -2022	**P-VALUE**
High-forested	0.21
Moderate-forested	0.94
Open-Forested	<0.05**
Moderate-High	0.53
Open-High	0.28
Open-Moderate	0.02*

Table A.C9: *Eigenvectors, how specified PC represent the original measured 11 variables. Each number can be interpreted as a correlation coefficient between each original variable and it's corresponding PC also referred to as contributions. The larger the coefficient of the original variable, the larger the contribution to the PC, in other words the PC "represents" this particular variable well. They can be interpreted the same way as correlation coefficients between the original variable and the PC. All coefficients that are blank, are very small and therefore have contributions that are considered negligible. PC1 therefore represents 5 geographical variables and years since fire well.*

	C.1	C.2	C.3	C.4	C.5	C.6	C.7	C.8	C.9	C.10	C.11
Aspect	**-**	0.27	0.486	0.52	0.34	0.42	0.33	-	-	-	-
Slope °	**-**	-0.34	-	-0.47	0.70	-	0.30	0.21	-	-	-
CBD	**-**	-0.34	-0.572	0.36	-0.27	0.26	0.46	0.19	-	-	0.11
CH	**-0.31**	-0.31	-	0.37	0.21	-0.28	-0.31	0.33	0.44	-0.32	-0.14
Lat ***	**-0.47**	-0.16	0.125	-	-0.12	-	0.10	-0.15	-0.16	0.31	-0.74
Long	**0.30**	-0.39	-	0.15	-	-0.18	0.21	-0.72	0.11	-0.28	-
SDD	**-0.29**	-	0.32	-0.22	0.29	-0.44	0.60	0.14	0.14	-0.14	0.17
Elev.*	**0.32**	-0.34	0.35	-	-0.17	-	-	0.39	**-0.59**	-0.27	-0.12
Ptmean*	**-0.32**	-0.19	0.16	0.33	-0.19	0.62	-0.13	-0.12	0.11	-0.46	0.17
Tmean*	**0.33**	-0.34	0.34	-	-0.26	0.13	-	0.14	0.50	0.51	-
YSF ***	**0.40**	0.33	-0.16	-0.17	-0.12	0.12	0.15	0.20	**0.33**	-0.36	-0.57

Table A.C10*: Importance of the component's eigenvalues corrected by the total variance in the dataset, where 190 is the sample size and. In this algorithm for line three each variance is calculated by dividing N instead of N-1. Thus we are correcting it by multiplying N/(N-1). The bottom line is the proportion of the variance explained by each PC. Corrected and PC 1 therefore explains 79% of the variance.*

	C1	C2	C3	C 4	C 5	C6	C7	C8	C9	C10	C11
SD	1.88	1.23	1.07	1.03	0.97	0.84	0.80	0.74	0.60	0.52	0.33
SD->VAR	3.56	1.53	1.15	1.06	0.94	0.71	0.64	0.56	0.36	0.27	0.11
	3.57	1.53	1.16	1.06	0.95	0.71	0.64	0.56	0.36	0.27	0.11
Prop. Ex	**0.79**	0.34	0.25	0.23	0.20	0.16	0.14	0.12	0.08	0.06	0.02

Table A.C11: *Importance of components (PC's), all PC (Comp.1 – Comp.11) often expressed as the proportion of variance explained. SD is the standard deviations of the principal components (its variance) which is related to it's eigenvalue. The third row is the cumulative proportion of the variance explained which should add up to 1.*

	C1	**C2**	**C3**	**C4**	**C5**	**C6**	**C7**	**C8**	**C9**	**C10**	**C11**
SD	1.88	1.23	1.07	1.03	0.97	0.84	0.80	0.74	0.60	0.52	0.33
PROP. VAR	**0.32**	**0.13**	**0.10**	**0.09**	0.08	0.06	0.05	0.05	0.03	0.02	0.01
Cum. Prop.	**0.32**	**0.46**	**0.57**	**0.66**	0.75	0.755	0.87	0.93	0.96	0.98	1.00